IMPACT OF AEROSOLS ON CONVECTIVE CLOUDS AND PRECIPITATION

Wei-Kuo Tao,[1] Jen-Ping Chen,[2] Zhanqing Li,[3,4] Chien Wang,[5] and Chidong Zhang[6]

Received 14 July 2011; revised 2 December 2011; accepted 18 December 2011; published 17 April 2012.

[1] Aerosols are a critical factor in the atmospheric hydrological cycle and radiation budget. As a major agent for clouds to form and a significant attenuator of solar radiation, aerosols affect climate in several ways. Current research suggests that aerosol effects on clouds could further extend to precipitation, both through the formation of cloud particles and by exerting persistent radiative forcing on the climate system that disturbs dynamics. However, the various mechanisms behind these effects, in particular, the ones connected to precipitation, are not yet well understood. The atmospheric and climate communities have long been working to gain a better grasp of these critical effects and hence to reduce the significant uncertainties in climate prediction resulting from such a lack of adequate knowledge. Here we review past efforts and summarize our current understanding of the effect of aerosols on convective precipitation processes from theoretical analysis of microphysics, observational evidence, and a range of numerical model simulations. In addition, the discrepancies between results simulated by models, as well as those between simulations and observations, are presented. Specifically, this paper addresses the following topics: (1) fundamental theories of aerosol effects on microphysics and precipitation processes, (2) observational evidence of the effect of aerosols on precipitation processes, (3) signatures of the aerosol impact on precipitation from large-scale analyses, (4) results from cloud-resolving model simulations, and (5) results from large-scale numerical model simulations. Finally, several future research directions for gaining a better understanding of aerosol-cloud-precipitation interactions are suggested.

Citation: Tao, W.-K., J.-P. Chen, Z. Li, C. Wang, and C. Zhang (2012), Impact of aerosols on convective clouds and precipitation, *Rev. Geophys.*, *50*, RG2001, doi:10.1029/2011RG000369.

1. INTRODUCTION

[2] Aerosols, and especially their effect on clouds and precipitation, are one of the key components of the climate system and the hydrological cycle. Yet the aerosol effect on clouds and precipitation remains poorly known. A recent report published by the U.S. National Academy of Science states that "The greatest uncertainty about the aerosol climate forcing—indeed, the largest of all the uncertainties about global climate forcing—is probably the indirect effect of aerosols on clouds" [*National Research Council* (*NRC*), 2005]. This "aerosol indirect effect" (AIE) includes the traditional "indirect," or "Twomey," effect on cloud droplet size and thus reflectance for a constant liquid water path [*Twomey*, 1977; *Twomey et al.*, 1984] and the "second indirect" effect on cloud extent and lifetime [*Albrecht*, 1989; *Hansen et al.*, 1997; *Ackerman et al.*, 2000]. Enhanced aerosol concentrations can also suppress warm-rain processes by reducing particle sizes and causing a narrow droplet spectrum that inhibits collision and coalescence processes [e.g., *Squires and Twomey*, 1961; *Warner and Twomey*, 1967; *Warner*, 1968; *Rosenfeld*, 1999]. The aerosol effect on precipitation processes, considered part of the second type of aerosol indirect effect [*Albrecht*, 1989], is even more complex, especially for mixed-phase convective clouds.

[3] Continued advancement of instrumental technology has provided the community with much improved research tools to gain insights concerning aerosol-cloud-precipitation interactions (ACPI). For instance, a combination of cloud top temperature and effective droplet sizes, estimated from the advanced very high resolution radiometer (AVHRR), has been used to infer the suppression of coalescence and precipitation processes by smoke [*Rosenfeld and Lensky*, 1998] and desert dust [*Rosenfeld et al.*, 2001]. Multisensor (passive/active microwave and visible and infrared) satellite

[1]Laboratory for Mesoscale Atmospheric Processes, NASA Goddard Space Flight Center, Greenbelt, Maryland, USA.
[2]Department of Atmospheric Sciences, National Taiwan University, Taipei, Taiwan.
[3]Earth System Science Interdisciplinary Center and Department of Atmospheric and Oceanic Sciences, University of Maryland, College Park, Maryland, USA.
[4]State Key Laboratory of Earth Surface Processes and Resource Ecology, College of Global Change and Earth System Science, Beijing Normal University, Beijing, China.
[5]Department of Earth, Atmospheric, and Planetary Sciences, Massachusetts Institute of Technology, Cambridge, Massachusetts, USA.
[6]Rosenstiel School of Marine and Atmospheric Science, University of Miami, Miami, Florida, USA.

8755-1209/12/2011RG000369
Paper number 2011RG000369

observations from the Tropical Rainfall Measuring Mission (TRMM) have also been used to identify the presence of nonprecipitating supercooled liquid water near cloud tops due to over-seeding from both smoke over Indonesia [*Rosenfeld*, 1999] and urban pollution over Australia [*Rosenfeld*, 2000]. In addition, aircraft measurements have provided evidence of sustained supercooled liquid water down to −37.5°C in continental mixed-phase convective clouds [*Rosenfeld and Woodley*, 2000]. These findings further suggest that an increase in continental aerosols can reduce the mean size of cloud droplets, suppressing coalescence and warm-rain processes, permitting more freezing of cloud droplets and associated latent heat release above the 0°C isotherm, and enhancing the growth of large hail and cold-rain processes [*Rosenfeld and Woodley*, 2000]. *Andreae et al.* [2004] analyzed in situ observations made during the Large-Scale Biosphere-Atmosphere Experiment in Amazonia–Smoke, Aerosols, Clouds, Rainfall, and Climate (LBA-SMOCC) campaign and found that increases in smoke and surface heat due to biomass burning tend to lead to higher cloud top heights and the enhancement of cold-rain processes over the Amazon basin. *Lin et al.* [2006] examined multiplatform satellite data over the Amazon basin and found that high biomass burning–derived aerosols are correlated with elevated cloud top heights, large anvils, and more rainfall. *Koren et al.* [2005] examined cloud properties derived from the Moderate Resolution Imaging Spectroradiometer (MODIS) and found strong evidence that aerosols from pollution, desert dust, and biomass burning systematically invigorate convective clouds over the Atlantic Ocean. Using long-term integrated TRMM-derived precipitation data, *Bell et al.* [2008] found a significant midweek increase in summertime afternoon thunderstorms over the southeastern United States, which coincides with a midweek increase in ground-measured aerosol concentration. Recently, *Li et al.* [2011a] and *Niu and Li* [2011] used long-term (10 year) sets of extensive ground-based and global A-Train (CloudSat, Cloud-Aerosol Lidar and Infrared Pathfinder Satellite Observation (CALIPSO), and MODIS) spaceborne satellite measurements to reveal unprecedentedly strong climatic effects of aerosols on clouds and precipitation. They also attempted to sort out conditions under which clouds and precipitation are suppressed or fueled by aerosols.

[4] These findings are consistent with the notion that aerosols have a major impact on the dynamics, microphysics, and electrification properties of continental mixed-phase convective clouds. In addition, high aerosol concentrations in urban environments could affect precipitation variability by providing a significant source of cloud condensation nuclei (CCN). Such pollution effects on precipitation potentially have enormous climatic consequences in terms of both feedbacks involving the land surface via rainfall and the surface energy budget and changes in latent heat input to the atmosphere. Table 1 summarizes observations of cloud system features in high-aerosol and low-aerosol continental environments. Basically, aerosol concentrations can influence cloud droplet size distributions, the warm-rain process, the cold-rain process, cloud top heights, the depth of the mixed-phase region, and the occurrence of lightning. The following review of observation-modeling studies of the AIE follows the general life cycle of a cloud from the germination of cloud droplets; warm-rain, cold rain, and mixed-phase rain processes; and deep convective clouds to thunderstorms. In each phase, aerosols exert different influences on the development of clouds that ultimately affect precipitation.

[5] The main objective of this paper is to review our current understanding of the interactive processes between aerosols, clouds, and deep-convective precipitation systems. Recent results from observations and modeling (from cloud-resolving models to global models) are reviewed. The paper has seven sections. It begins in section 2 with a brief description of fundamental theories regarding the effects of CCN and ice nuclei (IN) on microphysics and precipitation processes. The observational evidence of aerosol effects on cloud and precipitation processes is then reviewed in section 3. Section 4 presents the signatures of aerosol impacts on precipitation processes from large-scale analyses. Sections 5 and 6 summarize recent results from cloud-resolving model and large-scale numerical model simulations, respectively. In section 7, current and future research on aerosols and their interactions with precipitation are discussed.

2. FUNDAMENTAL THEORIES OF AEROSOL EFFECTS ON CLOUDS AND PRECIPITATION

2.1. Activation of Condensation Nuclei Into Cloud Drops

[6] Aerosol particles composed of hygroscopic materials are good surfaces upon which water vapor can condense, so they are called condensation nuclei (CN). CCN are the portions of CN that are capable of initiating cloud drop formation. Such a capability is strongly related to the mass and composition of their water-soluble component. *Köhler* [1936] explained this mechanism with the Köhler curve, which describes the equilibrium saturation ratio over the solution drop surface, S_d, as a function of the drop radius. For each droplet containing a fixed amount of dissolved salt, the solution (Raoult) effect reduces the water activity and thus surface vapor pressure, whereas the curvature (Kelvin) effect does the opposite by holding water molecules together. These two effects combine to form the Köhler curve, which shows a peak value in S_d at a unique drop size called the critical radius r^* (see Figure 1). The maximum S_d appearing on a curve corresponding to a given particle with dry size r_d or equilibrium size (wet size) r_e is commonly called the critical (or activation) saturation ratio, S^*, for that particle, presumably with a known composition and fixed solute mass. During cloud formation, once the ambient saturation ratio S_∞ exceeds the S^* of a particle, that particle can be activated into a cloud drop. Those particles that never meet the condition of $S_\infty > S^*$ will stay in a "haze state" and are called interstitial aerosols. This also means that whether CN can be regarded as CCN depends not only on the properties of the particle but also on the ambient conditions (i.e., S_∞). It is important to recognize that aerosols have a

TABLE 1. Key Observational Studies Identifying the Differences in Microphysical Properties, Cloud Characteristics, Thermodynamics, and Dynamics Associated With Clouds and Cloud Systems Developed in Dirty and Clean Environments[a]

Properties	High CCN[b] (Dirty)	Low CCN (Clean)	References (Observations)
Cloud droplet size and distribution	smaller and narrower	larger and broader	*Squires* [1958], *Radke et al.* [1989], *Ferek et al.* [2000], *Rosenfeld and Lensky* [1998], *Rosenfeld* [1999, 2000], *Rosenfeld et al.* [2001], *Rosenfeld and Woodley* [2000], *Andreae et al.* [2004], *Koren et al.* [2005], *Yuan et al.* [2008]
Warm-rain process	suppressed	enhanced	*Squires* [1958], *Radke et al.* [1989], *Albrecht* [1989], *Rosenfeld* [1999, 2000], *Rosenfeld and Woodley* [2000], *Rosenfeld and Ulbrich* [2003], *Andreae et al.* [2004], *Lin et al.* [2006], *Givati and Rosenfeld* [2004], *Li et al.* [2011a]
Cold-rain process	enhanced	suppressed	*Rosenfeld and Woodley* [2000], *Orville et al.* [2001], *Williams et al.* [2002], *Andreae et al.* [2004], *Lin et al.* [2006], *Bell et al.* [2008]
Mixed-phase region	deeper	shallower	*Rosenfeld and Lensky* [1998], *Williams et al.* [2002], *Andreae et al.* [2004], *Koren et al.* [2005, 2008, 2010a, 2010b], *Lin et al.* [2006], *Li et al.* [2011a], *Niu and Li* [2011]
Lightning	enhanced (downwind side)/ higher maximum flash	less and lower maximum flash	*Williams et al.* [2002], *Orville et al.* [2001], *Steiger et al.* [2002], *Steiger and Orville* [2003], *Yuan et al.* [2011]

[a]Updated and modified from *Tao et al.* [2007].
[b]Cloud condensation nuclei.

broad size range, and the sizes of CN are important in determining their role in cloud and precipitation formation. From Figure 1, one can see that larger aerosols have lower S^*, so they have the advantage of easier activation. Note that the solute amount in an aerosol particle may vary with time during its uptake of water either by absorbing gases (such as nitric acid or ammonia) from the ambient air or by dissolving its solid cores (e.g., mineral dust) [*Kulmala et al.*, 1993, 1997]. Besides solute mass (or particle dry size), the Köhler curve also varies with the solute chemical composition, which influences not only the Raoult effect (by altering the water activity) but also the Kelvin effect (by altering the surface tension). Temperature is another factor that determines Köhler curve characteristics. An aerosol particle may become warmer than its environment due to either latent heating from vapor condensation or absorption of solar radiation by its soot or mineral dust component. Such heating affects all three factors that determine the Köhler curve (i.e., saturation vapor pressure, surface tension, and solution activity) so the Köhler curve should not be calculated using the ambient temperature [*Conant et al.*, 2002; *Nenes et al.*, 2002]. The insoluble portion of the aerosol particle, such as soot and mineral dust, may also affect the Köhler curve, simply by adding to the particle size and thus reducing the Kelvin effect.

[7] The relationship between the initial number of cloud concentration (N_C) near cloud base and aerosol number spectra is an important issue in studying aerosol effects on cloud microphysics and radiation with regional and global atmospheric models. The Köhler theory is a first step in understanding this relationship. However, the Köhler theory can only tell us whether a condensation nucleus can be activated into a cloud drop under a particular ambient supersaturation, ss_∞ ($\equiv S_\infty - 1$). The maximum ss_∞ (hereinafter termed $ss_{\infty,\max}$) that can be reached must be known in order to determine the number of cloud drops activated at the cloud base. The ambient supersaturation is controlled by two factors, as indicated by the saturation development equation [*Squires*, 1952]

$$\frac{dss_\infty}{dt} = A_1 \frac{dz}{dt} - A_2 \frac{dq_w}{dt}, \tag{1}$$

where the coefficients A_1 and A_2 are properties of the ambient air, z is the height, and q_w is the cloud water content. In equation (1) the source term indicates an increase in ss_∞ due to expansion cooling (thus a decrease in saturation vapor pressure) in the updrafts, and the sink term is due to water

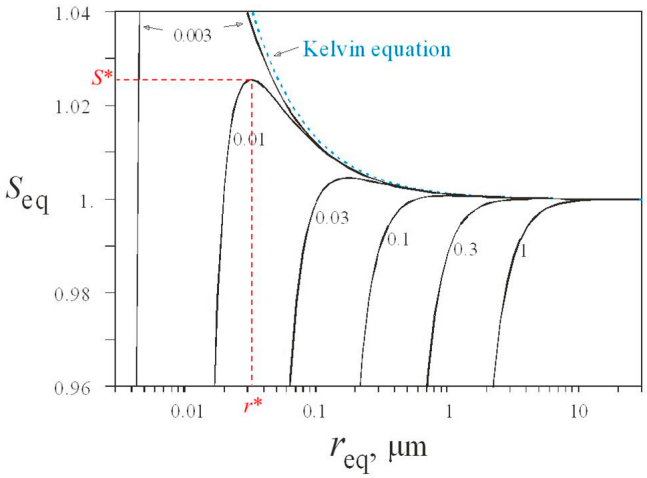

Figure 1. Relationship between the saturation ratio of drop surface (S_{eq}) and the equilibrium drop size (r_{eq}) according to the Köhler theory. All curves are for drops formed from ammonium sulfate particles with the dry radius in units of millimeters. By taking the 0.01 μm particle as an example, the red-dashed lines indicate the positions of critical saturation ratio S^* and critical radius r^*. Adapted from *Chen* [1994b].

vapor removal by condensation onto cloud drops. The condensation rate, dq_w/dt, is roughly proportional to ss_∞, cloud drop size, and N_C; N_C, in turn, is determined by the CN size spectrum and the variation in ss_∞. As more and more CCN turn into cloud drops, the sink term quickly surpasses the source term after which ss_∞ starts to decrease. Typically, this peak supersaturation, $ss_{\infty,\max}$, is reached within a few tens of meters above the cloud base. No more CN activation can occur deeper into the cloud unless ss_∞ rises again and surpasses the original $ss_{\infty,\max}$ due to enhanced updrafts or depletion of cloud drops by rain accretion [*Chen*, 1994a]. Although the relationship between N_C and the CN spectrum is quite convoluted, a unique solution for N_C at the cloud base exists when the CN spectrum and updraft speed (dz/dt) are given. In the following, we briefly describe the common form of the CN spectrum representation and how it can be used to derive N_C.

[8] One common type of CN spectra measurement is based on the Köhler theory discussed above. The aerosol particles to be measured are introduced into a diffusion chamber with controlled ss_∞, and then the number of cloud drops formed at that condition is counted. This specified ss_∞ represents the critical supersaturation, ss^* ($\equiv S^* - 1$), of the smallest CCN that can be activated. By sweeping through a range of ss_∞ values in the diffusion chamber, one can obtain a relationship between the number of CCN (N_{CCN}) and $ss_{\infty,\max}$. Earlier studies found that the measured CCN spectra can often be approximated empirically as

$$N_{CCN} = C \cdot ss^k_{\infty,\max}, \tag{2}$$

where C and k are time- and location-dependent coefficients of the CN spectra [*Twomey*, 1959a]. Figure 2 shows examples of the measured relationship between N_{CCN} (normalized by the number of CN, N_{CN}) and $ss_{\infty,\max}$, as well as that using equation (2) for several values of k. Note that $ss_{\infty,\max}$ here is often expressed in terms of the percentage of supersaturation. The power law formulation in equation (2) is simple and effective, but it has the weakness of producing unlimited CCN number concentrations with ever-increasing $ss_{\infty,\max}$. In reality, the number of CCN normally diminishes when the size gets too small or the supersaturation gets too high, causing a leveling off of N_{CCN}.

[9] Another common type of aerosol measurement is done by segregating aerosol particles according to their aerodynamic sizes and then counting the particle number in each size segment to obtain a size spectrum. Earlier studies using such techniques found that the number density distribution (or the size distribution) of aerosol particles with a dry size, r_a, greater than 0.1 μm can be approximated by a power law relationship [e.g., *Junge*, 1952, 1955],

$$n(r_a) \equiv \frac{dN(r_a)}{dr_a} = a_1 r_a^{-a_2}, \tag{3}$$

where $N(r_a)$ is the total number of CN with a dry size greater than r_a, and a_1 and a_2 are constants. Note that $ss_{\infty,\max}$ in equation (2) actually represents the critical supersaturation of the smallest CCN, and it can be related to the r_a of that particle by the approximation, $s^* \approx \alpha \cdot r_a^{-3/2}$, where α depends on the chemical composition. With this relationship, equation (2) can be converted into a size spectrum:

$$n(r_a) = \frac{dN_{CCN}}{dr_a} = \alpha \cdot C \cdot r_a^{-\left(1+\frac{3k}{2}\right)}. \tag{4}$$

One can easily recognize the equivalency between equations (3) and (4). As mentioned before, these formulas might not apply to $r_a < 0.1$ μm, yet under some conditions, such as in strong convection, very small CN do form cloud drops. To better describe the full size spectrum, many studies applied the trimodal lognormal function to represent the observed

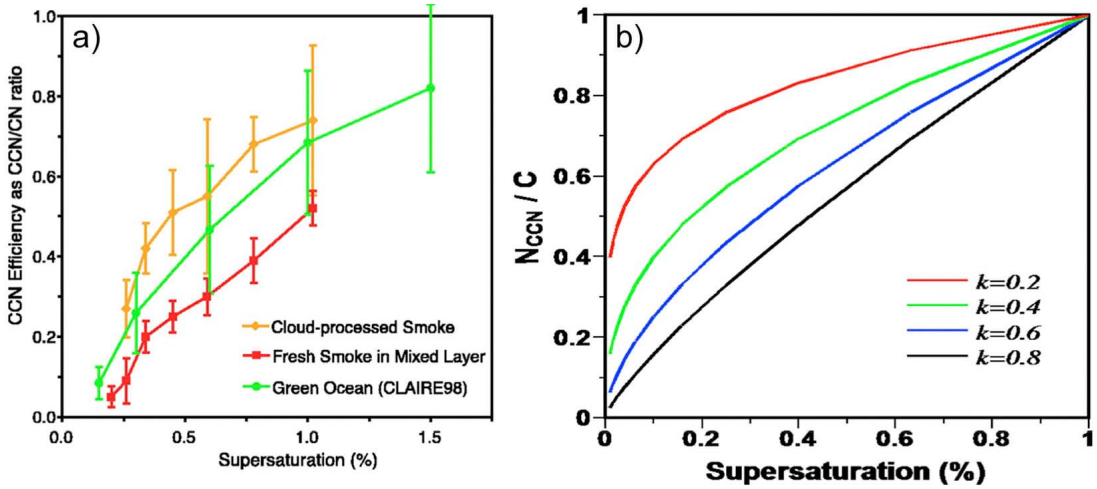

Figure 2. Cloud condensation nuclei (CCN) spectra expressed in terms of activation supersaturation. (a) Values observed for different aerosol types (adapted from *Andreae et al.* [2004]). (b) Values according to the empirical formula $N_{CCN} = C\ s^k$. Note that values of the vertical coordinate have been normalized against N_{CN} for Figure 2a and against the coefficient C for Figure 2b. Copyright AAAS. Reprinted with permission.

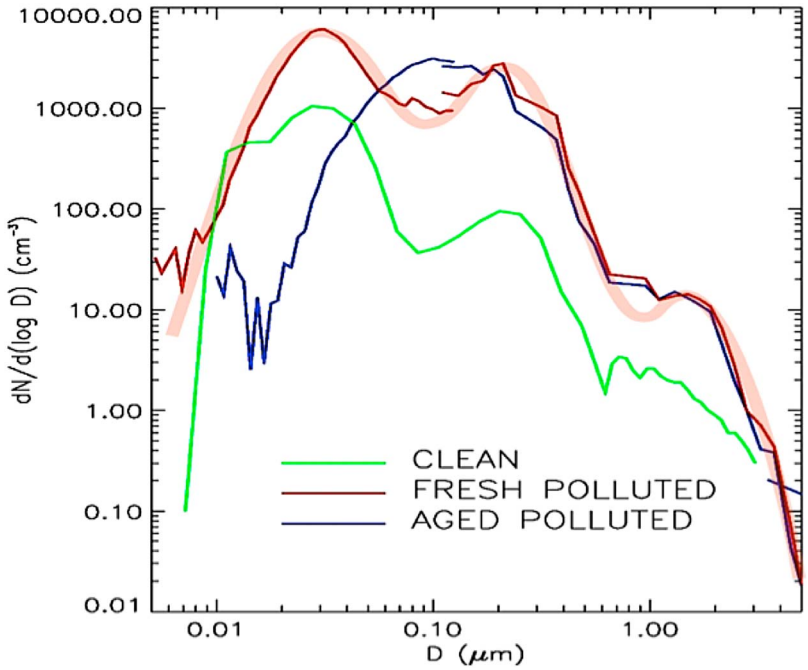

Figure 3. Examples of observed aerosol number size distribution (thin curves; adapted from http://research.metoffice.gov.uk/research/apr/ace-2.html) and the trimodal lognormal fit according to equation (5) for one of the curves (shaded curve).

aerosol spectra [e.g., *Whitby*, 1978; *Jaenicke*, 1993; *Brechtel et al.*, 1998],

$$n(\ln r_a) = \sum\nolimits_{i=1,3} \frac{N_i}{\sqrt{2\pi}\sigma_i} \exp\left[-\frac{\ln^2(r_a/r_{0,i})}{2\sigma_i^2}\right], \qquad (5)$$

where i is the modal index, and for each mode, N, σ, and r_0 are the number concentration, standard deviation, and modal radius, respectively. Examples of the trimodal lognormal size distribution are illustrated in Figure 3. Presenting the aerosol population in terms of size spectra such as those described by equations (3) or (5) has a disadvantage in that chemical composition must be known in order to calculate N_C, but such information is often not provided. In this regard, equation (2) may be a better formulation for CN spectra because it does not require additional information. Even if chemical compositions are known, the numerous chemical species in natural aerosols makes it difficult for model calculations. For this problem, *Petters and Kreidenweis* [2007] suggested a single hygroscopicity parameter, κ, which can be measured relatively easily and used effectively to model CCN activity.

[10] Quite a few cloud resolving models (CRMs) are capable of resolving ss_∞ and obtaining N_C directly by applying the Köhler theory to a specified CN spectrum such as those given in equations (2) and (5). These models include those using sophisticated bin microphysics [e.g., *Clark*, 1973; *Kogan*, 1991; *Khain et al.*, 2004; *Tao et al.*, 2007; *Morrison and Grabowski*, 2010], as well as those using bulk microphysics [e.g., *Feingold et al.*, 1994; *Ekman et al.*, 2006, 2007; *Cheng et al.*, 2007; *Morrison and Grabowski*, 2008]. But many global models and regional cloud models, such as those adopting the "saturation adjustment" assumption, do not resolve ss_∞ explicitly. Even for CRMs that do resolve ss_∞, the peak supersaturation is very often under-predicted because it occurs within roughly 50 m above the cloud base, which is not resolved in these models [cf. *Clark*, 1973; *Chen and Liu*, 2004]. Nevertheless, *Cheng et al.* [2007] showed that the calculation of supersaturation can be improved significantly by imbedding a Lagrangian parcel scheme. The Lagrangian-type calculation can also be applied in global models by running a parcel model, either online or offline, with given updraft speeds in order to derive N_C [*Nenes and Seinfeld*, 2003; *Roelofs et al.*, 2006]. But such calculations not only demand more computational resources but also require detailed calculations of thermodynamics and the aerosol activation process according to the Köhler theory. Alternatively, N_C may be derived by using diagnostic formulas introduced below.

[11] *Twomey* [1959b] was the first to link N_C to the CN spectrum in a diagnostic manner. By inserting equation (2) into equation (1) and applying a simplified condensation equation, he derived an asymptotic solution for N_C as a function of C, k, updraft speed, and air properties. As shown in Figures 4a and 4b, Twomey's solution predicts that N_C increases monotonically with N_{CN}. Recall that equations (2) and (4) yield an infinite number of N_{CN} if no upper limit is set for $ss_{\infty,\max}$ in equation (2) or no lower limit is set for r_a in equation (4). Yet, if the 0.1 μm cutoff size mentioned by *Junge* [1952, 1955] is applied to equation (2), the predicted N_C would unrealistically exceed N_{CN}. So a cutoff radius of 0.01 μm is applied to obtain the N_C in Figures 4a and 4b, and the chemical composition is assumed to be ammonium sulfate. Twomey's solution compares well with

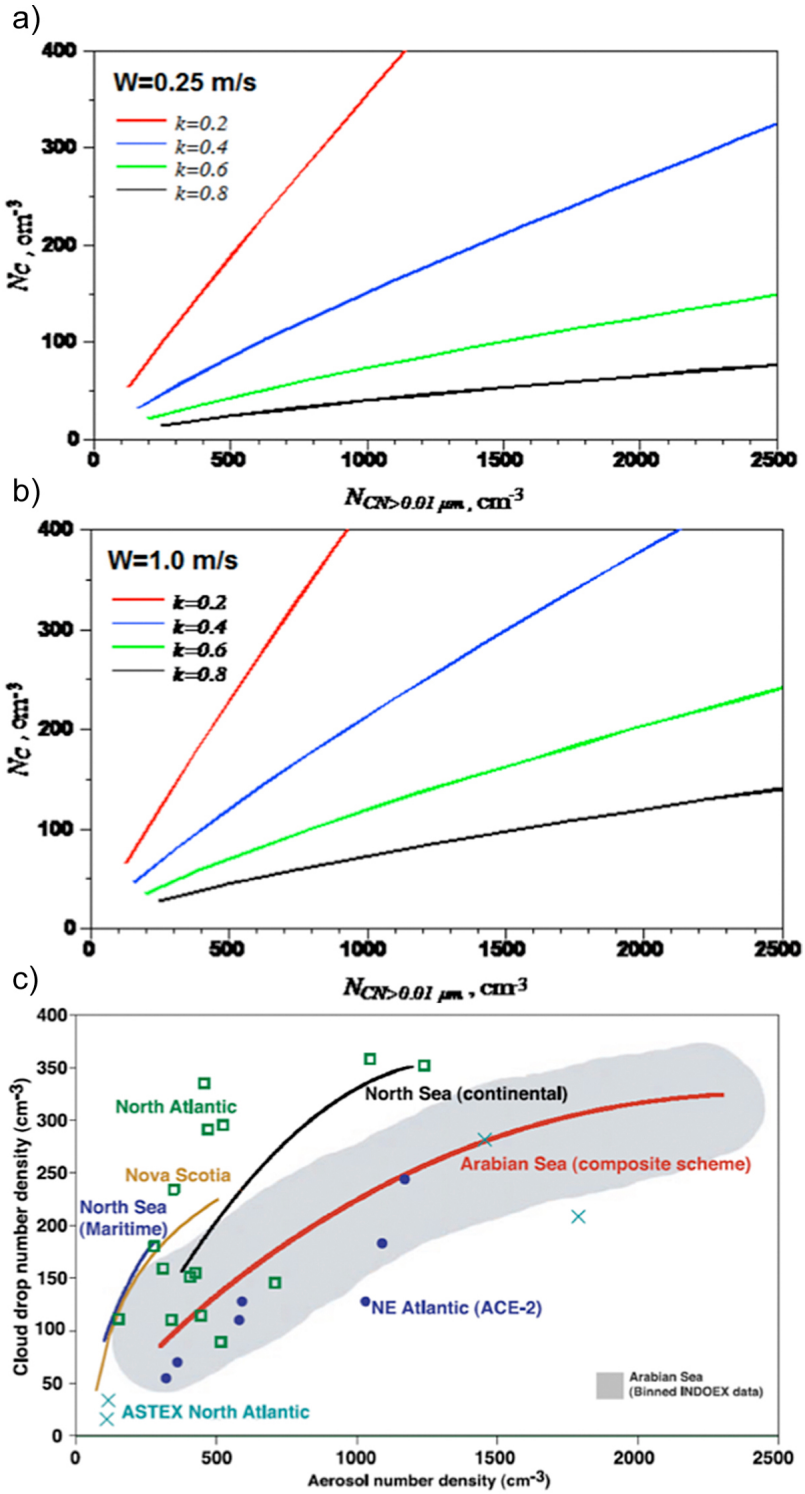

Figure 4. Relationship between the number concentrations (in cm^{-3}) of condensation nuclei (CN) and cloud drops. (a) Predictions from *Twomey*'s [1959b] quasi-analytical solution for a few typical k values and updraft speed W = 0.25 m/s. (b) Same as Figure 4a but for W = 1.0 m/s. (c) Observation results summarized by *Ramanathan et al.* [2001a]. In Figures 4a and 4b the CN concentration N_{CN} is calculated from equation (3) with a lower size limit of 0.01 μm. Copyright AAAS. Reprinted with permission.

the observational results summarized by *Ramanathan et al.* [2001a] (Figure 4c). The trends and the magnitudes are quite similar, and the regional differences in the observations seem to correspond to the variations in the coefficient k in equation (2). One feature that Twomey's prediction does not capture well is the leveling off of N_C toward higher N_{CN}. *Chen and Liu* [2004] examined Twomey's quasi-analytical solution by incorporating equation (2) into a parcel model

with detailed microphysics to obtain N_C. They found that Twomey's solutions significantly deviate from model calculations for large k and C values, partly because Twomey's solution is not exact and partly because its derivation omitted the solute effect and gas kinetic effect on condensation growth. Modification of Twomey's method has been performed by *Sedunov* [1967], *Ming et al.* [2006], *Khvorostyanov and Curry* [2009], and others, and the improvements include a refined asymptotic solution as well as considering more physical constraints such as soluble fraction, surface tension, and condensation (accommodation) coefficient. Parameterizations of CCN activation have also been developed using results from a parcel model that are fitted into various empirical functions [e.g., *Ghan et al.*, 1993; *Abdul-Razzak et al.*, 1998; *Lohmann et al.*, 1999; *Fountoukis and Nenes*, 2005] or by compiling results into lookup tables [*Saleeby and Cotton*, 2004]. Besides the theoretical approaches, prediction of N_C can also be obtained empirically by correlating N_C observed just above the cloud base with aerosol concentration (usually the mass of sulfate) observed below the cloud base. This method has been applied in various global climate models [e.g., *Boucher and Lohmann*, 1995; *Lohmann et al.*, 1999; *Roelofs et al.*, 1998; *Jones et al.*, 2001; *Tsai et al.*, 2010].

[12] Past studies of CCN focused mainly on the inorganic component of the aerosol. Yet around the globe, organic carbon is the second-most abundant component of fine aerosols after sulfate [*Novakov and Penner*, 1993; *Kanakidou et al.*, 2005; *Liu and Wang*, 2010]. Soluble organic compounds can decrease water activity and the surface tension of water [*Shulman et al.*, 1996; *Facchini et al.*, 1999; *Abdul-Razzak and Ghan*, 2004] just like inorganic solutes, but the effect is weaker for organics on the same mass basis. Such organic aerosol effects have been included in a few of the aforementioned studies [e.g., *Nenes and Seinfeld*, 2003]. One particular type of organic carbon called "surfactants" consists of polar (hydrophilic) and nonpolar (hydrophobic) segments, so these molecules stay preferentially on the droplet surface and form a monolayer film [*Langmuir and Langmuir*, 1927; *La Mer*, 1962]. Such a monolayer film does not influence the Köhler curve but can retard the condensation process through the gas-kinetic effect by reducing the water accommodation coefficient. *Deryaguin et al.* [1985] applied a one-dimensional model to show significant retardation of cloud drop condensation growth by the monolayer film. *Feingold and Chuang* [2002] further demonstrated that because of the slower growth of the activated cloud drops in an adiabatic cloud (i.e., the sink term in equation (1)), the monolayer film may cause a higher ambient supersaturation ss_∞ and thus promote activation of the smaller CN. Such a surface film effect is generally ignored in current cloud models due to its complexity as well as a lack of information on the characteristics of surfactants in aerosols.

2.2. CCN Effect on Rain Formation

[13] Rain formation processes can be categorized into two major pathways: warm-rain processes that do not involve ice crystals and cold-rain processes that do. CN may have a strong influence on warm-rain formation, mainly through their effect on N_C. As discussed above, N_C tends to increase with N_{CN} (see Figure 4). Because of competition of water vapor among cloud drops, a higher N_C necessarily leads to smaller cloud drops. Small cloud drops are ineffective in collision, partly due to lower fall speeds and partly due to smaller collision efficiencies. It is difficult for a cloud drop to grow into a raindrop (typically defined as drops with radii or diameters greater than 100 μm) merely by condensation, and collision coalescence is considered a necessary process for warm-rain initiation. But the collision coalescence process is inefficient unless some of the cloud drops can reach, by condensation growth, the so-called Hocking limit (around 19 μm in radius) [*Hocking*, 1959]. Once a raindrop is initiated, its further growth proceeds mainly by collecting cloud drops, and the efficiency of this process again depends heavily on cloud drop sizes.

[14] Another effect of increasing N_{CN} on warm-rain formation is the narrowing of the cloud drop size spectrum [*Fitzgerald and Spyers-Duran*, 1973; *Martin et al.*, 1994; *Liu and Daum*, 2002; *Andreae et al.*, 2004]. If we assume that the shape of the CN spectrum, as defined by the coefficient k in equation (2) or σ and r_0 in equation (5), remains fixed, then the increase in CN number concentration leads to a lower $ss_{\infty,\max}$ and thus a larger cutoff size for CN activation. According to the condensation growth equation, smaller drops grow faster in size than larger drops. This means that an increase in cutoff size (representing the smallest cloud drops) may lead to a narrower cloud drop size range. The difference in cloud drop sizes (and thus fall speeds) is important to the collision process because it requires that two colliding droplets have significant relative motions. Therefore a narrowed spectral width also leads to suppression of warm-rain formation. Note that the suppression of collision coalescence further enhances the narrowing of the cloud drop size spectrum.

[15] Note that the warm-rain suppression effect might not occur if the increase in N_{CN} comes with a change in the shape of the CN spectrum. An extreme example is the addition of a few very large CCN, which are often termed giant CCN (GCCN), with radii in the micrometer range or larger. One natural GCCN is large sea salt particles generated by the breakup of air bubbles in the ocean or by wave tearing [*de Leeuw et al.*, 2011]. Because of their inherently large sizes, GCCN may be activated directly into rain embryos and can readily initiate the warm-rain process [*Johnson*, 1982; *O'Dowd et al.*, 1997; *Feingold et al.*, 1999; *Lasher-Trapp et al.*, 2001; *Cheng et al.*, 2007]. In addition, because they also compete for water vapor, GCCN can lower $ss_{\infty,\max}$ and thus deprive small CN of the chance to activate into cloud drops [*Ghan et al.*, 1998; *Feingold et al.*, 1999; *Cheng et al.*, 2007]. Furthermore, because there are fewer cloud drops, each cloud drop can grow larger and thus is more efficient at converting into rain by collision coalescence. So GCCN counteract both Twomey's first and second indirect effects. Large insoluble particles such as mineral dust have a similar capability especially when they are coated with hygroscopic materials. The GCCN effect has been utilized for artificial rain enhancement. In the so-called

warm-cloud seeding procedure, GCCN-sized salt particles are introduced into clouds to accelerate rain initiation [*Mather et al.*, 1997; *Bruintjes*, 1999]. However, the effectiveness of GCCN depends on how efficiently rain can be initiated without them. In clean environments (e.g., low N_C), cloud drops are able to grow large enough by condensation to reach the so-called Hocking limit, after which the cloud drop can grow effectively by collision coalescence and convert into raindrops. So GCCN tend to be less important in such situations as demonstrated by *Feingold et al.* [1999] using detailed model simulations. They also noted that higher concentrations of GCCN are required at higher CCN concentrations for marine stratocumulus to produce drizzle. While CCN generally increases with CN for dusty events, its ratio tends to decrease sharply with increasing CN, implying that less GCCN become available under heavy loading conditions like dust storms [*Liu et al.*, 2011]. Having stated the roles of dust particles in serving as CCN, it is worth noting that dust has a very broad impact on global climate, ecosystems, human health, and agriculture, as recently reviewed by *Ravi et al.* [2011].

[16] The discussions above suggest that more CN leads to more cloud drops and less precipitation. Yet there are many examples showing that an increase in CCN does not lead to higher cloud water content or longer cloud lifetimes. For instance, *Ackerman et al.* [2004] demonstrated that the entrainment of overlying dry air above a deck of boundary layer stratocumulus cloud may result in a decrease in cloud water when the humidity of the overlying air is very low. Also, more and smaller cloud drops may enhance evaporation in the downdraft region of cloud edges, which leads to lower cloud fraction, cloud size, and cloud depth [*Teller and Levin*, 2006; *Xue and Feingold*, 2006]. A more detailed discussion on these effects is given in section 5.

[17] In cold clouds, such as the upper part of deep convective or high latitude clouds, CN's effects on cloud and precipitation are much more complicated than in warm clouds. Because of the Raoult effect of freezing point depression, soluble compounds tend to inhibit the freezing of liquid aerosols and cloud droplets and thus the formation of ice crystals. Yet liquid droplets normally cannot form without these soluble chemicals. So when the atmosphere is short of IN, the only viable way to form cloud ice is to freeze the water in aerosol particles or cloud drops. Such homogeneous nucleation occurs quite commonly in cirrus formed by slow lifting or in orographic wave flow at high altitudes where air temperature is generally below −40°C [*Heymsfield and Sabin*, 1989; *Heymsfield and Miloshevich*, 1993], as well as in the cirrus anvil generated in convective storms [*Knollenberg et al.*, 1993; *Heymsfield et al.*, 2005].

[18] Since N_C is largely controlled by N_{CN}, the number of ice crystals in such clouds is inevitably influenced by the amount of CN entering the clouds. Several model simulations showed that aerosols have strong influences on not only the microphysical structure but also the extent and lifetime of cirrus [*Chen et al.*, 1997; *Phillips et al.*, 2005; *van den Heever et al.*, 2006; *Carrió et al.*, 2007; *Ekman et al.*, 2007; *Fan et al.*, 2010a]. In regions where cloud drop freezing is slow (i.e., not all cloud drops can freeze), the number of cloud ice particles formed by cloud drop freezing depends not only on N_C but also on the cloud drop mass mixing ratio according to the classical nucleation theory. In this case, the number of cloud ice particles may increase with increasing N_{CN} due to the suppression of warm-rain processes, thus elevating cloud water content. But each cloud ice particle that formed would be smaller because of smaller cloud drop sizes. It is interesting to note that cloud ice particles with smaller initial sizes may not necessarily grow slower than larger ones due to the shape inertia effect [*Sheridan et al.*, 2009]. Another way to initiate cloud ice is by heterogeneous nucleation with the help of IN. Water may directly deposit onto IN as ice (called deposition nucleation) or as liquid and then freeze (called condensation-freezing nucleation). Such a process is very sensitive to ss_∞. As can be realized from equation (1), ss_∞ is strongly modulated by N_C and the size of cloud drops, so CN can influence ice nucleation indirectly through their effect on cloud drops.

[19] Besides nucleation, CN may also influence the growth of ice particles. When cloud ice crystals are first formed, they grow mainly by vapor deposition. The water vapor they need comes either from a continuous cooling of air by lifting or by the evaporation of cloud drops. The latter is called the Wegener-Bergeron-Findeisen (WBF) process, and this conversion from drops to ice is limited by the rate of cloud drop evaporation. With more cloud drops, the WBF conversion proceeds faster, so the deposition growth of cloud ice is influenced indirectly by CN.

[20] When cloud ice crystals are large enough, they can also grow by accreting cloud water, a process called riming. Just like the collision between cloud drops, the efficiency of riming is strongly dependent on the cloud particle size. Again, since cloud particle sizes are influenced by N_{CN}, so will the riming process. In general, the WBF process is enhanced but riming is suppressed with more CN. Therefore, the formation of snow, graupel, and hail, as well as the so-called cold rain that forms from their melting, is affected [*Khain et al.*, 2004; *van den Heever et al.*, 2006; *Tao et al.*, 2007; *Cheng et al.*, 2010]. The net outcome varies with the overall dynamic and thermodynamic structures of the clouds, as well as the availability of GCCN and IN. Note that all the CN effects on ice phase precipitation and cold-rain formation mentioned above are related to cloud particle size and number concentration. These effects can best be resolved in a model with binned microphysical schemes [e.g., *Khain et al.*, 2004; *Tao et al.*, 2007; *Morrison and Grabowski*, 2010] and, to some extent, by multimoment bulk microphysical schemes [e.g., *Feingold et al.*, 1994; *Morrison and Pinto*, 2005; *Cheng et al.*, 2007; *Li et al.*, 2008a; *Morrison and Grabowski*, 2008]. Single-moment bulk microphysical schemes are not suitable because they do not keep track of differing particle sizes or number concentrations.

2.3. Ice Nuclei Effect on Cold-Cloud Processes

[21] Cloud glaciation can be initiated by either homogeneous freezing, which requires very low temperatures, or by heterogeneous nucleation, which works at higher

temperatures with the aide of IN. The latter is considered very important to cloud physical processes, precipitation formation, and global radiation balances [*Pruppacher and Klett*, 1997; *Cantrell and Heymsfield*, 2005]. Just like CCN, the effect of IN on cloud microphysics comes mainly from their impact on the cloud ice number concentration, N_{CI}, which is particularly important in the mixed-phase zone of clouds where the balance between ice and liquid is sensitive to cloud ice number [*Korolev and Field*, 2008]. Because of insufficient knowledge about the particles that cause ice nucleation, mixed-phase zone processes are difficult to model [*Klein et al.*, 2009; *de Boer et al.*, 2010]. Nevertheless, relevant information about IN and ice nucleation rates is accumulating.

[22] The most common type of IN is probably mineral dust particles transported into the atmosphere by strong winds from bare lands, such as deserts, semiarid areas, agricultural uplands, and dry river beds. They have been implicated as possible atmospheric IN for over 50 years [*Isono et al.*, 1959]. More recently, emerging evidence has suggested that mineral particles may reach high into the upper troposphere where they serve as IN for cirrus cloud formation [*Heintzenberg et al.*, 1996; *Sassen*, 2002; *Sassen et al.*, 2003]. *DeMott et al.* [2003] detected IN concentrations up to 100 times higher than typical background values in and above the marine boundary layer in Florida during Saharan dust episodes. These IN were within the air layer that feeds thunderstorm development and subsequent cirrus anvil formation. Measurements of ice particle residuals from anvil cirrus [e.g., *Cziczo et al.*, 2004] and cloud model simulations [e.g., *van den Heever et al.*, 2006] all support the hypothesis that mineral dust modifies cloud microphysics and dynamics. Soot particles from anthropogenic or natural burning processes can also act as IN, but their ice nucleating efficiency is much weaker. Another source of IN are biological aerosols such as bacteria, pollen, fungi, spores, and even phytoplankton. These bioaerosols, especially some species of bacteria, are very efficient IN, but their number concentrations are generally low.

[23] IN may initiate ice formation via four different modes. Two were mentioned earlier: deposition nucleation and condensation-freezing nucleation, which are controlled mainly by supersaturation. IN may also cause cloud drops or raindrops to freeze by either immersion freezing or contact freezing, and temperature is their main controlling factor. Immersion freezing occurs when an ice nucleus enters a cloud drop (either by acting as a CCN or by collection inside the cloud) and keeps it unfrozen for some time, later initiating freezing when the air gets cold enough. Contact freezing occurs when an ice nucleus collides with a supercooled drop and immediately freezes. *Hoose et al.* [2010a] estimated that globally, immersion freezing by mineral dust is the dominant ice formation process, followed by immersion and contact freezing by soot. Ice formation from biological aerosols is significant only over certain areas over land (such as forests), where their concentrations are greater than anywhere else in the atmosphere.

[24] Similar to the activation of CN into cloud drops, not all IN can nucleate into cloud ice in a specific cloud environment. Two hypotheses have been offered to explain such a phenomenon. The "stochastic hypothesis" states that nucleation is a probabilistic and time-dependent process, i.e., only a portion of a specific kind of IN can be nucleated during a unit length of time, and the rate of nucleation depends on both particle properties and environmental conditions [cf. *Fletcher*, 1962; *Mason*, 1971]. A contrasting view is called the "singular hypothesis," which considers that nucleation is controlled by impurities or by the number of active sites on the surface of ice nuclei, where each site has a characteristic temperature (for freezing nucleation) or supersaturation (for deposition nucleation) [cf. *Dorsey*, 1948; *Vali and Stansbury*, 1966; *Fletcher*, 1969; *Vali*, 2008]. This means that singular nucleation is time-independent, so a particular kind of IN is nucleated all together once their threshold temperature or supersaturation is reached. Furthermore, ice nucleation occurring at different temperatures or supersaturations would imply the presence of different IN which can be of the same species and of the same size but possess different surface properties. More detailed discussions about these hypotheses are given by *Vali and Stansbury* [1966], *Vali* [2008], *Chen et al.* [2008], and *Niedermeier et al.* [2010].

[25] These two views of nucleation form the basis for the parameterization of ice nucleation from measurements and for use in cloud microphysical schemes. For example, IN concentrations (N_{IN}) in the atmosphere are often measured by sampling air in a cloud chamber and counting N_{CI} that form under a given temperature, pressure, and humidity. The measured N_{CI} are then used to represent N_{IN} by expressing it as a time-independent function of temperature or supersaturation [e.g., *Fletcher*, 1962; *Huffman*, 1973]. Note that such measurements usually cannot identify the type of IN so the functional dependence can be considered as empirical. There are also laboratory measurements of heterogeneous nucleation targeted on specific types of IN [e.g., *Yankofsky et al.*, 1981; *Diehl et al.*, 2001; *Archuleta et al.*, 2005; *Field et al.*, 2006; *Möhler et al.*, 2006]. Such results can be used in cloud microphysical models only when the types and size spectrum of IN are known or given. Empirical parameterization of heterogeneous nucleation according to the singular concept has been adopted in cloud microphysical schemes, such as the freezing parameterization from *DeMott et al.* [1998], condensation/deposition freezing from *Cooper* [1986] and *Meyers et al.* [1992], and nucleation in the contact mode from *Meyers et al.* [1992]. Examples of measurements and fitting functions for these ice nucleation modes are given in Figure 5. One can see in Figure 5b a large variability in IN concentration as well as in the inverse temperature dependence among data sets. The lack of general applicability in space and time is the main weakness of such empirical formulas. Note that the above N_{IN}-N_{CI} relationships have been converted into pseudorate equations by taking the rate change of temperature or supersaturation as the functional variable, such as that applied in the spectral bin models of

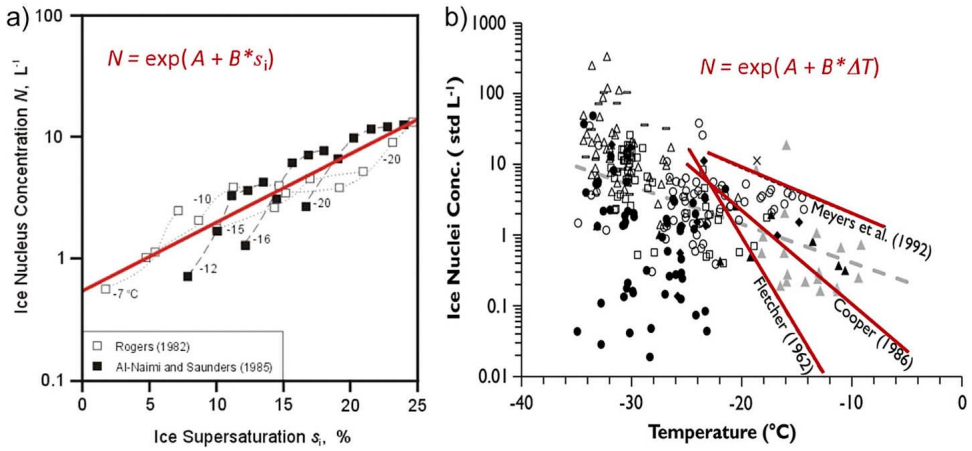

Figure 5. Ice nuclei concentration as functions of ice supersaturation or supercooling. (a) Deposition/condensation-freezing nucleation (adapted from http://www.ems.psu.edu/~lno/Meteo437/Icenucl1.jpg). (b) Immersion freezing (adapted from *DeMott et al.* [2010]). Various symbols represent different field measurements. The three solid red lines are parameterization from earlier studies, and the dashed gray line is a fitting to all data.

Chen and Lamb [1994] and *Khain et al.* [2000], so that the depletion of IN can be treated. The stochastic approach has also been adopted for interpreting measurement results and for application in regional microphysical schemes. For example, measurements of IN and their immersion freezing capability are often expressed as rate equations [e.g., *Bigg*, 1953; *DeMott*, 1990], which were used in several cloud schemes [e.g., *Reisin et al.*, 1998; *Diehl and Wurzler*, 2004; *de Boer et al.*, 2010; *Fan et al.*, 2010a, 2010b].

[26] The empirical type of ice nucleation parameterization is popular because it may be implemented without knowing IN types and even N_{IN}. These advantages are also the main weakness of such parameterizations because they cannot respond to the large spatial and temporal variations of natural IN species. The empirical treatment of IN is therefore one of the main uncertainties in current cloud microphysical simulations. Progress has been made toward the improvement of ice nucleation processes and their representation in cloud models. For example, many models have the capability of simulating the emission and transport of mineral dust particles and soot particles. A few recent efforts to simulate bacteria or other bioaerosols in the atmosphere have also been made [*Burrows et al.*, 2009; *Hoose et al.*, 2010a, 2010b]. New parameterizations of ice nucleating rates based on laboratory measurements are also emerging [e.g., *Marcolli et al.*, 2007; *Chen et al.*, 2008; *Fornea et al.*, 2009; *Kanji and Abbatt*, 2006; *Lüönd et al.*, 2010]. For example, *Chen et al.* [2008] presented a generalized parameterization that keeps the original mathematical form of the classical nucleation theory and includes thermodynamic parameters of the IN (i.e., contact angle and activation energy) derived from laboratory measurements. Furthermore, effects not considered in the measurements, such as solute or curvature effects on heterogeneous freezing, can be easily added by modifying the saturation vapor pressure in the classical nucleation rate formula with the Raoult or Kelvin equation. A comparison of such parameterizations against original measurements for several IN species is shown in Figure 6. Preliminary implementation of this parameterization has been done by *Hoose et al.* [2010b] to estimate the relative importance of different IN species on a global scale. Integration of such schemes into cloud microphysical models is likely to occur in the near future.

3. OBSERVATIONAL EVIDENCE OF PROCESSES AND MECHANISMS BEHIND THE AIE

[27] While various mechanisms have been proposed to describe how aerosols affect precipitation, they are essentially tied to two fundamental processes through which aerosols alter energy and water cycles and ultimately influence precipitation: scattering and absorption of solar radiation and

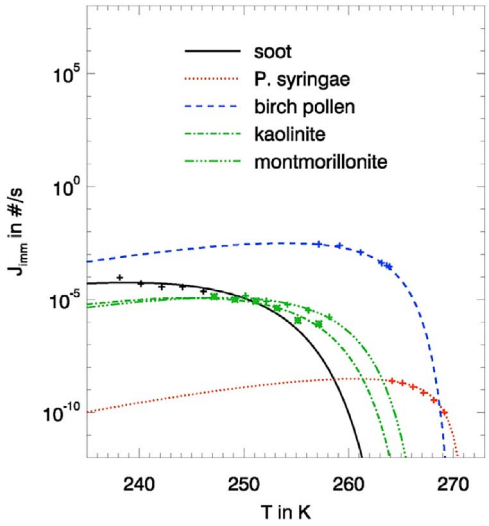

Figure 6. Immersion-freezing nucleation rate for a single ice nucleus as a function of temperature for individual particles. Symbols represent laboratory data, and curves are fittings following the parameterization method of *Chen et al.* [2008]. Adapted from *Hoose et al.* [2010a].

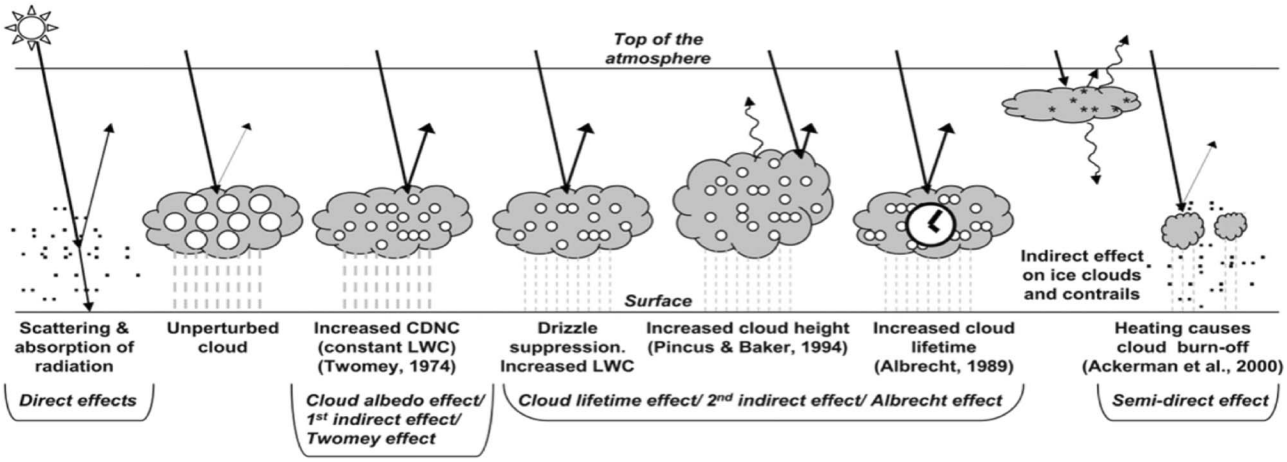

Figure 7. Various mechanisms proposed to explain how aerosols affect clouds and precipitation. Adapted from *Intergovernmental Panel on Climate Change* (*IPCC*) [2007].

serving as CCN or IN. Most, if not all, mechanisms proposed so far [e.g., *Intergovernmental Panel on Climate Change* (*IPCC*), 2007] can be traced either directly or indirectly to these fundamental processes but at different stages in a chain of actions, illustrated in Figure 7. Conversion of aerosol particles into CCN is the crux of the majority of the effects.

[28] Among the seven mechanisms illustrated in Figure 7, only the last one is linked to the radiative effect of aerosols, namely its absorption of solar radiation to burn off cloud droplets. All remaining mechanisms originate from the Twomey effect: increases in aerosol concentration leading to increases in cloud droplet number concentration (CDNC) for liquid clouds [*Twomey*, 1977]. For a fixed liquid water path, this leads to smaller cloud particle sizes and thus suppression of precipitation and prolonging of cloud lifetime [*Albrecht*, 1989]. The retention of liquid water to above the freezing level causes extra latent heat to invigorate the development of deep convective clouds and enhance precipitation [*Andreae et al.*, 2004; *Rosenfeld et al.*, 2008]. This invigoration effect may also increase cloud height. The aerosol effects on precipitation, cloud height, amount/liquid water path (LWP), and duration are lumped into a general term: the second aerosol indirect effect [*Albrecht*, 1989], which is much more complex than the first aerosol indirect effect.

[29] Comparing the latest IPCC report to earlier editions, the number of mechanisms governing aerosol-cloud-precipitation interactions has increased. For example, five mechanisms were described in the 2001 IPCC report [*IPCC*, 2001] and seven were presented in the 2007 report [*IPCC*, 2007]. These mechanisms are essentially contingent upon the series of constraints applied. By adding or changing constraints, one can, in principle, find more types of aerosol indirect effects. However, identifying them would become an increasingly more daunting task because these processes in nature are all coupled, although one may control them in a model. Many idealized coincidences are required to observe the AIE and to determine which hypothesized processes are behind it. In general, cloud and precipitation processes are dictated primarily by the dynamic and thermodynamic settings of the atmosphere and by cloud microphysics as well. Virtually all investigations concerning the AIE, especially observation-based ones, have been fraught with difficulties and uncertainties in removing or decoupling the influences of atmospheric dynamics and thermodynamics.

[30] To understand this, Figure 8 illustrates the major processes occurring in an atmospheric column. From the viewpoint of observation studies, we have snapshots of atmospheric variables (e.g., aerosols, clouds, and precipitation) in a column, and we try to relate them as a measure of the AIE. For satellite remote sensing, aerosols below clouds are obscured by the clouds themselves. Clouds and precipitation at any point in a spatial-temporal domain result from all processes taking place over a much larger domain. Other influential factors need to be taken into account in order to isolate and quantify aerosol effects on precipitation. For example, advection may move a cloud from outside to inside of the domain under study, and convection linking aerosols with locally generated clouds may occur. Vertical motion associated with convection supplies moisture that dictates the growth from cloud droplets to raindrops. The essence of

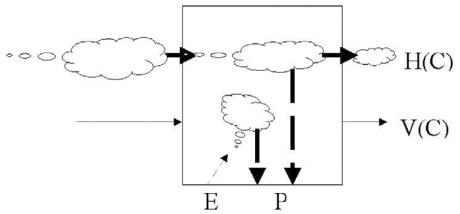

Figure 8. A schematic of the water budget for vertically integrated water vapor and cloud hydrometeors. H and V denote divergence and convergence of cloud water and water vapor, respectively. P and E stand for precipitation and evaporation, respectively. The dash and solid downward arrows represent precipitation from advective and convective clouds.

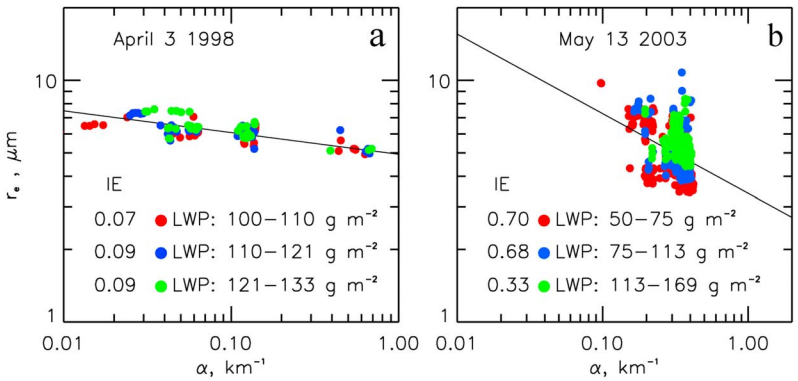

Figure 9. Cloud droplet effective radius (DER) estimated from a combination of ground-based remote sensing instruments (multifilter rotating shadowband radiometer (MFRSR) and microwave radiometer) and aerosol extinction coefficient near the cloud base from a lidar at the Atmospheric Radiation Measurement (ARM) Southern Great Plains (SGP) central facility site. Adapted from *Feingold et al.* [2003, 2006].

studying the AIE is to establish relationships between newly generated and/or the new growth of existing hydrometers with local aerosols. For stratiform clouds associated with large-scale atmospheric features such as frontal systems, local aerosols would have little to no bearing on clouds and precipitation. For convective clouds, the relationship would be closer.

[31] Despite the complex interaction between meteorological systems and aerosols, with adequate measurements and sound approaches, it is still possible to reveal the AIE by identifying favorable conditions, i.e., enhancing "signals" and suppressing "noise." Selection and study of dramatic events whose effects on clouds and precipitation exceed those exerted by other factors, such as ship tracks [*Ferek et al.*, 2000; *Coakley et al.*, 2000], fire smoke [*Kaufman and Fraser*, 1997; *Rosenfeld*, 1999; *Koren et al.*, 2004; *Andreae et al.*, 2004], heavy air pollution [*Rosenfeld*, 2000], and dust storms [*Rosenfeld et al.*, 2001], can help in this pursuit. Another kind of approach would be to track complete aerosol episodes or cycles during which aerosol loading goes up and down, as does the associated cycle of changes in cloud microphysics (e.g., effective radius) [*Schwartz et al.*, 2002; *Feingold et al.*, 2003]. A third approach is to use a large ensemble of cases to try to suppress or filter out the influences of fast atmospheric dynamics in order to single out the effects of aerosols, which are essentially partial derivatives of cloud/precipitation with respect to changes in aerosol properties under the same meteorological setting (in an ensemble sense). This is illustrated using long-term ground data [*Li et al.*, 2011a] and global satellite data [e.g., *Nakajima et al.*, 2001; *Niu and Li*, 2011].

3.1. Impact on Cloud Droplet Size Distributions and Warm-Rain Processes

[32] As stated above, the driving mechanism for the majority of other aerosol effects on clouds is the first aerosol indirect effect: the decrease in cloud droplet size with increasing aerosol number concentration for a fixed liquid water path (LWP) [*Squires*, 1958; *Twomey*, 1977]. Cloud albedo is enhanced in a cloud with constant LWP because there are a greater number of small cloud particles whose sum of cross sections is larger and thus reflect more radiation than fewer but larger droplets [*Twomey*, 1977]. This effect has been supported by ample evidence from satellite remote sensing [*Han et al.*, 1994; *Wetzel and Stowe*, 1999; *Nakajima et al.*, 2001; *Liu et al.*, 2003]. Satellites collect a multitude of aerosol measurements over the entire globe more readily than in situ or ground-based instruments. However, they suffer from several inherent retrieval problems (see *Z. Li et al.* [2009] for recent reviews of the satellite retrieval of aerosol parameters), such as difficulties in separating real effects from false ones [*Yuan et al.*, 2008]. There is also the inherent limitation that cloud and aerosol properties cannot be obtained at the same time over the same location. The majority of previous studies used large-scale data, which are described in more detail in section 4. Within a sufficiently large spatial and temporal domain, clear and cloudy scenes can be found but at different times and/or different locations. Given the large-scale variation in aerosols, significant uncertainties can be incurred due to both data mismatch and small-scale changes in cloud properties.

[33] These limitations can be overcome, or lessened, by ground and in situ observations [*Leaitch et al.*, 1996; *Feingold et al.*, 2003; *Penner et al.*, 2004]. Nevertheless, a large range of variation (by a factor of 3 or more) was found concerning the sensitivity of cloud microphysics to aerosols, as measured by the ratio of the change in cloud particle size to aerosol parameters. While some of the differences are related to the use of different analysis methods and/or observational data [*Rosenfeld and Feingold*, 2003], a large natural variation is often encountered [*Feingold et al.*, 2003; *Kim et al.*, 2003; *Yuan et al.*, 2008]. Figure 9 shows changes in cloud droplet size with aerosol extinction coefficient, a measure of aerosols' indirect effect, from ground-based measurements collected at the Atmospheric Radiation Measurement (ARM) Southern Great Plains (SGP) central facility site [*Feingold et al.*, 2003, 2006]. It is seen that the method is valid for a small range of variation in LWP and a large range of variation in aerosol loading (Figure 9a) but invalid under the opposite condition (Figure 9b).

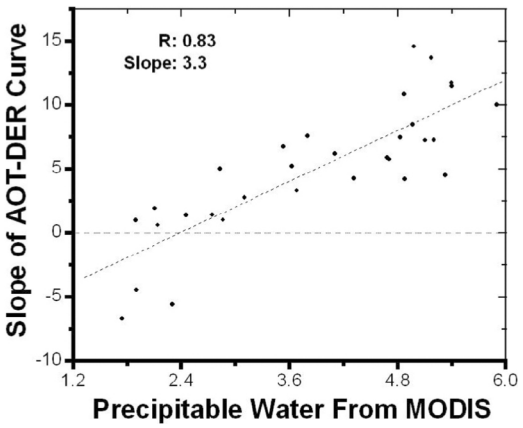

Figure 10. Dependence of the slope of regression between cloud DER and aerosol optical depth (AOD) aerosol indirect effect (AIE) on precipitable water (cm m^{-2}) over the southeastern United States from the Gulf of Mexico to inland. The correlation coefficient (R) and slope between these two quantities are given. Adapted from *Yuan et al.* [2008].

[34] The vast majority of previous studies showed a negative dependence of cloud particle size on aerosol loading. However, some satellite-based studies show a positive relationship [*Sekiguchi et al.*, 2003; *Storelvmo et al.*, 2006]. *Yuan et al.* [2008] conducted an extensive study that examined the relationship between cloud droplet effective radius (DER) and aerosol optical depth (AOD) for a large number of convective cloud scenes acquired around the world by the Moderate Resolution Imaging Spectroradiometer (MODIS) on board the Terra satellite. While inverse relationships between cloud particle size and aerosol loading for different types of aerosols predominated over most of the world, exceptional positive relationships were found in two regions: the Gulf of Mexico and the South China coast during summer when the atmospheric environment over both regions is predominantly influenced by monsoon circulations that blow moist air from oceans to polluted inland areas. The slope of the regression between cloud droplet size and AOD changes systematically from negative to positive with increasing precipitable water, as shown in Figure 10. This is partly because droplets have no great need to compete for water vapor in order to grow, thanks to the ample influx of water vapor from the Gulf of Mexico associated with the prevailing Bermuda high-pressure system in the summertime.

[35] Aerosols alter warm-rain processes by changing cloud microphysics and the LWP. Enhanced aerosol concentrations are generally believed to suppress warm-rain processes by enabling the formation of small cloud droplets and a narrow droplet spectrum; both inhibit collision and coalescence processes [e.g., *Squires and Twomey*, 1966; *Warner and Twomey*, 1967; *Warner*, 1968; *Radke et al.*, 1989; *Rosenfeld*, 1999; *Liu et al.*, 2003].

[36] A combination of cloud top temperatures and effective droplet sizes, estimated from the advanced very high resolution radiometer (AVHRR), has been used to infer the suppression of coalescence and precipitation processes for smoke [*Rosenfeld and Lensky*, 1998] and desert dust [*Rosenfeld et al.*, 2001]. Analysis of satellite observations indicated that, on average, both naturally transported and local anthropogenic dust aerosols can significantly reduce cloud water particle size, optical depth, and liquid water path [*Huang et al.*, 2006a, 2006b, 2010]. These results suggest that dust aerosols warm up clouds and increase evaporation of cloud droplets, further reducing cloud water path via the so-called semidirect effect. Such semidirect effects may play an important role in cloud development and act to exacerbate drought conditions over semiarid areas of northwestern China [*Huang et al.*, 2006a, 2006b, 2010].

[37] It should be pointed out that the above finding, as well as those from all previous satellite-based studies of the AIE, was based on retrievals of cloud droplet size at the cloud top only because the radiometric signal at mid-IR channels saturates rapidly [*Platnick*, 2000; *Chang and Li*, 2002]. Cloud top cloud droplet size is driven by many factors, such as atmospheric stability, available water vapor, and cloud thickness. For adiabatic processes, cloud droplet size increases linearly with cloud top height, which is further linked to potential energy [*Rogers and Yau*, 1989]. Linear cloud droplet size profiles can be retrieved using multiple IR channels of varying absorption strength [*Chang and Li*, 2002, 2003]. *Matsui et al.* [2004] employed column-mean cloud droplet sizes derived from microwave-based retrievals of LWP and cloud optical depth (COD) and showed a negative correlation between these cloud droplet sizes and the aerosol index (AI). They also investigated the impact of the lower tropospheric static stability (LTSS) on the AIE using observational data. *Chen et al.* [2007] found systematic biases in the retrieval of LWP when using the conventional visible-IR approach, which casts a doubt on the use of optical remote sensing products alone to investigate the AIE. Sensitive to column amount, microwave-based LWP retrievals are somewhat more accurate.

[38] It should be stated that an increase in cloud droplet size does not necessarily lead to an increase in precipitation; that is, the first indirect effect is not a necessary cause for an increase in precipitation, nor does it lead to it. Precipitation is controlled by many factors that are dynamical, thermodynamical, and microphysical in nature.

3.2. Impact on Ice and Mixed-Phase Clouds: Aerosol Invigoration Effect

[39] While most research into aerosol effects on clouds has focused on low-lying stratiform clouds, some investigators have noted possible aerosol effects on cirrus clouds as well [e.g., *Sassen et al.*, 1995; *Ström and Ohlsson*, 1998]. However, the findings are much less conclusive. *Sherwood* [2002] analyzed changes in ice particle effective radius at the top of tropical cumulonimbus clouds (using data from the International Satellite Cloud Climatology Project) with respect to the aerosol index from the Total Ozone Mapping Spectrometer (TOMS) and found that the two quantities were negatively correlated. They attributed this to the smaller size of water droplets that were frozen and lifted to high altitudes by the deep convective cloud system. *Chýlek et al.* [2006], however, found the opposite trend using

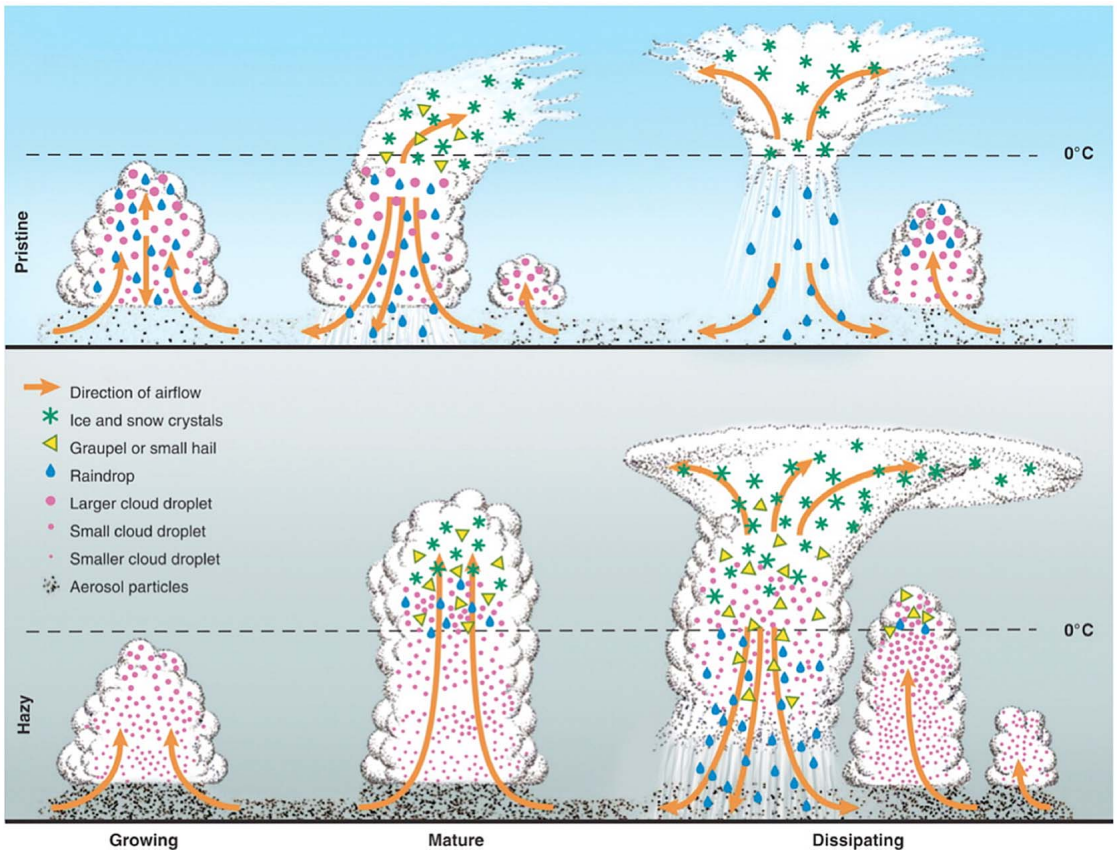

Figure 11. Schematic illustrating the aerosol invigoration effect. The plots correspond to (top) clean and (bottom) dirty environments. Adapted from *Rosenfeld et al.* [2008]. Copyright AAAS. Reprinted with permission.

MODIS data over the Indian Ocean during winter. Over the same region, *Massie et al.* [2007] found little change in ice particle size with increase in aerosol loading. By combining MODIS ice cloud particle size, Aura carbon monoxide content (a proxy of aerosols), and TRMM precipitation, *Jiang et al.* [2008] found that the influence of aerosols on ice clouds is contingent upon moisture content, which is somewhat similar to the finding of *Yuan et al.* [2008] for warm clouds. In a dry environment, aerosols tend to reduce ice crystal size and suppress precipitation; they have little impact on ice crystal size and precipitation in a wet environment. On the basis of this finding, ice particle effective size was parameterized as a function of ice water content and aerosol optical depth for different geographic regions [*Jiang et al.*, 2011].

[40] TRMM data were used to infer the presence of nonprecipitating supercooled liquid water near the cloud top due to over-seeding from smoke over Indonesia [*Rosenfeld*, 1999] and urban pollution over Australia [*Rosenfeld*, 2000]. Aircraft measurements have also provided evidence of sustained supercooled liquid water (down to −37.5°C) in continental mixed-phase convective clouds [*Rosenfeld and Woodley*, 2000]. These findings further suggest that continental aerosols reduce the mean size of cloud droplets, suppressing coalescence and warm-rain processes, permitting more freezing of cloud droplets and associated latent heat release above the 0°C isotherm, and enhancing the growth of large hail and cold-rain processes [*Rosenfeld and Woodley*, 2000]. This is now known as the aerosol invigoration effect [*Andreae et al.*, 2004, *Rosenfeld et al.*, 2008]. Figure 11 illustrates the effect for two deep convective cloud systems that developed under clean and dirty atmospheric conditions. Owing to the aerosol invigoration effect, the cloud in a dirty atmosphere tends to grow higher and becomes a stronger thunderstorm than it would under cleaner atmospheric conditions.

[41] *Andreae et al.* [2004] analyzed in situ observations made during the LBA-SMOCC campaign. They found that increases in smoke and surface heat due to biomass burning tend to lead to higher cloud top heights and the enhancement of cold-rain processes over the Amazon basin. This is shown in Figure 12 with in situ measurements made over the Amazon and Thailand. The "blue" and "green" cases in Figure 12 represent clean clouds over the ocean and the Amazon, respectively. The two "pyro" cases are the most extreme forms of smoky clouds. All other cases except for the two "Thai" cases are clouds with moderate concentrations of smoke. Substantial differences in the cloud drop size, D_L, are evident. Observations made in Thailand on 2 May 1998 show that cloud bases had to exceed 6400 m to produce warm rain under smoky conditions. Once these clouds extended above the freezing level, they become quite

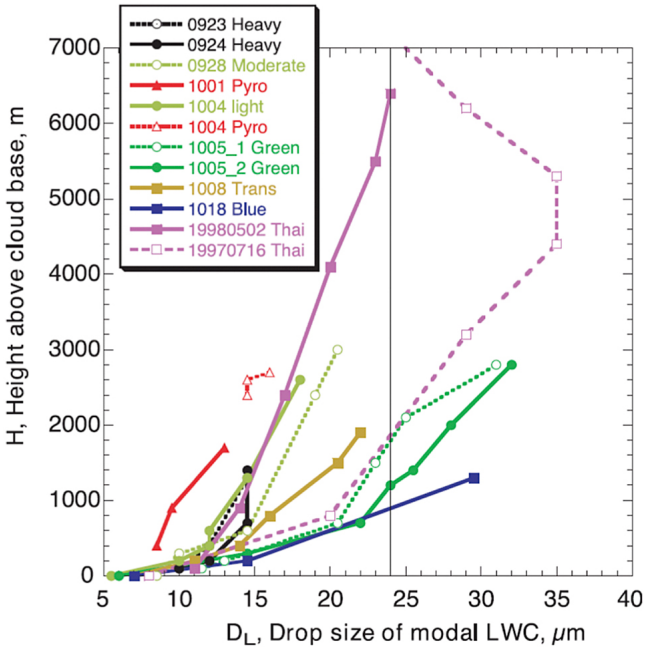

Figure 12. The dependence of cloud drop diameter (x axis) on distance above cloud base (y axis) for different regimes. The vertical line at $D_L = 24$ μm denotes the onset of warm rain. Adapted from *Andreae et al.* [2004]. Copyright AAAS. Reprinted with permission.

vigorous with intense showers, thunderstorms, and sometimes hail events. These observations indicate that the shift of the onset of precipitation to a higher level under polluted conditions leads to enhanced formation of ice hydrometers and more vigorous convection. *Koren et al.* [2005] examined cloud properties derived from the MODIS and found strong evidence that aerosols from pollution, desert dust, and biomass burning systematically invigorate convective clouds over the Atlantic Ocean. A theoretical explanation for such an effect is given by *Rosenfeld et al.* [2008] using a parcel model to demonstrate the buoyancy changes in four scenarios (see Figure 13): (1) suppressing rainfall and keeping all condensed water, without freezing; (2) precipitating all condensed water, without freezing; (3) precipitating all condensates, with freezing at $T < -4$°C; (4) suppressing precipitation until $T = -4$°C, and then freezing and precipitating all condensed water above that temperature. Their model results suggest the importance of cloud height and phase in determining if aerosols invigorate cloud development and its strength, and if they suppress or enhance precipitation.

[42] Both aerosol microphysical and invigoration effects were confirmed through use of a long-term (10 year) set of data acquired under the U.S. Department of Energy's Atmospheric Radiation Measurement (ARM) program [*Li et al.*, 2011b]. The extensive and high-quality set of aerosol, cloud, and meteorological measurements helped reveal unprecedented strong "climate" signals of aerosols' impact on clouds and precipitation and provided a valuable means of sorting out various influential factors and mechanisms. As seen in Figure 14a, aerosol invigoration occurs only for mixed-phase clouds with warm bases (>15°C) and cold tops (<−4°C). Mean cloud top heights (from averaging all single-layer cloud top heights found over the 10 years of data analyzed) increase systematically and significantly with increasing concentrations of condensation nuclei (CN) as measured from the ground. No such effect is observed for pure liquid clouds or for ice clouds. As CN (measured before any precipitation occurs) increases, the frequencies of light and heavy rains decrease (suppression) and increase (enhancement), respectively, as shown in Figure 14b. The finding of opposite roles played by aerosols in modulating rain has major scientific and social implications because it suggests that increases in aerosol pollution could make moist regions or seasons wetter and arid regions or seasons drier.

[43] The location of clouds in the atmosphere has a role in determining the nature of the invigoration effect. If the cloud base is high, for example, very close to the freezing level, there will not be very much liquid water to release latent heat because the distance for cloud particles to grow before reaching the freezing level is too short. Yet a switch in opposite effects of aerosols on the frequency of clouds occurs for clouds with tops below and above the mean freezing level (around 3.3 km), as determined from ARM's multiple sensors [*Li et al.*, 2011a]. The freezing level is thus a key factor whose height can be determined with a newly proposed method using passive satellite imaging data like those from MODIS [*Yuan et al.*, 2010]. At present, a complete picture of cloud geometry can be obtained for most

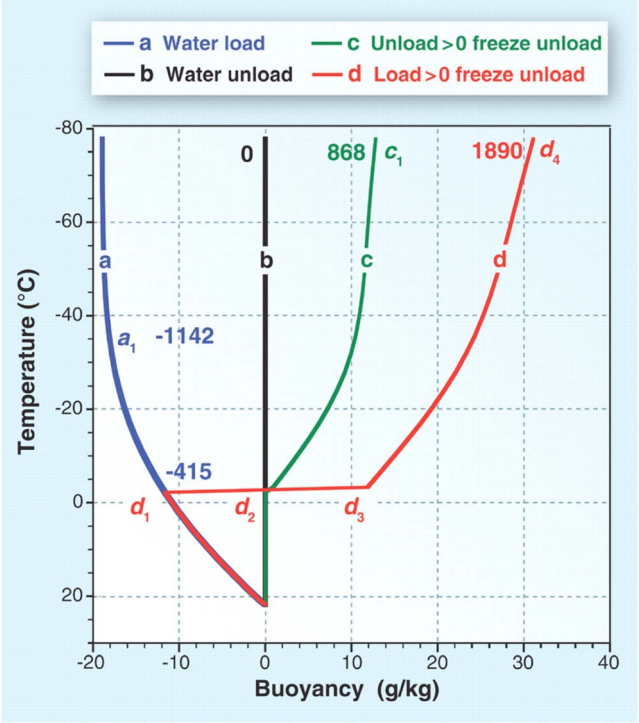

Figure 13. Buoyancy of an unmixed adiabatically rising air parcel. Numbers near the lines show the released static energy (in J kg^{-1}). Adapted from *Rosenfeld et al.* [2008]. Copyright AAAS. Reprinted with permission.

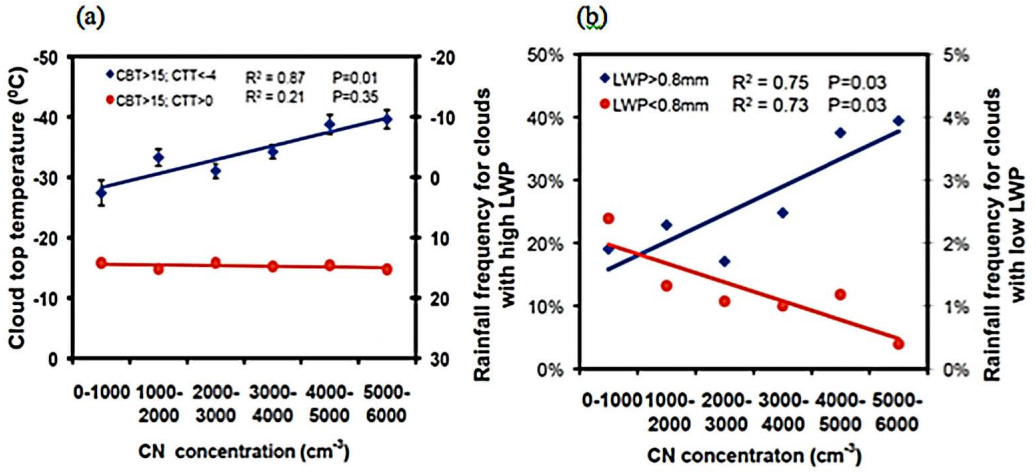

Figure 14. Responses of (a) cloud top temperature and (b) precipitation frequency to increases in aerosol number concentration (CN) measured at the SGP central facility site over a period of 10 years. Clouds are differentiated by cloud top temperature (CTT), bottom temperature (CBT), and rainfall amount. Adapted from *Li et al.* [2011a].

clouds, except for really thick clouds, using ground-based and spaceborne active sensors [*Clothiaux et al.*, 2000; *Stephens et al.*, 2002; *Mace and Benson*, 2008]. Data from the MODIS multichannel passive sensor, though, were used successfully to identify single- and dual-layer clouds of thin cirrus above water clouds which account for the majority of the world's clouds [*Chang and Li*, 2005]. Historical high-resolution radiosonde data could also be used to reconstruct cloud geometry at sounding station sites [*Zhang et al.*, 2010]. Such a potentially rich source of information has yet to be developed and exploited for studying the AIE.

[44] The invigoration effect is driven by latent heat release, which is rooted to the first indirect effect. This effect, in turn, further depends on aerosol hygroscopic properties, which may be collectively referred to as the aerosol microphysical effect. For absorbing aerosols like smoke, the thermodynamics of the atmosphere can be altered through heating of the aerosol-laden atmosphere and cooling of the surface. This enhances atmospheric stability and reduces the moisture content due to evaporation [*Ackerman et al.*, 2000], thus inhibiting the formation of clouds and precipitation. For smoke aerosols that have the capability of serving as CCN, the two competing effects lead to boomerang-shaped responses of cloud top height and cloud fraction as theorized and confirmed by *Koren et al.* [2008] over the Amazon region (Figure 15).

3.3. Impact of Aerosols From Urbanization on Thunderstorms and Lightning

[45] As the major emission source of anthropogenic aerosols, urban areas may disturb the atmospheric environment enough so that the regional climate is modified. There are two types of major disturbances: land cover changes and atmospheric emissions. The latter includes both aerosols and greenhouse gases. The greenhouse effect generally has a much larger spatial and long-term impact than the aerosol effect. Aerosol and land cover changes can leave strong footprints, but it is a nontrivial task to separate the effects of these two changes.

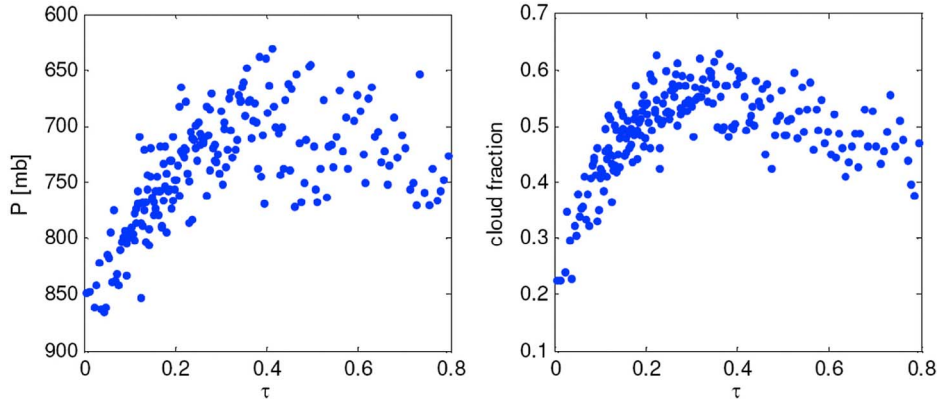

Figure 15. Cloud top pressure and cloud fraction as a function of aerosol optical depth obtained over the Amazon during the dry season of 2005. Adapted from *Koren et al.* [2008].

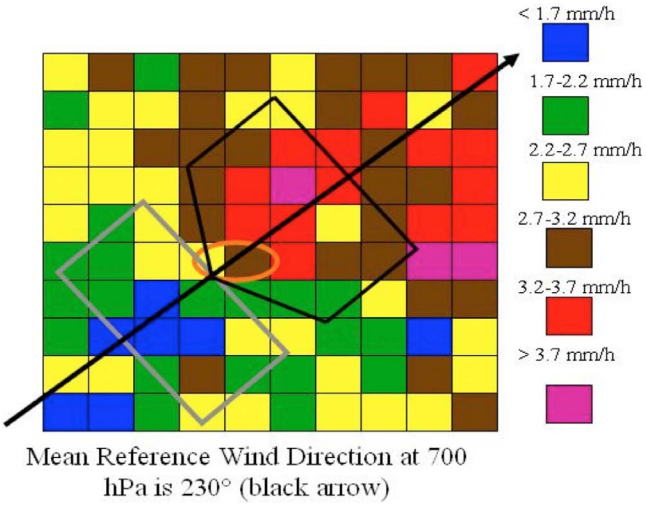

Figure 16. Spatial distribution of mean rain rate in the Houston, Texas, metropolitan and surrounding areas with the mean prevailing wind vector at 700 hPa. Adapted from *Shepherd and Burian* [2003].

[46] Enhancement of rainfall downstream of some major metropolitan areas has been documented for a long time, such as in Chicago [*Changnon et al.*, 1981], Tokyo [*Ohashi and Kida*, 2002], Houston [*Shepherd and Burian*, 2003] (see Figure 16), and New York City [*Jin et al.*, 2005]. High aerosol concentrations in urban environments could affect precipitation variability by providing an enhanced source of CCN. Hypotheses were made to explain the effect of urban regions on convection and precipitation [*van den Heever and Cotton*, 2007; *Shepherd*, 2005]. It is unclear if the urban heat island effect or the aerosol effect, or both, causes the enhancement. With the theory of aerosol invigoration, we may now take a new look at this phenomenon. Heavily polluted cities are an ideal setting for inducing and enhancing invigorated clouds, especially cities near lakes and along coastlines in summertime. During this season, warm moist air can blow from seas or lakes to land, providing the following conditions favorable to cloud invigoration: (1) a plentiful supply of highly hygroscopic anthropogenic aerosols, (2) the heat island effect which fuels convection, and (3) moist hot air that can provide large amounts of potential energy to sustain strong convection.

[47] This seems to corroborate the finding of a midweek anomaly in precipitation and convection, and intensified lightning over urban areas. Using long-term integrated TRMM-derived precipitation data, *Bell et al.* [2008] found a significant midweek increase in summertime afternoon thunderstorms over the aerosol-laden southeastern United States, which coincides with a midweek increase in ground-measured aerosol concentration, wind convergence at 1000 hPa and divergence at 300 hPa, and vertical velocity at 500 hPa (see Figure 17). These coincidental findings are consistent with the notion that aerosols have a major impact on the dynamics of continental mixed-phase convective clouds [*Rosenfeld and Woodley*, 2000; *Williams et al.*, 2002].

[48] Enhancement of the lightning flash density was found to be centered over and downwind of a metropolitan area [*Orville et al.*, 2001], as shown in Figure 18. Possible causes include enhanced convergence associated with the urban heat island effect and altered microphysical processes associated with anthropogenic pollution. *Steiger and Orville* [2003] compared 14 years' worth of cloud-ground flash density distributions with the locations of PM10 (particulate matter less than 10 μm in diameter) sources in Louisiana. They concluded that pollution plays a key role in lightning enhancement, while urban and sea breeze effects are negligible. *Yuan et al.* [2011] examined 2005 lightning data from the lightning-imaging sensor on board the TRMM satellite and MODIS AOD (Figure 19). They found anomalously high lightning activity in the presence of high aerosol loading, which was traced to volcanic activity; no connection was found with any anomalies in meteorology. They further quantified the response of lightening to AOD: A ~60% increase in aerosol loading leads to a more than 150% increase in lightning flashes. Aerosols could influence lightning activity through modification of cloud microphysics. Cloud ice particle sizes are reduced and cloud glaciation is delayed to colder temperatures when aerosol loading is increased. Despite the seemingly convincing evidence linking aerosols with

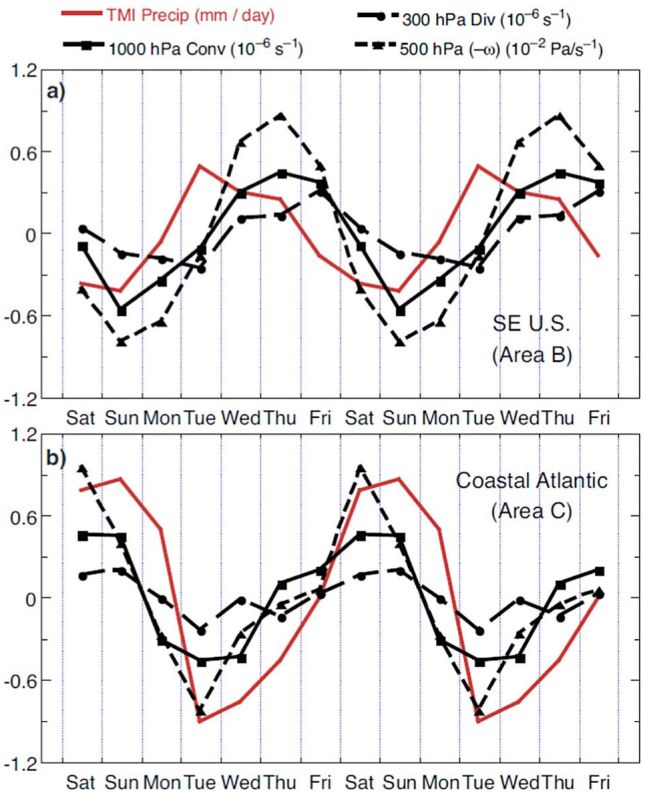

Figure 17. Weekly cycles of precipitation, 1000 mbar convergence, 300 mbar divergence, and 500 mbar vertical wind from National Centers for Environmental Prediction (NCEP2) reanalysis over the southeastern United States and the coastal Atlantic during the summers of 1998–2005. Adapted from *Bell et al.* [2008].

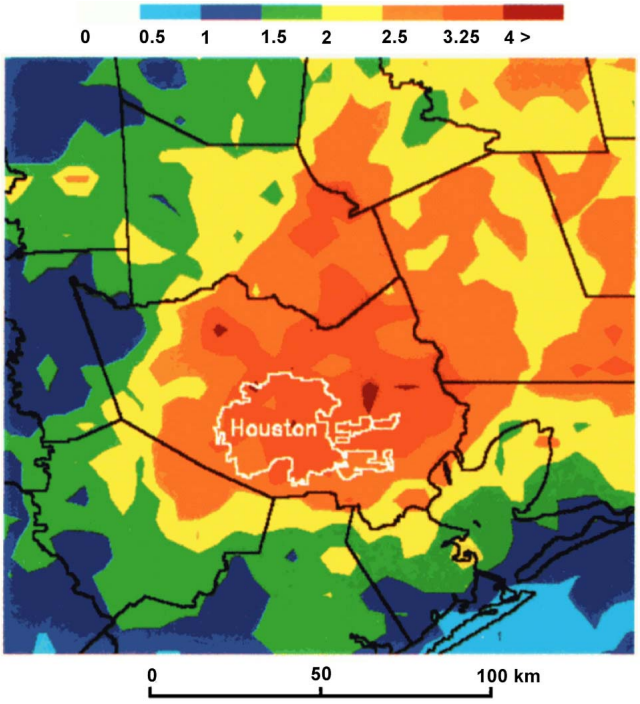

Figure 18. The 12 year summer (June, July, and August) flash density in flashes per square kilometer from 1989 through 2000 at Houston, Texas. Adapted from *Orville et al.* [2001].

lightning activity, their real connection is far more complex, especially in light of many other influential factors associated with urban regions, as demonstrated by simulations with a state-of-the-art land surface model and a cloud-resolving model (see section 5 and *van den Heever and Cotton* [2007]).

4. LARGE-SCALE OBSERVATIONAL DIAGNOSTICS OF THE AEROSOL EFFECT ON PRECIPITATION

[49] In general, a main purpose of large-scale observational analyses of aerosol-precipitation relationships is to reveal statistically significant signals that may suggest influences on the large-scale distribution and variability of precipitation by radiation and/or CCN effects of aerosol. This is different from the analyses discussed in section 3 that seek physical processes governing the AIE. On large scales (especially the global scale), total precipitation is constrained by the moisture budget, which is mainly dictated by surface evaporation. Unless aerosol effects alter surface evaporation, they may modify only the timing and location of precipitation but not its total amount. A local signal of aerosol effects on precipitation is usually a manifestation of such changes in timing and location of precipitation.

4.1. Isolating Aerosol Effects

[50] Large-scale observational analyses of aerosol effects on precipitation face no less of a challenge than the theoretical, modeling, and field observational approaches discussed elsewhere in this review. All large-scale observational studies must adequately address issues of data quality, analysis methods, robustness of the results (i.e., statistical significance), and causality. The issue of causality manifests itself in observational studies of aerosol effects on precipitation in two problems: aerosol effects on precipitation versus precipitation effect on aerosols (i.e., rainout and washout), and effects on precipitation by other meteorological factors covarying with aerosol.

[51] The simplest way to remove the rainout/washout effect on aerosol and cloud contamination from an aerosol-precipitation analysis is to avoid relationships between coincidental measurements of aerosol and precipitation. Aerosols upwind can be included in an analysis based on back-trajectory calculations [*Hui et al.*, 2008; *Huang et al.*, 2009b]. An equivalent approach is to include time lags with aerosol signals leading precipitation [*Lau and Kim*, 2006; *Bollasina and Nigam*, 2009]. Another method is to exclude aerosol data near cloud scenes or within a grid box with a large cloud fraction [*Koren et al.*, 2010a]. In a target precipitation area that is remote from aerosol sources,

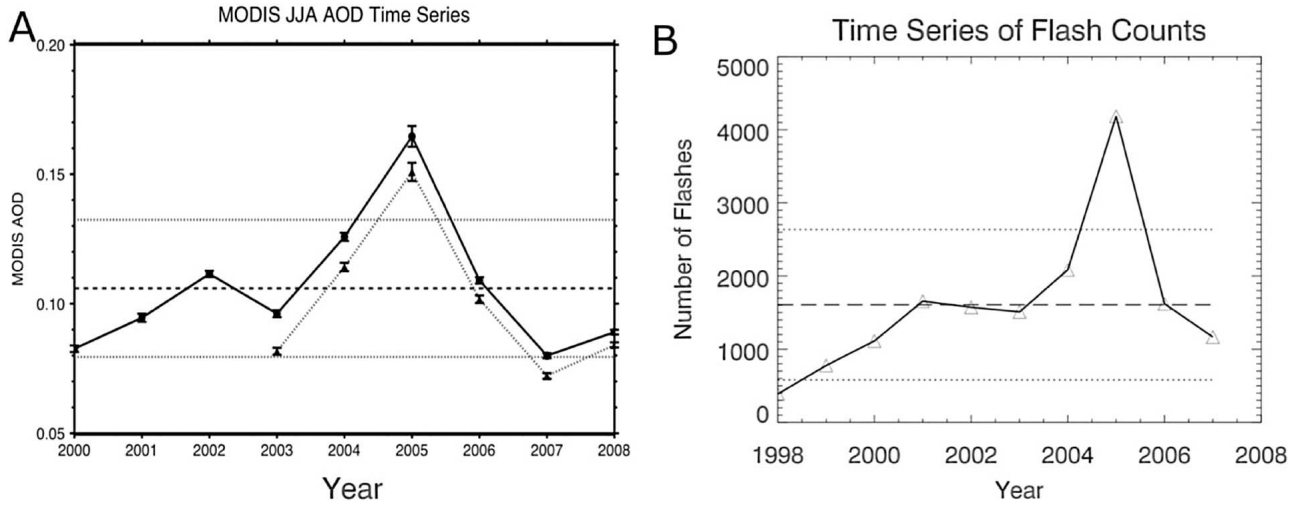

Figure 19. Time series of Moderate Resolution Imaging Spectroradiometer (MODIS) AOD and flash counts from 2000 to 2008 over the western Pacific Ocean east of the Philippines. Adapted from *Yuan et al.* [2011].

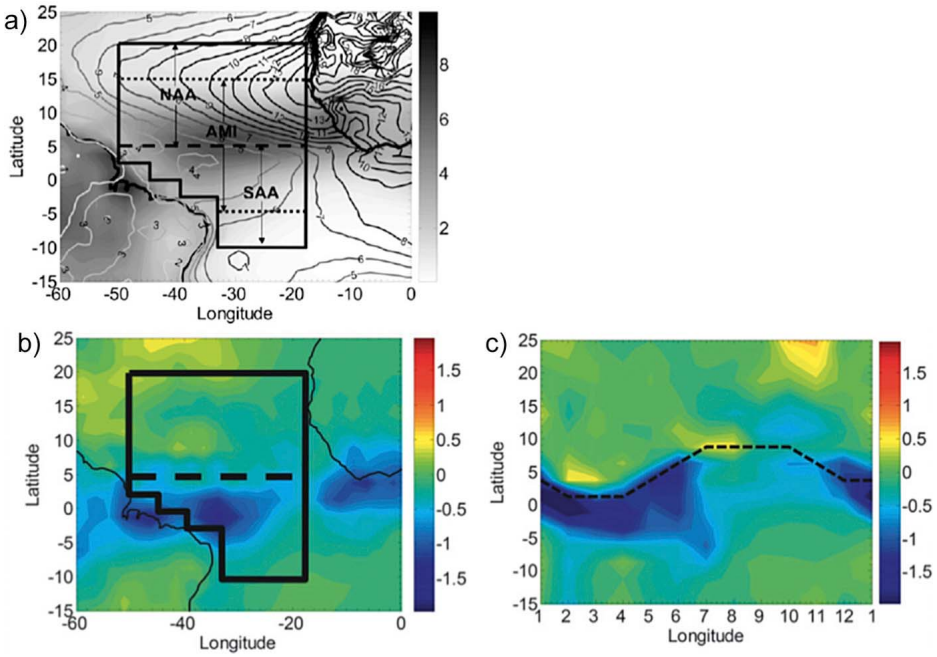

Figure 20. (a) Analysis domains from *Huang et al.* [2009b]. Aerosol variability was estimated within the Atlantic aerosol domain (AA, solid boundaries) and the two subdomains separated at 5°N (dashed line): NAA to the north and SAA to the south. Precipitation variability was calculated within the Atlantic marine Intertropical Convergence Zone (ITCZ) domain (Atlantic marine ITCZ (AMI), centered at the dashed line at 5°N and bounded to the north and south by dotted lines at 15°N and 5°S). Shades are for climatological mean precipitation (mm d^{-1}) and contours for Total Ozone Mapping Spectrometer (TOMS) mean aerosol index. (b) Annual mean difference in precipitation (mm d^{-1}) between the top and bottom tercile months of TOMS aerosol indices within the AA domain. (c) Seasonal cycle of difference in precipitation (mm d^{-1}) between the top and bottom tercile months of TOMS aerosol indices averaged over the latitude of the AA domain. Adapted from *Huang et al.* [2009b].

fluctuations in aerosols independent of precipitation should be the same as those outside and upwind of the precipitation region. On the basis of this, *Huang et al.* [2009, 2009a] used aerosols averaged over a large domain containing rainbands over the tropical Atlantic Ocean and West African monsoon region and broad areas of no precipitation to represent large-scale fluctuations in aerosols in the rainband regions (Figure 20a).

[52] Several methods have been used in previous studies to isolate the aerosol effect on precipitation from other effects. One is to examine the variability of other factors (e.g., water vapor) that may potentially cause fluctuations in precipitation. Observed aerosol-precipitation covariability might indicate aerosol effects on precipitation only if the observed precipitation variability is not coherent with these other factors. The following examples illustrate some approaches that have been applied attempting to isolate aerosol effects on precipitation from other effects.

[53] *Qian et al.* [2009] observed a decreasing trend in light rain (<10 mm d^{-1}) and an increasing trend in heavy rain (>50 mm d^{-1}) over East China from 1956 to 2005. This is the same period of large increases in pollution in the same part of China (Figure 21), although their trends are not the same nor are they monotonic. No correlation was found between decreasing trends in light rain with water vapor transport as deduced from a global reanalysis product. This led the authors to rule out the possibility that the trend in light rain was caused by changes in large-scale meteorological conditions. They subsequently conjectured that the increase in aerosols due to pollution observed during the same period was the likely cause of the observed decreasing trend in light rain through the known suppressing effect of aerosols that shifted the rain distribution from light to heavy. They did not, however, discuss whether the change in the total amount of water corresponding to the observed trend in light rain over the time period in question is within the uncertainties of the water vapor transport data.

[54] *Wilcox et al.* [2010] observed a northward shift of rainfall in the Intertropical Convergence Zone (ITCZ) over the tropical Atlantic Ocean during African dust outbreaks. They examined differences in temperature profiles and lower tropospheric zonal wind between African dust outbreaks and low dust conditions. They postulated that the northward shift of rainfall was caused by lower tropospheric warming attributable to advection of the warm Saharan air layer (SAL), enhanced subtropical subsidence, and radiative heating of dust.

[55] Similarly, *Lau and Kim* [2006] compared composites and lag regressions of aerosols, wind, temperature, and precipitation over the Indian summer monsoon region. They proposed an "elevated heat pump" hypothesis, namely, that anomalously high concentrations of absorbing aerosols

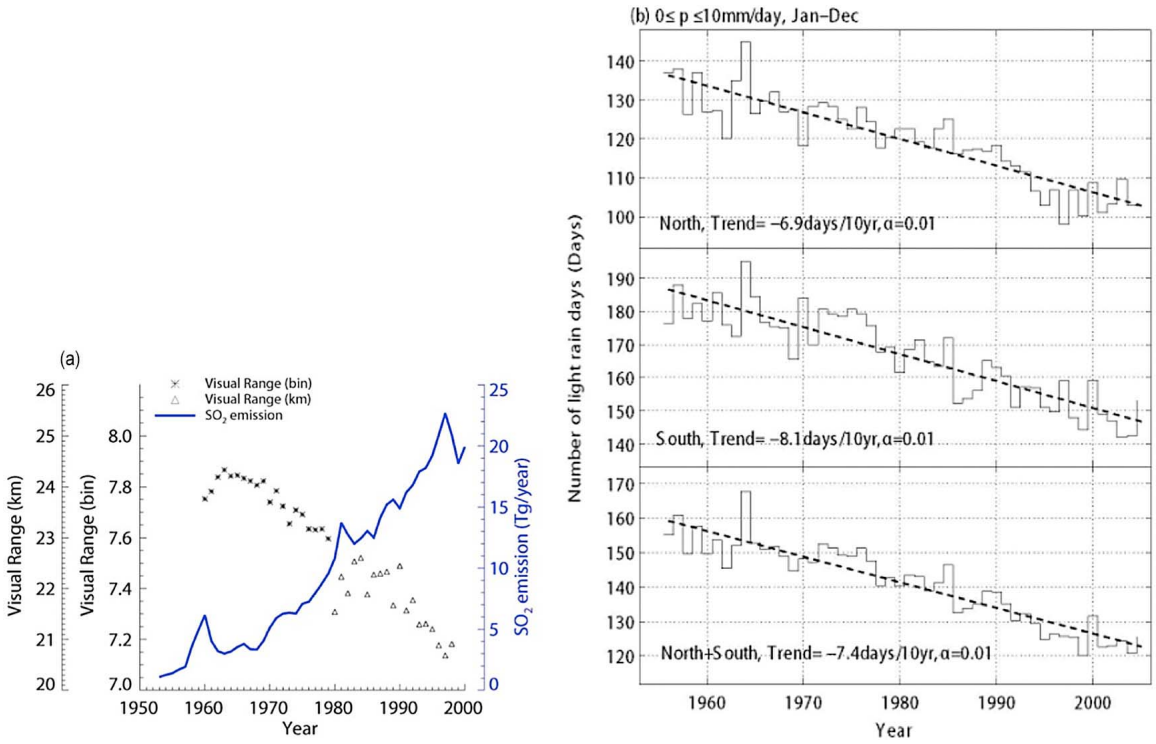

Figure 21. (a) Time series of China total SO_2 emission (Tg a^{-1}) for 1953–2000 and corrected visual range (bin before 1980 and km after 1980) over East China for 1960–2000. (b) Time series of number of days of light rain (less than 10 mm d^{-1}) from 1956 to 2005 over northern East China, southern East China, and all of East China (days). Adapted from *Qian et al.* [2009].

during the premonsoon season are associated with anomalous warming that is responsible for changes in the large-scale circulation leading to an increase in monsoon rainfall over India. In the work of both *Lau and Kim* [2006] and *Wilcox et al.* [2010], possible contributions of aerosols to the observed variability of rainfall were compared to but not separated from other factors. Therefore, their hypothesis is plausible but not without ambiguity, even though the observed signals are consistent with those numerical simulations (see section 6), where the attribution of changes to specific physical processes is much clearer. The same sets of observations have been subject to different interpretations and result in contradictory conclusions [*Nigam and Bollasina*, 2010].

[56] The importance of examining the covariability between aerosols, precipitation, and other factors has been explicitly explored. In a study of the rainfall trend over Israel, *Alpert et al.* [2008] pointed out that urban dynamics (e.g., the heat island effect), if not fully taken into consideration, may lead to erroneous interpretations of data and to the incorrect conclusion that an observed decreasing rainfall trend is due to the suppression effect of increasing urban pollution from upwind regions. By comparing submonthly evolution patterns of aerosols, precipitation, and other meteorological variables during the premonsoon period over South Asia, *Bollasina and Nigam* [2009] reproduced the earlier monthly observations [*Bollasina et al.*, 2008] and showed that anomalous aerosol buildup in May can delay the onset of monsoon rainfall due to the aerosol radiative effect (i.e., cooling of the land surface). But they acknowledged that the pervasive influence of advection precludes a robust analysis of the aerosol impact.

[57] Various statistical tools have been used either to remove the dependency of precipitation on other factors before its relationship with aerosols is established or to determine the importance of different factors to observed variability in precipitation so that the role of aerosols versus others can be determined. The following are examples of studies that used these tools.

[58] In an attempt to identify the aerosol effect on rainfall over the Amazon basin during the biomass burning season (September 2006), *Jones and Christopher* [2010] applied the principle component analysis (PCA) method, a commonly used statistical tool in geosciences. This method encompassed precipitation and 23 other parameters including meteorological environmental variables (winds, humidity, and temperature), cloud information (optical thickness, top pressure, liquid water path, fraction, and droplet effective radius), aerosol optical thickness, and locations. They interpreted the weighting of each parameter and its sign relative to precipitation in each principle component (PC) as a signal of the potential physical connection between the two. On the basis of this interpretation, they found that atmospheric environmental variables (e.g., zonal wind, relative humidity, lapse rate, and vertical motion) are the dominant factors for rainfall variability, with the largest weighting for the first principal component (PC1) which explains 25% of total rainfall variance. Following the same argument, they

identified the radiative effect of aerosols as the second most important factor for rainfall, which is represented by the second principal component (PC2) that explains 15% of total rainfall variance. Their results suggest a suppressing effect of smoke on rainfall. The orthogonality requirement for each PC may, however, obscure the physics intended to be disclosed.

[59] In a study of the aerosol effect on precipitation over the tropical Atlantic Ocean and in the West African monsoon region, *Huang et al.* [2009, 2009a, 2009c] used a multivariable linear regression method to remove the variability in aerosols and precipitation that is coherent with water vapor and sea surface temperature (SST) related to known climate modes (e.g., El Niño–Southern Oscillation (ENSO), North American Oscillation (NAO), and Tropical Atlantic Variability (TAV)). The resulting anomalous time series of aerosols and precipitation are considered linearly independent of other weather and climate factors. They then compared the spatial distribution and seasonal cycle in anomalous precipitation between months of high versus low aerosol anomalies (top and bottom terciles of all months) averaged over a large domain (Figure 20a). The comparison revealed decreases in precipitation during months of high aerosol anomalies at the southern edge of the rainbands during boreal winter, the season of frequent biomass burning over equatorial and southern Africa (Figures 20b and 20c). The spatial pattern and the seasonal cycle of the rainfall reduction do not match those of expected aerosol wet deposition. Numerical simulations with only the radiative effect of black carbon aerosol included have reproduced this observation (see section 6). They concluded that the reduction in rainfall is due to the radiative effect of smoke from biomass burning. The linear regression can only account for simultaneous relationships. So the removal of the coherent variability between precipitation and other factors may not be complete.

[60] A highly recommended method of isolating the aerosol effect from other effects is to examine aerosol-precipitation relationships in different regimes [*Stevens and Feingold*, 2009]. Regimes can be defined in various ways depending on data and analysis targets. They include convective characteristics (e.g., cloud working function; see below), environmental conditions for cloud (e.g., static stability), or cloud microphysics (e.g., LWP, ice path), as demonstrated in the following examples.

[61] In a study of the aerosol effect on rainfall during the biomass burning seasons (August–October of 2000 and 2003) in the Amazon, *Lin et al.* [2006] examined relationships between aerosol optical depth versus precipitation and clouds stratified by bins of cloud working function (CWF). CWF is defined as a vertical integration of work by buoyancy per unit mass flux, or the kinetic energy generation per unit mass flux [*Arakawa and Schubert*, 1974]. Instigation of convection in some numerical models is determined by the CWF passing a given threshold. CWF was used in this study to define regimes of the large-scale meteorological forcing for rainfall and convection. The CWF-stratified analysis indicates that elevated AOD was associated with increases in precipitation, occurrence of intense rainfall events, cloud cover, cloud top height, water path, and formation of ice. This is in contrast to the result from *Jones and Christopher* [2010] discussed above.

[62] *Sorooshian et al.* [2009] proposed to stratify the environmental effect in terms of LWP in a concept of precipitation susceptibility, which is defined as $S = -d\ln R/d\ln N_d$, where R is the precipitation rate and N_d is the CDNC or a subcloud N_{CCN} proxy. Using satellite data, a cloud parcel model and large eddy simulations, they demonstrated different vulnerabilities of precipitation to aerosols in three regimes: (1) low LWP, where clouds do not precipitate and are relatively insensitive to N_d, (2) intermediate LWP, where precipitation forms by interaction of cloud drops and is progressively more effectively suppressed by increasing N_d, and (3) high LWP, where susceptibility begins to decrease because there is ample LWP to drive the precipitation process. To remove ambiguity in whether the microphysical response is a result of a change in aerosols or a change in meteorological conditions (e.g., available liquid water), *Sorooshian et al.* [2010] further proposed to separate the precipitation susceptibility into two parts: $S_r = -(\partial\ln R/\partial\ln r)(\partial\ln r/\partial\ln N_d)$ and $S_\tau = -(\partial\ln R/\partial\ln\tau)\ (\partial\ln\tau/\partial\ln N_d)$, where r is the cloud droplet effective radius and τ is the cloud optical depth. They concluded that this separation provided more confidence in the results from the original precipitation susceptibility.

[63] *Panicker et al.* [2010] calculated the aerosol indirect effect, AIE = $d\ln r/d\ln t$ [*Feingold et al.*, 2003], for July and September 2001–2004 in four Indian summer monsoon regions. Similar to *Yuan et al.* [2008], they used MODIS AOD data for the fine mode fraction (FMF), cloud liquid water path (CLWP), cloud ice path (CIP), cloud ice radius (CIR), and cloud water radius (CWR). They used binned CLWP and CIP to define regimes. They found a positive AIE (the Twomey effect) for fixed CLWP and CIP in years when the monsoon rainfall was below normal, but a negative AIE (the anti-Twomey effect) in years of normal and above-normal rainfall. They suggested that the AIE depends on large-scale circulation patterns that may advect different types of aerosols from different sources. As pointed out earlier, ambiguity in the aerosol effect on precipitation on the seasonal time scale could be reduced by a careful water budget analysis.

[64] From the above discussion, it is obvious that each approach for isolating the aerosol effect on precipitation from other factors has it pros and cons. Large-scale diagnostics of the aerosol effect on precipitation, through either radiation or CCN changes or both, are incomplete without considering microphysics (clouds, aerosols, and precipitation), mesoscale cloud dynamics, and the large-scale background environment (aerosol transport, water budget). This requires unprecedented collaboration and coordination among subdisciplines within the atmospheric science field.

4.2. Applications of Satellite Data in Revealing ACPI

[65] A unique advantage of satellite data is their global coverage (in comparison to in situ observations). Observational evidence has been obtained from satellite data

TABLE 2. Statistical Relationships Between Cloud Parameters and Warm Rain for January and July 2008[a]

	Raining Threshold		Optimal HSS		Correlation	
	January	July	January	July	January	July
DER[b] (μm)	18.369	19.450	0.172	0.236	0.088	0.161
TAU	16.887	16.973	0.463	0.400	0.363	0.448
LWP[c] (mm)	0.187	0.180	0.524	0.500	0.434	0.530
T (°C)	10.280	11.180	0.055	0.071	0.009	−0.060

[a]HSS is the Heidke skill score. Only raining cloud samples are used to calculate the correlation coefficients. Adapted from *Chen et al.* [2011].
[b]Droplet effective radius.
[c]Liquid water path.

following somewhat different approaches from those based on other types of data as discussed earlier and large-scale models as discussed later in this review. Satellite observations can be used to effectively remove high-frequency weather variability and isolate signals of the AIE, as previously demonstrated [*Han et al.*, 1998; *Wetzel and Stowe*, 1999; *Nakajima et al.*, 2001; *Liu et al.*, 2003]. The advent of multiple advanced Earth Observations System (EOS) sensors aboard the A-Train [e.g., *Koren et al.*, 2008; *L'Ecuyer et al.*, 2009; *Niu and Li*, 2011] has substantially increased this capability. The most tangible and direct evidence of the AIE is linked to the microphysical properties of clouds, which are more readily measured by satellite observations despite various retrieval uncertainties and limitations [*Z. Li et al.*, 2009].

[66] Among a handful of microphysical variables retrievable from satellites (DER, LWP, COD), LWP plays the most significant role in precipitation [*Sorooshian et al.*, 2009; *Chen et al.*, 2011], even though these variables are not independent. Using matched rainfall data from CloudSat and cloud microphysics from MODIS aboard the A-Train, *Chen et al.* [2011] examined the predictability of rainfall from warm clouds. They found that LWP is by far the dominant factor, followed by DER and COD, as illustrated by the prediction skills in Table 2. As such, detection of any effects of aerosols on precipitation may begin with their effects on these key cloud variables.

[67] Given the dominant influence of LWP (or its primary proxy, COD) on precipitation, it is critical to understand whether and how aerosols change LWP, which is much more difficult than deducing the effect of aerosols on DER. Contrasting findings have been reported showing positive relationships [*Sekiguchi et al.*, 2003; *Storelvmo et al.*, 2006; *L'Ecuyer et al.*, 2009], negative relationships [*Twohy et al.*, 2005; *Matsui et al.*, 2006; *Brenguier et al.*, 2000], or mixed results [*Nakajima et al.*, 2001; *Coakley and Walsh*, 2002; *Han et al.*, 2002; *Kaufman et al.*, 2005]. Several mechanisms have been postulated. The enhancement of entrainment and droplet evaporation by aerosols reduces LWP [*Ackerman et al.*, 2004], whereas suppression of coalescence inhibits precipitation and thereby increases LWP [*Lebsock et al.*, 2008]. On the other hand, the scavenging effect of drizzle can remove aerosols, leading to a seemingly

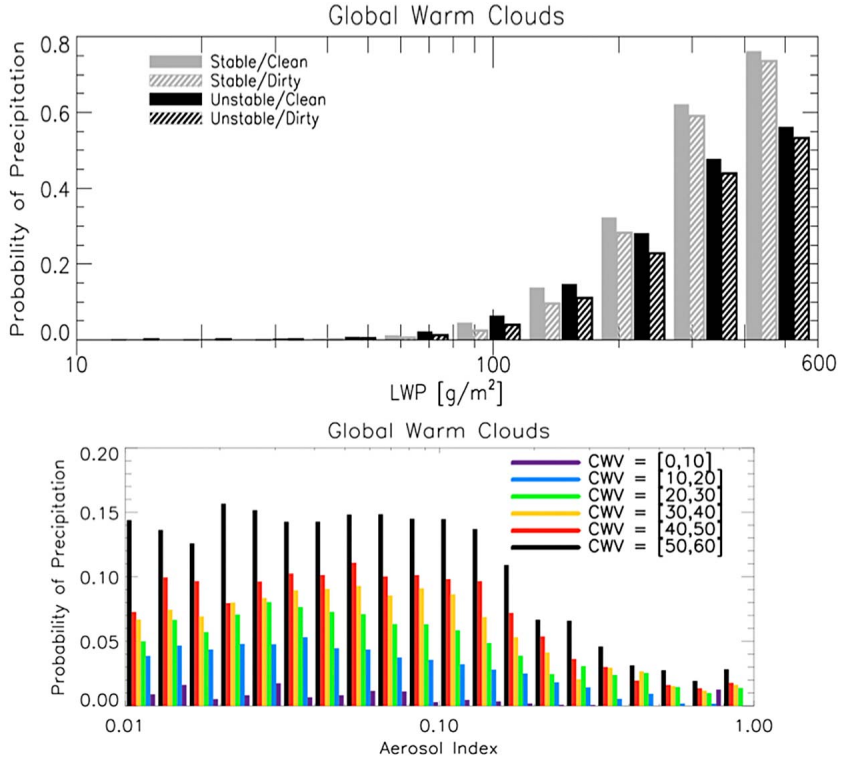

Figure 22. Changes in precipitation rate with (top) liquid water path (LWP) under different conditions of atmospheric stability and (bottom) aerosol index for different column water vapor (CWV) contents. The data were extracted from multiple A-Train sensors and reanalysis. Adapted from *Lebsock et al.* [2008].

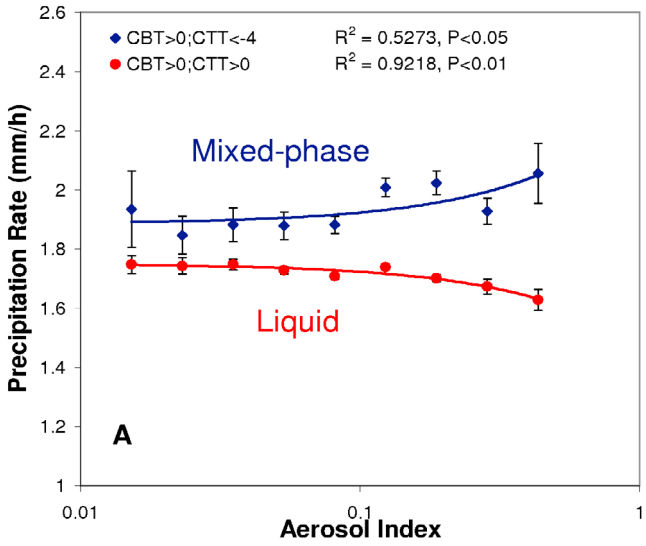

Figure 23. Variation of precipitation rate with aerosol index over the tropical oceans from CloudSat and MODIS satellite products for warm liquid clouds with cloud base temperatures (CBT) and cloud top temperatures (CTT) above 0°C and mixed-phase clouds with CTT below −4°C. Adapted from *Niu and Li* [2011].

negative relationship that undermines any real causal relation [*Twohy et al.*, 2005].

[68] Taking advantage of the unprecedented superior quality and quantities of A-Train sensors [*Stephens et al.*, 2002], thorough investigations of the AIE on warm clouds have been conducted under a wide range of conditions on a global scale [*Lebsock et al.*, 2008; *Berg et al.*, 2008; *L'Ecuyer et al.*, 2009; *Sorooshian et al.*, 2009; *Niu and Li*, 2011]. *Lebsock et al.* [2008] and *L'Ecuyer et al.* [2009] attempted to sort out various factors influencing warm rain or drizzle using a combination of precipitation data from CloudSat, cloud microphysics from MODIS, LWP and column water vapor (CWV) from Advanced Microwave Scanning Radiometer-EOS (AMSR-E), meteorological variables from a global reanalysis product, and a global aerosol transport model (distributions of aerosol species in both cloudy/raining and clear-sky scenes). As shown in Figure 22, the probability of precipitation increases with increasing LWP and CWV, and is moderately affected by atmospheric stability. For the same LWP, CWV, and stability, dirty clouds are less likely to rain than clean clouds. Not all types of aerosol particles inhibit precipitation. One exception is sea salt aerosols, because a large portion of them are within the GCCN size range and thus may serve as rain embryos (see section 2).

[69] Analyzing MODIS aerosol products (optical depth over land and aerosol index over oceans) for the entire global tropics (between 20°N and 20°S) where convective clouds are more dominant than at the middle to high latitudes, *Niu and Li* [2011] found distinct patterns of changes in precipitation rate with aerosol index for warm and mixed-phase clouds, as shown in Figure 23. Light rain associated with warm clouds occurs less frequently with increasing AI, whereas it increases with AI for mixed-phase clouds. This finding corroborates ground-based findings of *Li et al.* [2011a]. Both support the theories of aerosol microphysical effect and invigoration effect, namely, aerosols significantly invigorate convection through ice processes, while precipitation from liquid clouds is suppressed due to competition for limited water. It is worth noting that CloudSat is particularly good at detecting drizzle but not as capable of detecting moderate to heavier rainfalls due to its high-frequency (95 GHz) radar. This is remedied by the TRMM satellite. It carries two rain sensors: the TRMM Microwave Imager (TMI) and the Precipitation Radar (PR) at 35 GHz with sensitivities to different rain attributes. The TMI is most sensitive to LWP, while the PR is sensitive to large drops. By virtue of these differences in sensitivity, *Berg et al.* [2006, 2008] discovered a region where the largest discrepancies between the two sets of rain estimates was found, which was construed as a smoking gun of the strongest AIE on precipitation. It is located around the coast of East Asia and the western Pacific (Figure 24), the outlet of pollutants and dust from the world's most populated region. While continental-scale transport can bring some aerosols generated over Europe and Asia to this region [*Chin et al.*, 2004], local emissions are by far the largest source of aerosols, as shown by extensive measurements of aerosol optical, physical, and chemical properties collected during two major field experiments conducted in China [e.g., *Li et al.*, 2007, 2011b]. Using the 2008 intensive field campaign data acquired by the ARM Mobile Facility in southeastern China [*Li et al.*, 2011b], *Fan et al.* [2012] confirmed the significant role played by aerosols on precipitation. This was corroborated indirectly by the analysis of *Qian et al.* [2009].

5. CLOUD-RESOLVING MODEL SIMULATIONS

[70] The statistics of precipitating mesoscale convective cloud systems (MCS) have been quantified from space in terms of its correlation with rainfall estimated from the TRMM precipitation radar and microwave imager retrievals. Figure 25 shows that MCSs are the dominant heavy-rain producers in the tropics and subtropics; they generate more than 50% of rainfall in most regions. The global average annual rainfall exceeds 3 mm d^{-1} and up to 90% of the rainfall occurs over certain continental areas, e.g., the La Plata Basin of South America. Here we review mainly cloud resolving model (CRM) simulations associated with MCSs to examine the sensitivity of precipitation processes (rainfall) to aerosol concentrations. Other cloud-scale modeling simulations (including large-eddy simulations) associated with warm clouds, stratocumulus, orographic clouds, and Arctic stratus clouds are given by *Levin and Cotton* [2009].

5.1. Major Methodology

5.1.1. Cloud-Resolving Model

[71] One of the most promising methods to test the representation of cloud processes used in climate models is to use observations together with CRMs (see a recent review

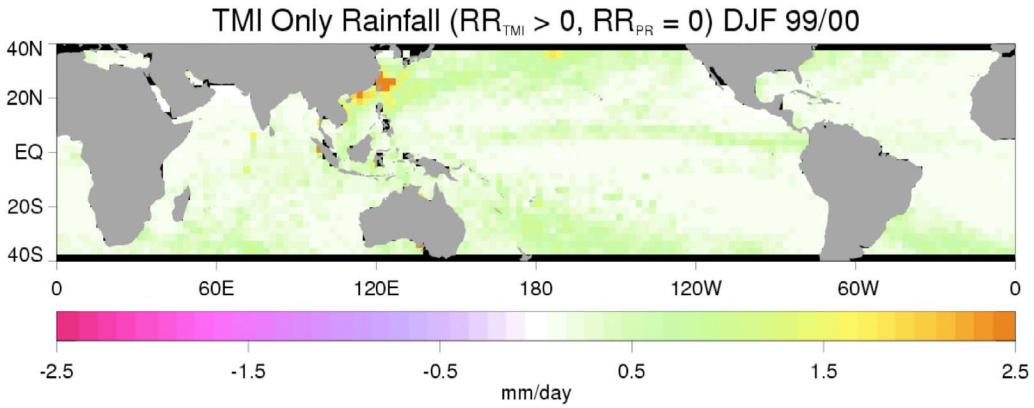

Figure 24. Rainfall estimates from the Tropical Rainfall Measuring Mission (TRMM) Microwave Imager (TMI) only when no rainfall was detected from the Precipitation Radar (PR) aboard TMMM. Adapted from *Berg et al.* [2006].

by *Tao and Moncrieff* [2009]). The CRM has to be nonhydrostatic, and its flow can either filter out (anelastic) [*Ogura and Phillips*, 1962] or allow (compressible) [*Klemp and Wilhelmson*, 1978] the presence of sound waves. Sound waves are not important in thermal convection, but their presence can place severe restrictions on the time step in numerical integrations. For this reason, most CRMs use an anelastic system of equations in which sound waves have been removed by neglecting the local variation of air density with time in the mass continuity equation. A three-dimensional diagnostic (elliptic) pressure equation can be solved using direct (e.g., Fourier transform) or iterative methods. In the compressible system, a very small time step (e.g., 2 s for a 1000 m spatial resolution) is needed for time integration due to the presence of sound waves. However, *Klemp and Wilhelmson* [1978] developed a semi-implicit time-splitting scheme, in which the equations are split into sound wave and gravity wave components to achieve computational efficiency. One advantage of the compressible system is that its numerical code remains a set of explicit prognostic equations, and adjustments due to factors such as surface terrain can be incorporated into the numerical model without complicating the solution procedure.

[72] Compared to typical global circulation and climate models, CRMs use more sophisticated and relatively realistic representations of cloud microphysical processes, and they can reasonably well resolve the structure and life cycles of clouds and cloud systems (with sizes ranging from about 2 to 1000 km). CRMs also allow for explicit interactions between clouds, outgoing longwave (cooling) and incoming solar (heating) radiation, as well as ocean and land surface processes (see reviews by *Tao* [2003, 2007] and *Tao and Moncrieff* [2009]). Observational data are required to initialize CRMs and to validate their results. *Browning et al.* [1993] and *Randall et al.* [2003] recommended that improved CRMs be used as a test bed to develop and evaluate cloud parameterizations in large-scale models.

[73] There are several major advantages in using CRMs to study the interactive processes between clouds, precipitation, and aerosols. For example, the use of a fully explicit microphysics scheme (liquid and ice) and a fine horizontal resolution can provide relatively realistic cloud optical

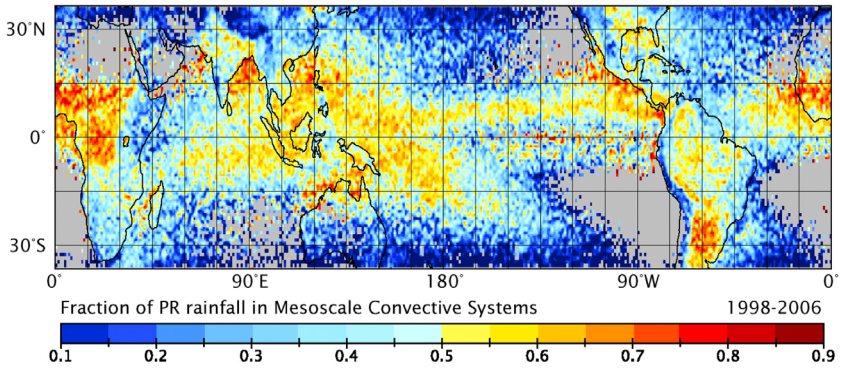

Figure 25. Fraction of estimated rainfall from precipitation features ≥100 km in maximum dimension as measured by the TRMM PR from January 1998 through December 2006. Mesoscale convective systems (MCSs) are shown to be the dominant rainfall producer in the most heavily raining areas of the tropics and subtropics. Adapted from *Nesbitt et al.* [2006].

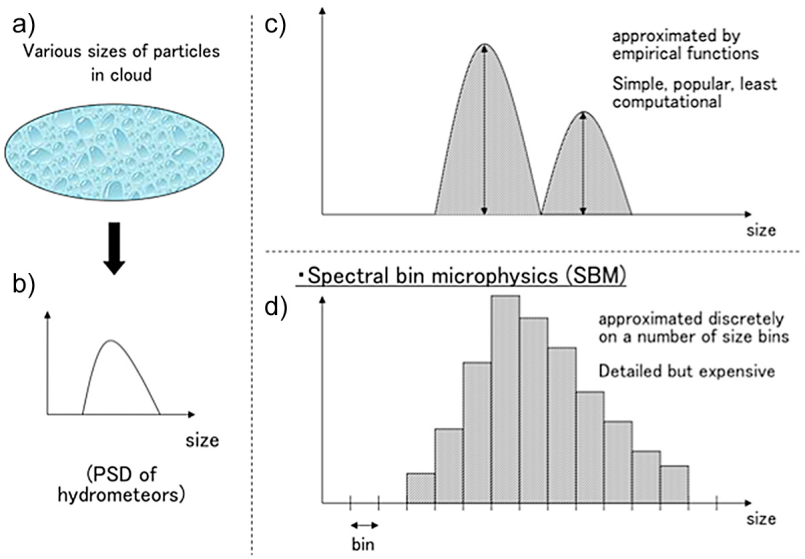

Figure 26. (a) Particles in clouds have various sizes. (b) They can be arranged in the form of particle size distribution (PSD). In general, two microphysical approaches are used to represent PSD numerically: a bulk microphysics and a spectral bin microphysics. In the framework of bulk microphysics, an analytical distribution function is assumed to give a form of PSD, and the model prognosticates the integrated variables such as (c) mass content. This approach is simple, popular, and the least computational. In the framework of spectral bin microphysics, PSDs are approximated discretely by (d) a number of size bins. This approach is detailed but computationally very expensive.

properties, which are crucial for determining radiation budgets. With a high spatial resolution, each atmospheric layer is considered either completely cloudy (overcast) or clear; no partial cloudiness is assumed. In addition, the applied microphysics scheme is realistic enough to simulate the life cycle of clouds, precipitation, and aerosols. The CRM can also have better cloud dynamic processes in terms of the transport of aerosols (see reviews by *Thompson et al.* [1997], *Ekman et al.* [2004, 2006], and *Yin et al.* [2005]).

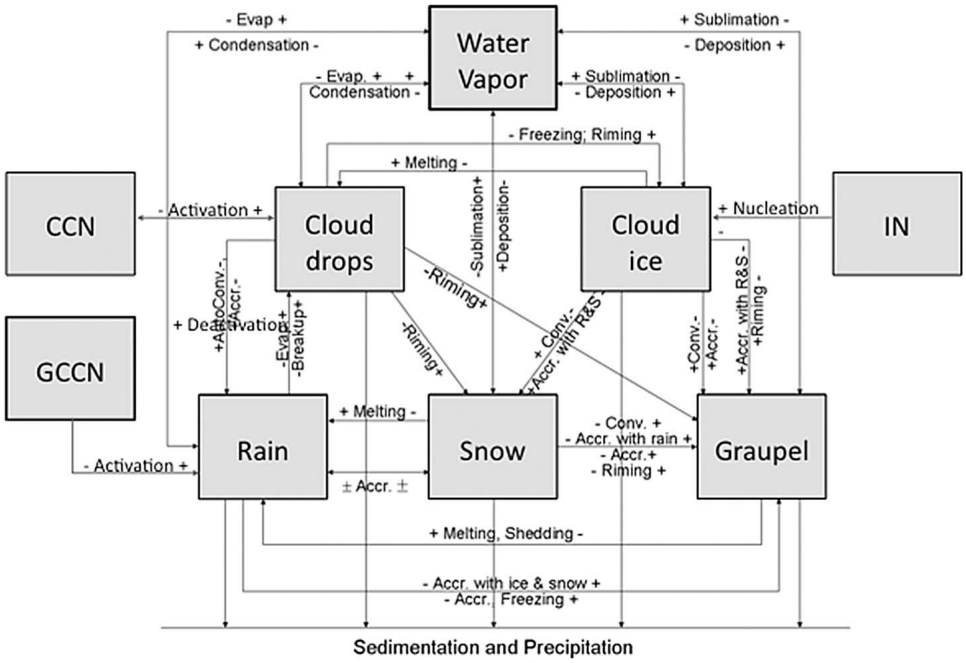

Figure 27. Schematic of the bulk microphysical processes in the typical two-water and three-class ice scheme. Boxes represent the bulk classes of water and aerosol particles, and the arrows represent conversion pathways, with plus and minus signs indicating the direction of the named conversion process. In addition to predicting the mass of cloud water species (cloud drops, rain, cloud ice, snow, and graupel), the number concentration of cloud water species is also predicted.

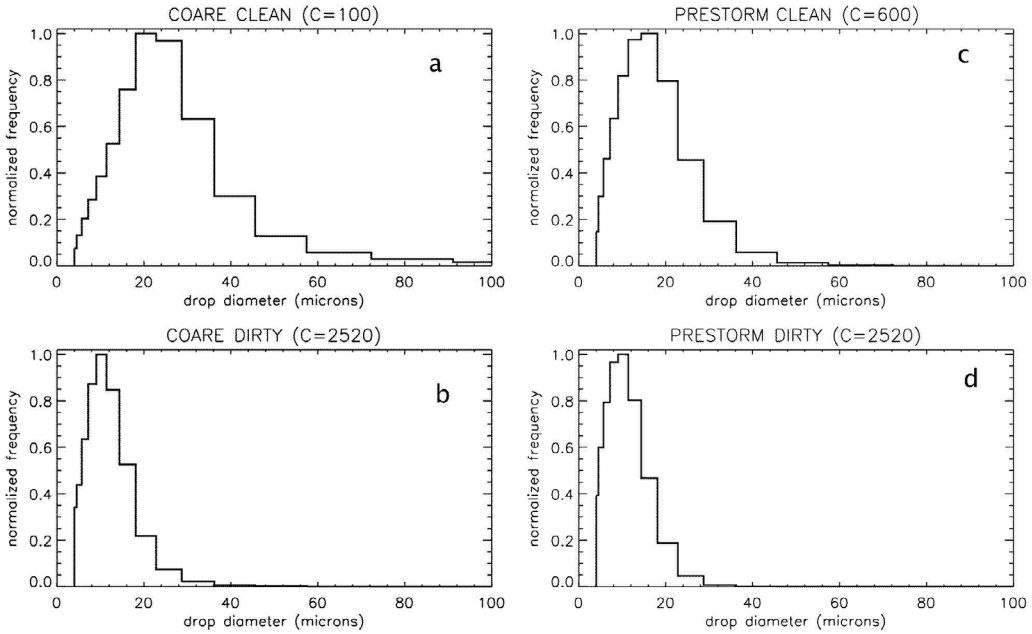

Figure 28. Simulated cloud drop size distributions. The simulations are for two mesoscale convective systems: (a) a tropical oceanic squall system observed during the Tropical Ocean and Global Atmosphere Coupled Ocean-Atmosphere Response Experiment (TOCA COARE), which occurred over the Pacific Ocean warm pool from November 1992 to February 1993), and (c) a midlatitude continental squall system observed during the Preliminary Regional Experiment for STORM-Central (PRE-STORM), which occurred in Kansas and Oklahoma during May–June 1985. (b and d) Same as Figures 28a and 28c except that they represent high CCN concentration cases. Adapted from *Tao et al.* [2007].

5.1.2. Microphysics Used in CRMs

[74] In order to use a CRM to study the impact of aerosols on cloud and precipitation processes, CCN activation and IN nucleation need to be considered in its microphysical scheme (see section 2). Two-moment bulk or spectral bin microphysics (SBM) schemes are required to study the impact of CCN, GCCN, and IN on cloud and precipitation formation. One of the major differences between the two-moment bulk and spectral bin microphysics schemes concerns the representation of cloud particle size spectra (Figure 26). Two-moment schemes typically combine the main features of single-moment schemes by calculating the mixing ratios of hydrometeors, and then adding additional variables for the number concentrations of all particles. Warm-cloud (ice-free) microphysics assumes a bimodal population of water particles. One population is for small cloud droplets whose terminal velocities are negligible compared to the vertical velocity of air, and the other is for large raindrops that have significant fall speeds. Ice microphysics typically assumes three types of particles: small cloud ice whose terminal velocity is negligible, snow whose terminal velocity is about a few tens of centimeters, and large graupel or hail that fall even faster. Only recently have some CRMs included frozen drops or hail as a fourth kind of particle. Graupel has a low density and a high intercept in the Marshal-Palmer distribution (high number concentration), while hail has a high density and a low intercept. Only raindrops, snow, graupel, and hail have a chance to reach the ground level. Graupel is representative for tropical oceanic convection, and hail is representative for midlatitude storms [*McCumber et al.*, 1991]. More than 25 transformations occur among water vapor, liquid particles, and ice particles, such as growth of ice crystals by vapor deposition and riming, the aggregation of ice crystals, the formation of graupel and hail, the growth of graupel and hail by the collection of supercooled cloud drops, the shedding of water drops from hail, the rapid growth of ice crystals in the presence of supercooled water, and the melting and sublimation of all forms of ice (see Figure 27). Certain mathematical functions such as the Khrgian-Mazin distribution function for cloud drops and the Marshall-Palmer distribution function

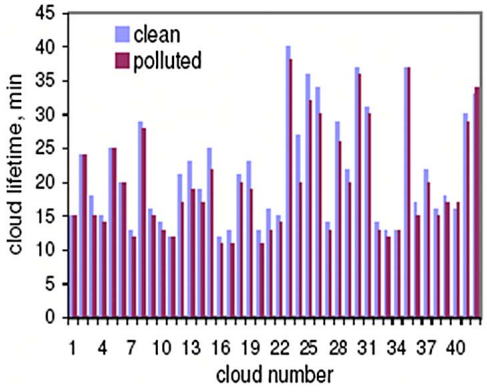

Figure 29. Cloud lifetimes for pairs of clouds initialized from identical dynamical conditions but different N_a. Adapted from *Jiang et al.* [2006].

TABLE 3. Key Papers Using Cloud Resolving Models to Study the Impact of Aerosols on Precipitation[a]

	Dimension	Microphysics	Turbulence	Radiation	Domain	Grid Size and Time Step	Lateral Boundary Conditions	Cases	Integration
Khain et al. [2004]	2-D	spectral bin (33 bin), six types of ice	1st order	no	64 × 16 km	dx = 250 m dz = 125 m dt = 5 s	closed	squall lines (east Atlantic) and a convective cloud (Texas)	~2 h
Khain and Pokrovsky [2004]	2-D	spectral bin (33 bin), six types of ice	1st order	no	64 × 16 km	dx = 250 m dz = 125 m dt = 5 s	closed	convective cloud (Texas)	2.5 h
Khain et al. [2005]	2-D	spectral bin (33 bin), six types of ice	1st order	no	128 × 16 km	dx = 250 m dz = 125 m dt = 5 s	closed	two squall lines (east Atlantic and Oklahoma) and a convective cloud (Texas)	2 and 4 h
Fridlind et al. [2004]	3-D	spectral bin (16 bins), one type of ice	1st order	no	48 × 48 × 24 km	dx = dy = 500 m dz = 375 m dt = 5 s	closed	convective cloud (Florida)	3 h
Wang [2005]	3-D	two moment bulk scheme	1st order	six broad bands for solar and 12 for IR; four-stream discrete-ordinate scattering, k-distribution	400 × 200 × 25 km	dx = dy = 2000 m dz = 500 m dt = 5 s	cyclic	squall line (ITCZ)	4 h
van den Heever et al. [2006]	3-D	two moment bulk scheme	1st order	broadband two- stream for solar and an emissivity for IR	145 × 145 × 20 km	dx = dy = 500 m dz = stretched dt = 1 s	radiative open	thunderstorm (CRYSTAL-FACE)	1–2 h
Cheng et al. [2007]	3-D	two moment bulk scheme (warm rain only)	1st order	simple broadband solar and emissivity (IR)	810 × 810 km × 100 Pa	dx = dy = 3000 m dz = stretched dt = 5 s	radiative open	shallow stratus (ARM-SGP)	72 h
Cheng et al. [2010]	3-D	two moment warm-rain scheme + Reisner cold rain	1st order	simple broadband solar and emissivity (IR)	810 × 810 km × 100 Pa	dx = dy = 3000 m dz = stretched dt = 5 s	radiative open	mixed-phase cold front (Taiwan)	72 h
Lynn et al. [2005a, 2005b]	3-D	spectral bin (33 bin), three types of ice and bulk scheme	TKE	broadband two- stream for solar and an emissivity for IR	400 × 199 × 25 km	dx = dy = 1000 m dz = stretched dt = 9 s	radiative open	squall line (Florida)	13 h
Fan et al. [2007a]	2-D	spectral bin (33 bin), six types of ice	TKE	no	512 × 22 km	dx = 500 m dz = stretched (250–1260 m) dt = 6 s	radiative open	sea breeze–induced convective event (Houston, Texas)	3 h
Teller and Levin [2006]	2-D	spectral bin (33 bin), three types of ice	1st order	no	30 × 8 km	dx = 300 m dz = 300 m dt = 2 s	closed	winter convective cloud, eastern Mediterranean	80 min

TABLE 3. (continued)

	Dimension	Microphysics	Turbulence	Radiation	Domain	Grid Size and Time Step	Lateral Boundary Conditions	Cases	Integration
van den Heever and Cotton [2007]	3-D	two moment bulk scheme	1st order	broadband two- stream for solar and an emissivity for IR	228 × 228 × 22 km	dx = dy = 1500 m dz = stretched dt = 2 s	radiative open	thunderstorm (St. Louis)	26 h
Lee et al. [2008a, 2008b, 2009a]	2-D	two moment bulk scheme	TKE	yes	168 × 20 km	dx = 2000 m dz = 500 m dt = ? s	cyclic with prescribed large-scale forcing	mesoscale convective ensembles (ARM-SGP CART)	24 h
Fan et al. [2009]	2-D	spectral bin (33 bin), six types of ice	TKE	no	768 × 24 km	dx = 300 m dz = 100–400 m dt = 2 s	cyclic	convection embedded in monsoon (East China, northern Darwin)	3 h
Lerach et al. [2008]	3-D	two moment bulk scheme (IN, CCN, and GCCN)	1st order	broadband two- stream for solar and an emissivity for IR	38.44 × 21.78 × 22 km	dx = dy = 111 m dz = stretched dt = 2 s	radiative open	supercell-tornadogenesis	2 h
R. Zhang et al. [2007]	3-D	two moment bulk scheme	TKE	multiple spectral bands (a simple short wave)	100 × 100 × 20 km	dx = dy = 3 km dz = 500 m	close	Pacific storm	12 h
Li et al. [2008b]	3-D	two moment bulk scheme	TKE	multiple spectral bands (a simple short wave)	1050 × 1050 × 20 km	dx = dy = 2 km dz = 500 m	close	deep convective precipitation	3 h
G. Li et al. [2009]	3-D	two moment bulk scheme	TKE	multiple spectral bands (simple short wave)	300 × 300 × 20 km	dx = dy = 750 m dz = 100–1000 m	close	squall line	24 h
Yin et al. [2005]	1.5-D axisymmetric	34 bins, one liquid and three ice categories	1st order	no	6 km × 12 km	150 m (radial) × 300 m (vertical) dt = 2.5 s (condensation/ deposition) dt = 5 s (others)	open	deep convection	80 min
Storer et al. [2010]	3-D	two-moment bin-emulating bulk scheme	1st order	a broadband two- stream for solar and an emissivity for IR	300 km × 500 km × 23 km	Dx = dy = 1 km	radiative	supercells	5.5 h
van den Heever et al. [2011]	2-D	two-moment bin-emulating bulk scheme	1st order	a broadband two- stream for solar and an emissivity for IR	10,000 km × 26 km	Dx = 1 km	periodic	tropical convection (trimodal distribution)	100 days
Saleeby et al. [2010]	3-D	two-moment bin-emulating bulk scheme	1st order	broadband two- stream for solar and an emissivity for IR	nested grids	Dx = dy = 1.25 km on finest grid	radiative	precipitating cloud systems over the East China Sea	48 h

[a]Model dimensionality (2-D or 3-D), microphysical schemes (spectral-bin or two-moment bulk), turbulence parameterization (first- or 1.5-order turbulent kinetic energy (TKE)), radiation (with or without), domain size (km), resolution (m), time step (s), lateral boundary condition (closed, cyclic, or radiative open), and case and integration time (h) are all listed. Updated and modified from *Tao et al.* [2007].

for raindrops, snow, and graupel or hail are assumed to represent their size distributions.

[75] With increasing computing power, explicit bin-microphysical schemes have been applied more commonly in CRMs to study cloud-precipitation-aerosol interactions. The formulation of explicit microphysical processes is based on solving equations for mass advection by condensation growth and stochastic collision kinetics for the size distribution functions of water droplets (cloud droplets and raindrops together as one continuous category). Ice particles are much more complicated due to their different shapes, so they are often classified into various growth habits such as columnar, plate-like, dendrites, snowflakes, graupel, and frozen drops. Each type is described by a discretized size distribution containing as many as 30 or more categories (bins). Spectral bin microphysics include the following processes: (1) activation (nucleation) of cloud droplets; (2) nucleation of ice particles [*Pruppacher and Klett*, 1997; *Meyers et al.*, 1992], including homogeneous freezing, deposition nucleation, condensation-freezing nucleation, immersion freezing [*Vali*, 1994], and contact freezing; (3) ice multiplication [*Hallett and Mossop*, 1974; *Mossop and Hallett*, 1974]; (4) detailed melting [*Khain et al.*, 2004]; (5) condensation or evaporation of liquid drops [*Pruppacher and Klett*, 1997; *Khain et al.*, 2000]; (6) deposition or sublimation of ice particles [*Pruppacher and Klett*, 1997; *Khain et al.*, 2000]; (7) drop/drop, drop/ice, and ice/ice collision/coalescence [*Pruppacher and Klett*, 1997; *Pinsky et al.*, 2001]; (8) turbulence effects on liquid drop collisions [*Pinsky et al.*, 2000, 2008]; and (9) collisional breakup [*Low and List*, 1982; *Seifert et al.*, 2005]. Sedimentation of liquid and ice particles is also considered, and for the latter, crystal shape is an important factor. Spectral bin microphysics is specially designed to take into account the effect of atmospheric aerosols on cloud development and precipitation formation by calculating the activation of aerosols explicitly according to the Köhler theory [*Pruppacher and Klett*, 1997]. Section 2 describes in more detail processes associated with the initialization of CCN, GCCN, and IN.

5.2. CCN Effect on Clouds

[76] It is commonly believed that clouds in a clean environment (low CCN concentration) produce fewer droplets but with larger sizes due to greater condensational and collectional growth, leading to a broader size spectrum in comparison to the high CCN situation. Figure 28 shows simulated cloud drop size distributions under low and high CCN concentrations [*Tao et al.*, 2007]. The results are very similar to those observed and shown by *Fletcher* [1962] and *Squires* [1958]. *van den Heever et al.* [2006] and *Carrió et al.* [2007] also found that smaller cloud droplets are found with a narrow spectrum under dirty conditions. The numerical results are in good agreement with observations, indicating that the microstructure of clouds depends strongly on cloud-aerosol interactions. The Twomey effect was well simulated. The width of the drop size distribution could have an impact on precipitation processes. For example, smaller cloud droplets would reduce the chance to form raindrops from cloud drop coagulation. This result is in agreement with observations [i.e., *Twomey et al.*, 1984; *Albrecht*, 1989; *Rosenfeld*, 1999].

[77] The effects of increases in aerosol concentration on cloud lifetime for warm convective clouds have been studied using CRMs and large-eddy simulations (a special type of cloud model with a resolution of 100 m or smaller). *Teller and Levin* [2006] showed that a polluted cloud produces less precipitation, which leads to an increase in the lifetime of the cloud under the same meteorological conditions. This result is in agreement with the second aerosol indirect effect on cloud lifetime [*Albrecht*, 1989; *Ackerman et al.*, 2000]. However, a separate modeling study shows that an increase in aerosol concentration from very clean to highly polluted conditions does not increase cloud lifetime (Figure 29), even though precipitation is suppressed. In rare cases (two cases in Figure 29), long-lived polluted clouds may have longer lifetimes than clean clouds due to the merging of individual clouds. This result is contrary to the observation that increases in aerosol concentration leads to prolongation of cloud lifetimes. But the model results do agree with observations of precipitation suppression under polluted conditions. *Jiang et al.* [2006] proposed that the small changes in cloud lifetime are due to the competing effects of precipitation suppression and enhanced evaporation for shallow clouds. The differences between results from *Teller and Levin* [2006] and *Jiang et al.* [2006] could be due to the differences in aerosol concentration (mildly polluted versus highly polluted) and/or environmental conditions.

5.3. CCN Effect on Precipitation

5.3.1. Impact of CCN on Surface Precipitation

[78] Recently, many CRMs have been used to examine the role of aerosols on mixed-phase convective clouds (Table 3). These modeling studies have many differences in terms of model configuration (two- or three-dimensional), domain size, grid spacing (150–3000 m), microphysics (two-moment bulk, simple or sophisticated spectral-bin), turbulence (first- or 1.5-order turbulent kinetic energy (TKE)), radiation, lateral boundary conditions (i.e., closed, radiative open, or cyclic), cases (isolated convection, tropical or midlatitude squall lines), and model integration time (e.g., 2.5 to 48 h). A simple metric, changes in time-integrated precipitation ($dP = 100 \times (P_{dirty} - P_{clean})/P_{clean}$) as a result of increases in the number concentration of CCN ($dN_0 = N_{dirty} - N_{clean}$), was used to examine the impact of aerosol concentration on surface rainfall (Table 4). Among these modeling studies, the most striking difference is that cumulative precipitation can either increase or decrease in response to higher concentrations of CCN. *Phillips et al.* [2002], *Khain et al.* [2004, 2005], *Khain and Pokrovsky* [2004], and *Teller and Levin* [2006] changed the number concentrations of CCN gradually and found robust decreases in cumulative precipitation for higher concentrations of CCN. This is completely opposite to the results of *Wang* [2005], *Khain et al.* [2005], *Lee et al.* [2009a], and *Fan et al.* [2007b].

TABLE 4. Summary of Precipitation Sensitivity (dP) to Increases in the Number of CCN (dN_0) for Different Studies[a]

Reference	Case	dN_0 (N_{clean}) (cm^{-3})	dP (%)
Tao et al. [2007]	TOGA COARE	2400 (100)	+58.
	PRE-STORM	1900 (600)	−24.
	CRYSTAL	1900 (600)	−13.
Phillips et al. [2002]	New Mexico	1950 (800)	−14.
		4200 (800)	−30.
Khain et al. [2004]	GATE	1160 (100)	−3.
Khain and Pokrovsky [2004]	Texas	40 (10)	−16.
		90 (10)	−19.
		290 (10)	−53.
		1250 (10)	−88.
Khain et al. [2005]	PRE-STORM	1160 (100)	+258.
Teller and Levin [2006]	wintertime eastern Mediterranean	210 (100)	−27.
		510 (100)	−55.
		810 (100)	−73.
		1260 (100)	−93.
Wang [2005]	ITCZ	400(100)	+180.
		800 (100)	+340.
		1200(100)	+540.
		1500 (100)	+700.
Lynn et al. [2005b]	Florida	1250 (10)	−5.
van den Heever et al. [2006]	CRYSTAL-FACE	350 (300)	−22.
Lee et al. [2008a, 2008b, 2009]	ARM-A	900 (100)	+18.
Lee and Feingold [2010]	TWP-ICE	450 (50)	+9.
Fan et al. [2007a]	sea breeze–induced convective event (Houston, Texas)	30,000 (3000)	+9.
Fan et al. [2009]	TWP-ICE and China	1100 (110)	± (depends on the wind shear
Cheng et al. [2010]	front system (northern Taiwan)	9000 (1000)	−12%
		900 (100)	∼0%

[a]Note that *van den Heever et al.* [2006] used a linear CCN concentration profile that ranged from 300 cm^3 at 4 km above ground level to 1000 cm^3 near the surface; GCCN and IN effects from *van den Heever et al.* [2006] and *Teller and Levin* [2006] are excluded; only five of the total 30 cases from *Wang* [2005] are displayed. Updated and modified from *Tao et al.* [2007].

[79] *Tao et al.* [2007] used a two-dimensional CRM with detailed spectral-bin microphysics to examine the aerosol impact on a tropical oceanic mesoscale convective system, a summertime midlatitude continental squall line, and a short-lived Florida sea breeze convective storm. Rain suppression in the high CCN concentration runs is evident in all three case studies but only during the first hour of the simulations (Figure 30). Rain reaches the ground early in all the clean cases. This result suggests that microphysical processes dominate the initial stage of cloud development, during which the transition of cloud droplets from condensational to collectional growth is very sensitive to cloud drop size. Compared to the case under polluted conditions, clouds in a clean environment (low CCN concentration) produce fewer but larger cloud droplets, leading to a better chance for raindrop formation from cloud drop coagulation. This result is in good agreement with many observations [e.g., *Rosenfeld*, 1999, 2000] and other CRM studies [*Khain and Pokrovsky*, 2004; *Khain et al.*, 2005; *Teller and Levin*, 2006; *Seifert and Beheng*, 2006; v*an den Heever et al.*, 2006; *Carrió et al.*, 2007; *van den Heever and Cotton*, 2007; *Lee et al.*, 2009a] and is in agreement with Twomey's second indirect effect. During the mature stage of the simulations, the effect of increasing CCN concentration ranges from rain suppression in the midlatitude continental case to little effect in the Florida sea breeze case to rain enhancement in the Pacific oceanic case. These results suggest that model simulations of the whole life cycle of a convective system are needed in order to assess the impact of aerosols on precipitation processes associated with MCSs and thunderstorms. These results also show the complexity of aerosol-cloud-precipitation interactions within deep convection.

[80] *Khain et al.* [2008] and *Khain* [2009] recently conducted a number of numerical experiments to identify the factors that determine the impact of aerosols on precipitation. A scheme (Figure 31) was proposed to classify aerosol effects on clouds and cloud systems under different environments. It shows that if the ambient relative humidity is high, then the condensation gain (loss) is large and the condensation loss (gain) is low, which could lead to an increase (decrease) in precipitation. *Seifert and Beheng* [2006], *Khain et al.* [2008], and *van den Heever et al.* [2011] have also showed that the impact of aerosols on precipitation and convection structure depends on cloud type. A decrease in precipitation with an increase in aerosol concentration usually occurs for isolated cumulus clouds and cloud systems that develop within a relatively dry environment and/or within regions of large wind shear or stratocumulus clouds. *Fan et al.* [2009] also found that the increase in CCN concentration always suppresses convection under strong wind shear conditions but enhances convection under weak wind shear conditions. On the other hand, an increase in precipitation with an increase in aerosol concentration often occurs for clouds forming in a moist environment, such as coastal zones, within cloud ensembles or tropical squall lines. Such a result can also be found in other CRM studies [*Wang*, 2005; *Tao et al.*, 2007; *Fan et al.*, 2007b] (see also Figure 30b) and is consistent with the LES study by

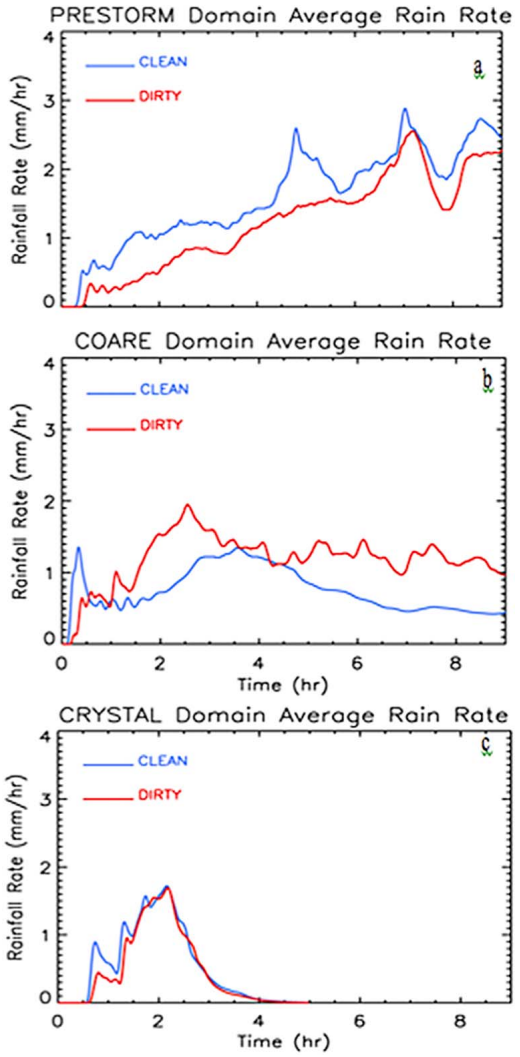

Figure 30. Time sequences of Goddard Cumulus Ensemble (GCE) model-estimated domain mean surface rainfall rate (mm h^{-1}) for (a) PRE-STORM, which occurred in Kansas and Oklahoma during May–June 1985, (b) TOGA COARE, which occurred over the Pacific Ocean warm pool from November 1992 to February 1993, and (c) Preliminary Regional Experiment for STORM-Central (CRYSTAL), which occurred in Kansas and Oklahoma during May–June 1985. cases. The solid and dashed lines represent clean and dirty conditions, respectively. Adapted from *Tao et al.* [2007].

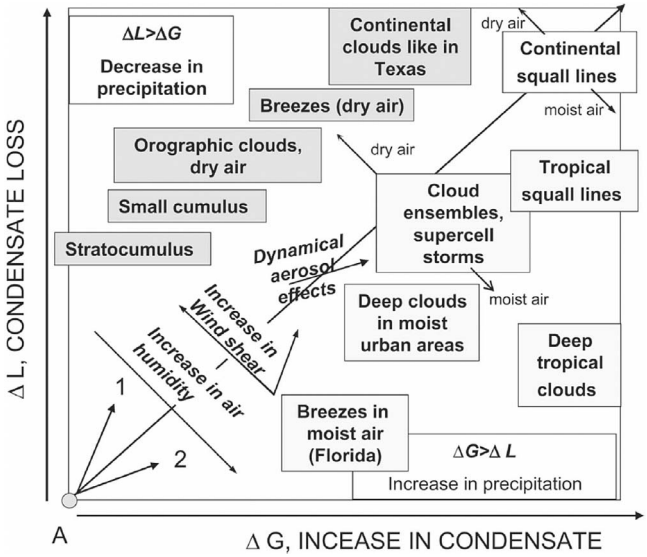

Figure 31. A schematic diagram of aerosol effects on clouds and cloud systems of different types. The zone above the diagonal corresponds to a decrease in precipitation with aerosol concentration. The zone below the diagonal corresponds to an increase in precipitation with an increase in the aerosol particle concentration. Adapted from *Khain et al.* [2008].

Ackerman et al. [2004]. Note that *Wang* [2005], *Tao et al.* [2007], *Khain et al.* [2008], *Fan et al.* [2007a], and *Lee* [2011] all showed that aerosols have a larger effect on precipitation under more humid conditions.

[81] Recently, *van den Heever et al.* [2011] made use of large-scale (e.g., 10,000 km), long-duration (100 days), high-resolution (1 km) radiative-cloud-equilibrium (RCE) simulations to investigate the impacts of enhanced CCN concentrations on a wide variety of storm types that developed under a wide range of different environmental conditions. They found that high CCN concentrations led to a reduction in surface precipitation from shallow clouds, but an enhancement in the precipitation produced by deep convective clouds, with a mixed response from more moderate convective storms such as cumulus congestus. They also noted that the frequency of lighter precipitation-producing systems was decreased under more polluted conditions, while the frequency of heavy precipitation-producing systems was enhanced, concluding that polluted conditions

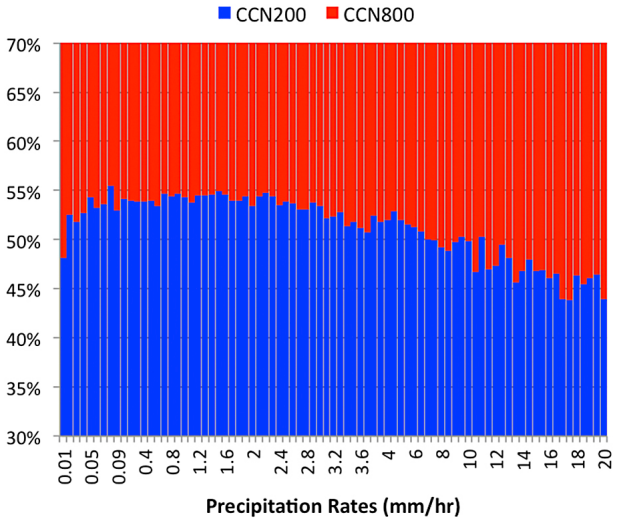

Figure 32. Precipitation rate (mm h^{-1}) frequency distribution plot for clean (CCN200) and polluted (CCN800) cases. The frequencies are expressed in a relative sense where, for example, 50% implies that the frequency for a given precipitation rate is the same for both cases. Adapted from *van den Heever et al.* [2011].

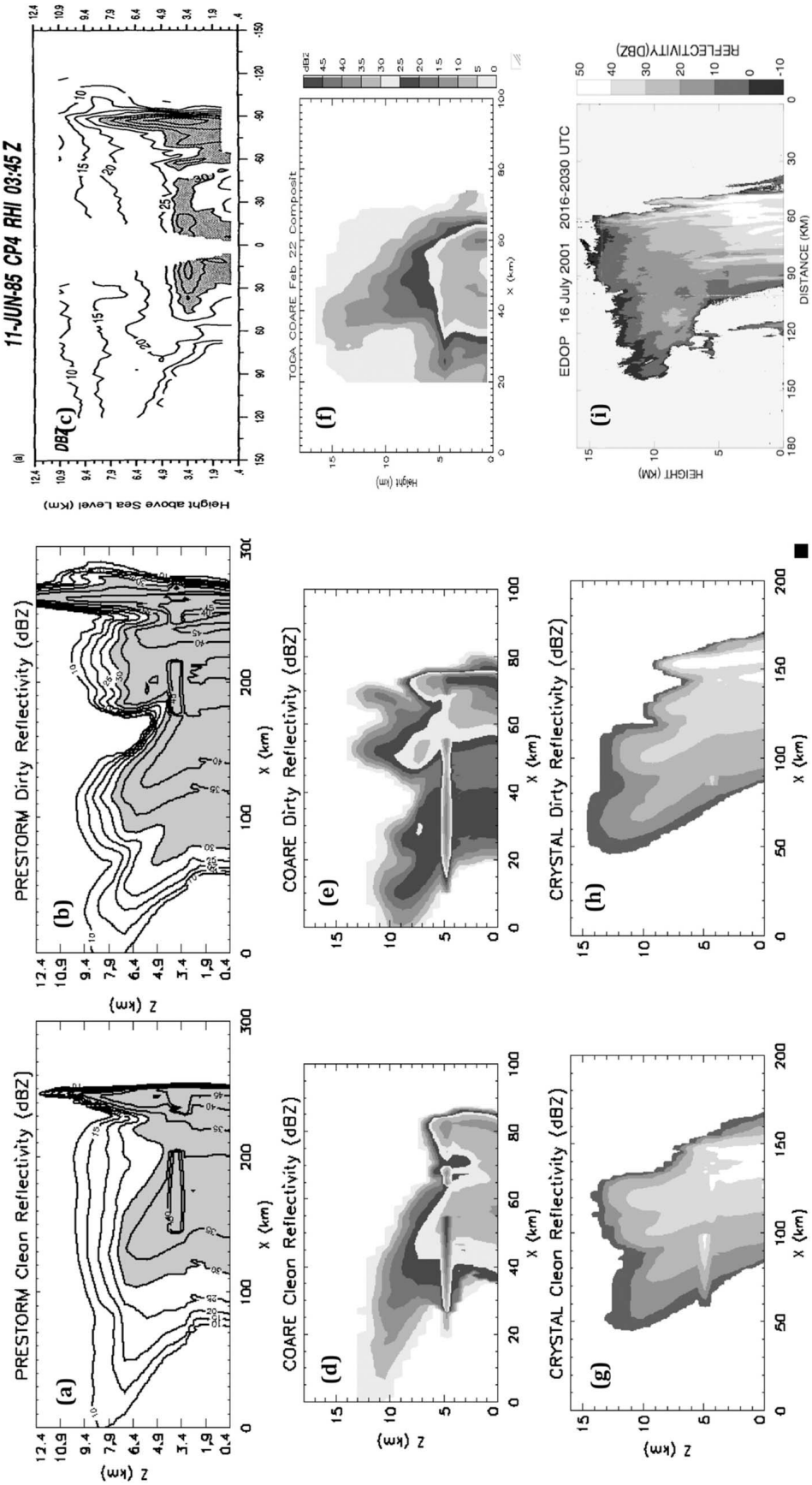

Figure 33. Observed and simulated radar reflectivity for the TOGA COARE, PRE-STORM, and CRYSTAL-FACE cases under dirty and clean conditions: (a) PRE-STORM clean, (b) PRE-STORM dirty, (c) PRE-STORM observed, (d) COARE clean, (e) COARE dirty, (f) COARE observed, (g) CRYSTAL clean, (h) CRYSTAL dirty, and (i) CRYSTAL observed. Adapted from *Tao et al.* [2007].

result in a greater frequency of more intense rainfall-producing systems (Figure 32).

[82] In almost all of the above cases, idealized aerosol concentrations were used in the model simulations. Some of the CRM domains were too small to resolve the observed clouds or precipitation systems (the domain size has to be at least twice as large as the simulated features). Furthermore, very few of these CRM studies compared model results with observed cloud structures, organization, and radar reflectivities (Figure 33). Note that model simulations may capture well storm sizes and structures under different environmental conditions. For example, the leading convection and the extensive trailing stratiform rain areas compared well with the radar reflectivity observed during the mature stage of the continental case [*Rutledge et al.*, 1988]. Clean cases (i.e., the control experiments) generally agree better with observations. In terms of radar reflectivity magnitudes, the agreement between simulations and observations is better at lower levels where only liquid phase cloud or rainwater exist. Simulated radar reflectivities tend to be higher than observations at upper levels and in the anvil area where ice phase particles dominate. This reflects the inadequate description of various ice phase mechanisms in this calculation, particularly those related to aerosol effects.

5.3.2. Physical Processes Behind the CCN Effect on Precipitation

[83] Observational studies suggest that enhanced aerosol concentrations could suppress warm rain processes by producing a narrow drop size spectrum that inhibits collision and coalescence processes [e.g., *Squires and Twomey*, 1966; *Warner and Twomey*, 1967; *Warner*, 1968; *Rosenfeld*, 1999]. In addition, more aerosols would reduce precipitation and rainfall. This is because more aerosols could produce smaller cloud droplets, resulting in less efficient collision coalescence and consequently less rainfall. Many cloud-resolving modeling studies simulated these processes during the early stage in the development of isolated convective systems and found that sometimes, more rainfall is produced under polluted (high CCN concentration) conditions.

[84] Several cloud-resolving modeling studies also examined the physical processes that could lead to aerosol-induced changes in precipitation. In general, three mechanisms were proposed to explain the enhancement of precipitation by changing (increasing or decreasing) the aerosol concentration (see Figure 34). The first mechanism involves the creation of stronger updrafts or downdrafts resulting from enhanced latent heat release as CCN suppress warm-rain formation and thus retain more liquid water in the cloud to be frozen at upper levels. This effect could be termed as the *latent heat–dynamic effect. Wang* [2005] showed precipitation increases in tropical deep convection due to higher CCN concentrations through this latent heat effect. *Khain et al.* [2005] also found that for cases where there was enhanced precipitation with high CCN concentrations, clouds were associated with stronger updrafts or downdrafts as well as stronger convergence in the boundary layer, which provides a better chance to trigger secondary clouds and prolong the lifetime of the convective system. *van den Heever and Cotton* [2007], *Lee et al.* [2008a], and *Storer et al.* [2010] also demonstrated the influences of aerosols on secondary storm development and its effect on increasing precipitation.

[85] The second mechanism is stronger evaporative cooling due to more but smaller raindrops under high CCN concentration conditions. Stronger evaporative cooling could enhance the strength of the near-surface cold pool. When the enhanced cold pool interacts with lower level wind shear, convergence could become stronger, producing more vigorous convection that ultimately leads to enhanced surface precipitation. This positive feedback mechanism could be termed as the *cool pool effect.* It seems to be occurring in the oceanic convective case (Figure 35), in which evaporative cooling in the lower troposphere is more than twice as strong for the polluted scenario compared to the clean scenario. Note that stronger evaporative cooling occurs in the developing stage of convective cloud systems. *Lee et al.* [2009a] also demonstrated that stronger evaporative cooling occurred under high aerosol concentrations and consequently led to enhanced surface precipitation.

[86] The third mechanism is the CCN effect on cloud microphysics. *Wang* [2005] suggested that with higher CCN concentrations, there is a greater increase in total water content consisting of numerous small liquid particles, leading to more vigorous convection and cold-rain processes. As a result, rain production is mainly from ice phase microphysics in the modeled tropical deep convective case for which precipitation is increased due to more CCN (with similar processes as the above continental convective case). *Cheng et al.* [2010] further showed that increasing the CCN concentration leads to more cloud drops and cloud ice, but that there is uncertainty in the magnitude of its effect on surface precipitation due to various responses of cold-rain production (this could be termed as the *cold-microphysics effect*). Figure 36 shows four different microphysical processes that would affect surface precipitation. The CCN effect on precipitation in the low-CCN case is dominated by suppressed warm-rain formation (effect A) and enhanced riming (effect C). On the other hand, in the high-CCN case where changes in snow-raindrop accretion are small, decreases in snow riming (due to reduced collection efficiency, effect B) and melting are big enough to dominate the change in cold-rain production, leading to suppressed surface rainfall. Overall, the CCN effect on precipitation in the high-CCN case is dominated by effect A and effect B.

[87] However, these three physical mechanisms can affect each other, making it difficult to isolate each mechanism independently. For example, a stronger evaporative cooling (cold pool effect) in the low troposphere for the high CCN-enhanced precipitation case (latent heat–dynamic effect) is evident in Figure 34a. On the other hand, the stronger cooling could be due to more evaporation associated with a stronger convective downdraft (latent heat–dynamic effect). The microphysics effect can affect both latent heat and the cool pool and vice versa. More smaller cloud drops may enhance the WBF process (i.e., snow deposition growth at the expense of evaporating cloud drops) so that the latent

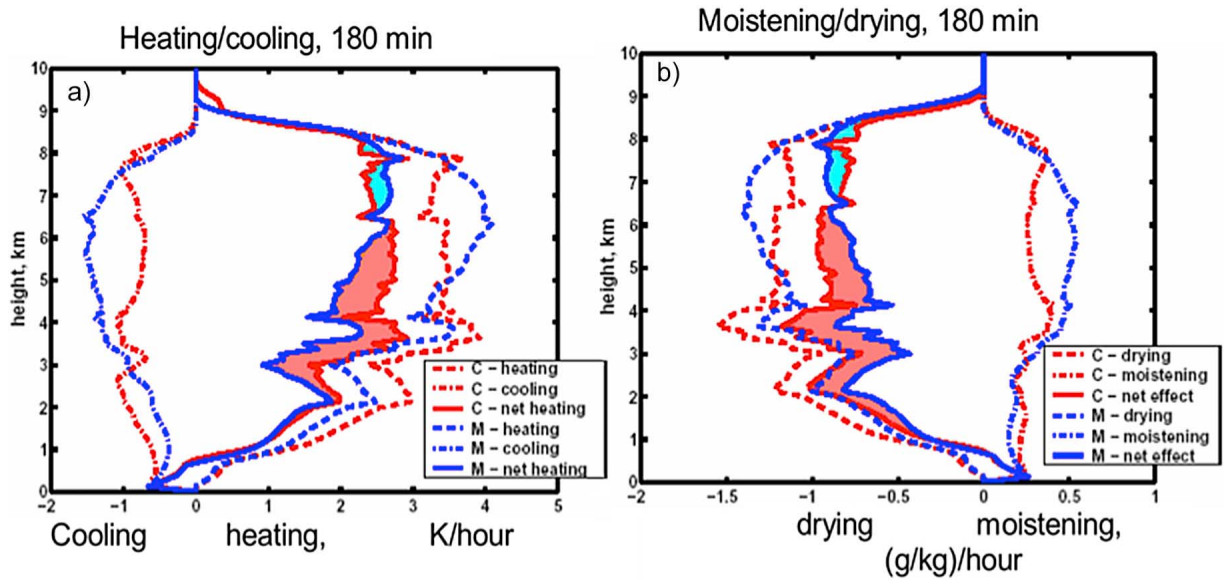

Figure 34. Vertical profiles of horizontally averaged (a) heating and cooling and (b) moistening and drying in a hail storm in southern Germany calculated for low (blue curves) and high (red curves) aerosol concentrations. Areas marked pink and light blue denote zones where net heating and drying are larger and smaller in the high aerosol concentration case, respectively. Adapted from *Khain et al.* [2008].

heat release becomes larger. But the reduced riming efficiency has the opposite effect on latent heat release. More numerous cloud drops (due to more CCN) could also lead to more ice nucleation and thus a higher number of snow and graupel particles, which, when melted, form more but smaller raindrops that cause stronger evaporative cooling below the cloud base. Convection may be strengthened due to either the latent heat effect or the cold pool effect, and the stronger updraft leads to higher supersaturation and thus enhanced ice deposition nucleation.

5.4. CCN Effect on Convective Precipitation Using Nested Cloud/Regional-Scale Models

[88] Regional-scale models (mainly the fifth-generation Pennsylvania State University–National Center for Atmospheric Research (Penn State-NCAR) Mesoscale Model (MM5), Weather Research and Forecasting Model (WRF), and Regional Atmospheric Modeling System (RAMS)) with fine resolutions (utilizing interactive nesting techniques) have also been used to study the impact of aerosols on

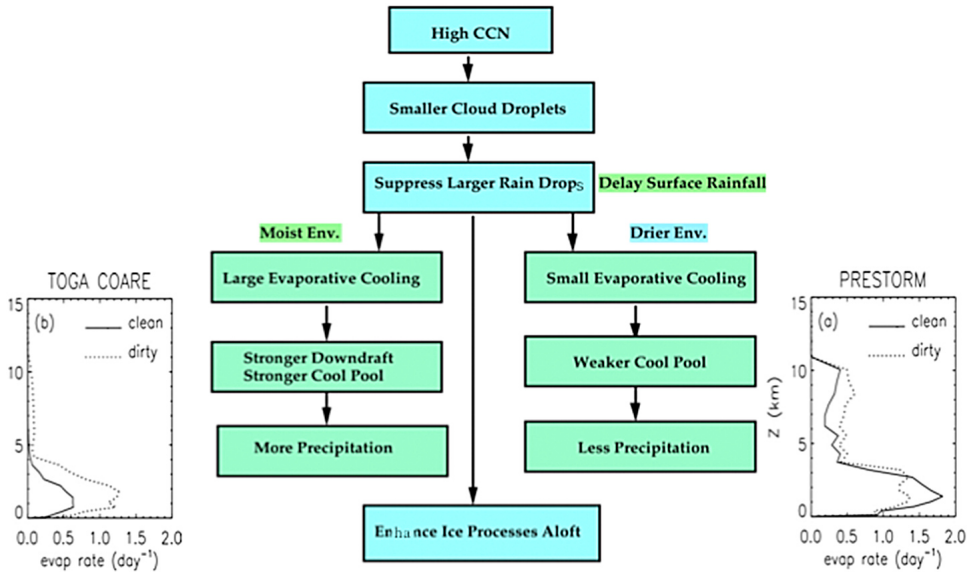

Figure 35. Schematic showing the physical processes that lead to either enhancement (oceanic convective case) or suppression (midlatitude continental convective case) of precipitation in a dirty environment. Their respective evaporative coolings are also shown. Note that differences in cooling occurred in the early stage of model simulations. Adapted from *Tao et al.* [2007].

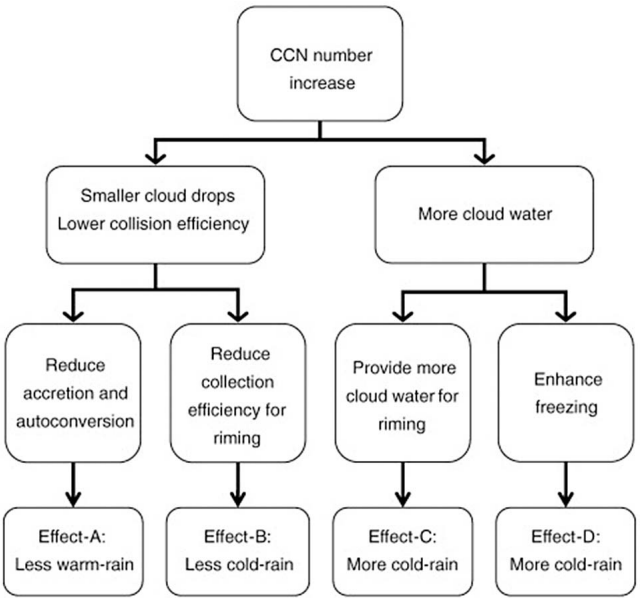

Figure 36. Schematic of the major CCN effects on warm-rain and cold-rain processes. Adapted from *Cheng et al.* [2010]. Copyright Elsevier. Reprinted with permission.

convective precipitation events associated with the Florida sea breeze, the urban heat island effect, tropical cyclones and hurricane, supercells, and tornadoes [i.e., *van den Heever et al.*, 2006; *van den Heever and Cotton*, 2007; *Lynn et al.*, 2005a, 2005b; *H. Zhang et al.*, 2007; *R. Zhang et al.*, 2007; *Zhang et al.*, 2009; *Li et al.*, 2008a, 2008b; *Lerach et al.*, 2008; *Khain et al.*, 2010; *Storer et al.*, 2010]. An advantage of this approach is that the model initial and lateral-boundary conditions are provided by large-scale analyses with realistic meteorological fields, and model simulations can be conducted with realistic terrain and land surface characteristics.

[89] *Lynn et al.* [2005a, 2005b] used spectral-bin microphysics (a simplified version of Khain's scheme [*Khain et al.*, 2004]) and the MM5 to simulate a cloud that approached the west coast of Florida, prior to the sea breeze development. The use of a continental CCN concentration led to a delay in the development of rainfall. The increase in CCN concentration led to convective invigoration and the formation of stronger secondary clouds [*Lynn et al.*, 2005b]. Simulations of rain events over the whole peninsula for this day showed significant invigoration of squall lines. There was an increase in precipitation rate and precipitation amount for a squall line that formed in the vicinity of the east coast of Florida. At the same time, continental CCN concentrations resulted in a 5% reduction in precipitation over the whole computational domain (containing a significant fraction of Florida) versus maritime values.

[90] *van den Heever et al.* [2006] used the RAMS and a two-moment bulk microphysical scheme [*Meyers et al.*, 1997; *Saleeby and Cotton*, 2004] to examine the aerosol effect on the formation of a thunderstorm over the peninsula of Florida. Note that the two-moment bulk scheme used by *van den Heever et al.* [2006] emulates a bin scheme by including the explicit activation of aerosols [*Saleeby and Cotton*, 2004]. Sensitivity tests show that different combinations of CCN, GCCN, and IN result in different amounts and temporal patterns of cloud-water/ice contents and rainfall. Their study showed that a high CCN reduces cumulative precipitation by 22% compared to low CCN. In addition, high amounts of GCCN and IN enhanced surface precipitation for the first 6 h of integration due to the initial broadening of the cloud droplet spectra. However, the total (12 h integration) accumulated precipitation is greatest for the clean (low CCN, GCCN, and IN) case. Rapid wet deposition of GCCN during the first 6 h of integration may be the reason for this. All their experiments involving high CCN resulted in high cloud-water content and weak surface precipitation.

[91] Using a similar modeling configuration, *van den Heever and Cotton* [2007] examined the sensitivity of urban-induced convective clouds over and downwind of St. Louis, Missouri. Their results indicate that downwind convergence (dynamic processes) induced by urban land cover appears to be the dominant factor in determining whether or not moist convection actually develops downwind of St. Louis. Once moist convection is initiated, urban-enhanced aerosols play a major role in determining the microphysical and dynamical characteristics of convective storms, particularly when background aerosol concentrations are low (Figure 37). Complicated relationships and feedbacks between microphysical and dynamical processes obscure the general understanding of urban-enhanced aerosol effects on precipitation. Note that *Lynn et al.* [2005b], *van den Heever et al.* [2006], and *van den Heever and Cotton* [2007]

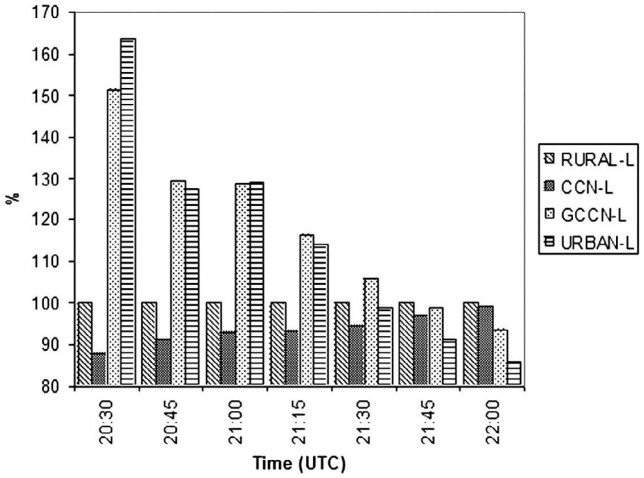

Figure 37. Time series of accumulated volumetric precipitation in the downwind region expressed as a percentage of the RURAL-clean background simulation. RURAL-L stands for the simulation with clean CCN and giant CCN (GCCN) background aerosols; CCN-L stands for the effects of the increase in CCN concentrations relative to clean background concentrations; GCCN-L represents the effects of GCCN concentrations relative to clean background concentrations; and URBAN-L stands for the effects of CCN and GCCN concentrations relative to clean background aerosols. Adapted from *van den Heever and Cotton* [2007].

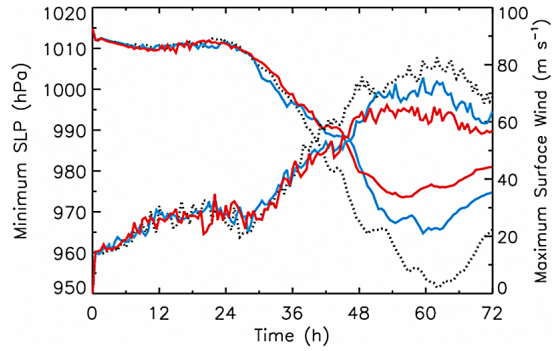

Figure 38. Temporal evolution of the minimum sea level pressure (MSLP) and maximum surface wind for clean (dotted curve), polluted (1000 cm^{-3}, blue curve), and doubly polluted (2000 cm^{-3}, red curve). Adapted from *H. Zhang et al.* [2007].

explicitly represent mesoscale forcing (i.e., sea breeze convergence and urban heat island convergence). This is important because cold pools can interact with these kinds of circulation, introducing another level of dynamic complexity. For example, if the cold pool outruns these mesoscale convergence fields, precipitation is reduced; when they remain coupled, precipitation is enhanced (cool pool effect in section 5.3.2). *van den Heever and Cotton* [2007] also found that the response of convective rainfall to urban-enhanced aerosols becomes stronger when the background aerosol concentrations are low.

[92] The role that aerosols or dust in the SAL play on tropical storms has recently been studied using regional-scale models [i.e., *H. Zhang et al.*, 2007; *Zhang et al.*, 2009; *Cotton et al.*, 2007]. The impact of dust acting as CCN in the SAL on the evolution of a tropical cyclone (TC) was examined through simulations initialized with an idealized pre-TC mesoscale convective vortex (MCV) using the RAMS [*Cotton et al.*, 2007]. Dust in the SAL can affect the simulated TC intensity by 22 hPa depending on CCN concentrations (Figure 38). High CCN concentrations could weaken the TC intensity. It can also affect eye wall development directly through release of latent heat by the enhanced activation and condensation growth of cloud droplets, and indirectly through modulating rainband development. Convection in the rainbands was negatively correlated with that in the eye wall in all simulations. The development of rainbands promotes latent heat release away from the eye wall, blocks the surface inflow, and enhances cold pools. The convection in the eye wall and rainbands did not show a monotonic relationship to the CCN input due to the nonlinear feedback of heating from a myriad of microphysical processes on storm dynamics (Figure 39). The impact of CCN on storm intensity was sensitive to the background GCCN vertical profile and presumably other environmental factors.

[93] The WRF with a spectral bin microphysics scheme was used to investigate the potential impact of aerosols on the structure and intensity of Hurricane Katrina as they were ingested into the storm's circulation during its passage through the Gulf of Mexico in 2005 [*Khain et al.*, 2010]. Continental aerosols invigorated convection largely at the TC periphery, which led to its weakening prior to landfall. The minimum pressure increased by 15 hPa, and the maximum velocity decreased up to 15 m s^{-1}. Aerosols substantially affected the spatial distribution of cloudiness and hydrometeor contents. The results are in good agreement with those of *Zhang et al.* [2009]. Figure 40 shows how the TC intensity is weakened due to the aerosol effect. Three processes are responsible for the decrease in intensity: (1) an increase in cloud updraft velocity at the TC periphery, causing enhanced vertical mass flux at the periphery and thus less air mass and water vapor penetrating to the central part of the TC; (2) extra convective heating at the periphery, lowering the surface pressure at the TC periphery and decreasing the horizontal pressure gradient; and (3) competition between two zones of convection (at the eye and at the periphery). Compensatory downdrafts caused by convection at the TC periphery also tend to damp convection in the TC eye. The diagram shown in Figure 40 agrees well with results of Saharan dust effects on TC intensity reported by *Zhang et al.* [2009]. They found that convection in TC rainbands was negatively correlated with that in the eye wall in all simulations.

[94] *Li et al.* [2008a] implemented a two-moment bulk microphysical scheme into the WRF model to investigate the effects of aerosols on cloud and precipitation processes. A deep cumulus cloud and precipitation event was simulated and a sensitivity study was carried out using a set of initial aerosol profiles at the surface level to examine the response of precipitation efficiency to the increase in aerosol concentration. Precipitation increased with aerosol concentration from clean to polluted conditions but was considerably reduced and completely suppressed under extremely polluted conditions (Figure 41). Enhanced precipitation with increasing aerosols at lower CCN is attributable to the suppressed conversion of cloud droplets to raindrops, which causes less efficient warm-rain processes but more efficient mixed-phase processes. At extremely high CCN, ice production is inhibited because ice nucleation becomes inefficient and anvil formation is hindered due to a large mass loading of small droplets (reduced buoyancy) and less latent heat from droplet freezing. Cloud coverage and core updrafts

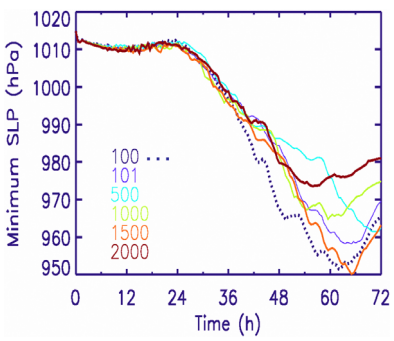

Figure 39. Temporal evolution of the MSLP and maximum surface wind for cases with different CCN concentrations. Adapted from *H. Zhang et al.* [2007].

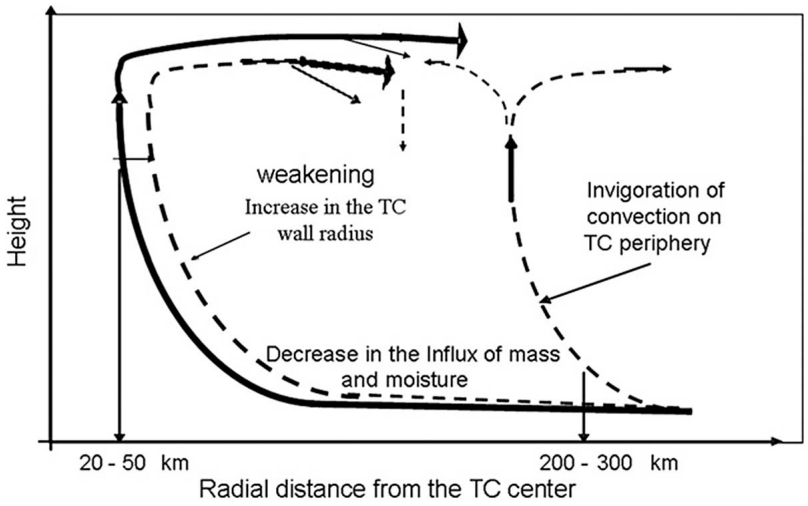

Figure 40. A scheme showing the aerosol effects on tropical cyclone (TC) structure leading to TC weakening. The dashed lines represent the run with high CCN concentrations at the TC periphery leading to convective invigoration. Invigoration of convection along the TC periphery due to high CCN could reduce the low-level influx of moisture and mass into the TC core and therefore reduce the TC intensity. Adapted from *Khain et al.* [2010].

exhibited similar nonmonotonic behaviors to precipitation under different aerosol loadings (Figures 41a and 41d). Under a similar modeling framework, aerosol effects on precipitation for different regional-scale systems were further investigated, including a mesoscale squall line in the southern plains of the United States [*G. Li et al.*, 2009] and a wintertime storm over the North Pacific [*R. Zhang et al.*, 2007; *Li et al.*, 2008b]. In these scenarios, precipitation enhancement under polluted conditions was reported along with more efficient mixed-phase processes and intensified convection.

[95] *Lerach et al.* [2008] used the RAMS to study the impact of aerosol indirect effects on the development of a

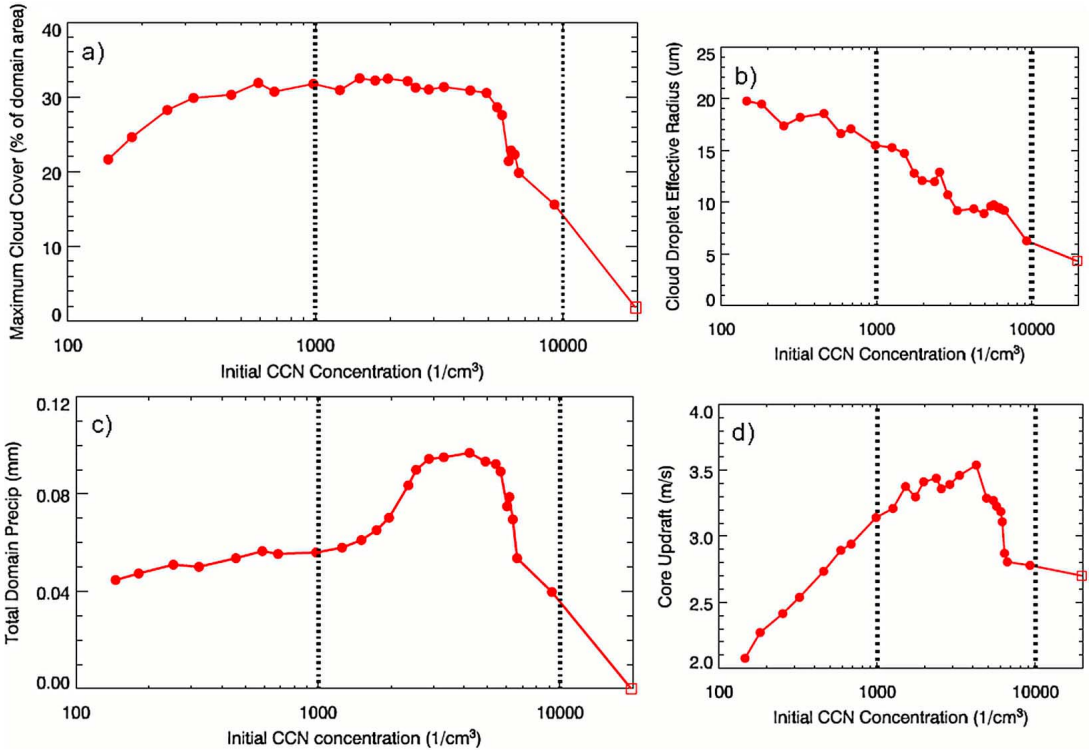

Figure 41. Modeled (a) maximum cloud cover, (b) cloud effective radius, (c) surface precipitation, and (d) core updraft as a function of the initial CCN. The number concentrations range from 200 to 50,000 cm^{-3}. Adapted from *Li et al.* [2008a].

supercell storm and its associated tornadogenesis. Their results indicated that a polluted environment (dust-laden CCN and GCCN concentrations of 2000 cm^{-3} and 0.2 cm^{-3}, respectively) would provide a favorable environment for tornadogenesis rather than a clean environment (clean continental CCN and GCCN concentrations). Their results indicated that both warm rain and cold rain are reduced in the polluted environment, and a longer-lived supercell is simulated. An EF-1 (surface wind speeds exceeding 40 m s^{-1}) tornado was produced due to weak evaporative cooling near updraft and downdraft interfaces close to the rear flank of the supercell. *Storer et al.* [2010] also made use of RAMS to simulate supercell development under clean and more polluted conditions. The aim of their study was to assess the relative importance of variations in convective available potential energy (CAPE) and aerosol concentration on the microphysical and dynamical characteristics of supercells (Figure 42). When comparing results from changes in CAPE and aerosol concentrations, they found that the total precipitation produced by storms is primarily driven by CAPE but that the increase in aerosol concentrations produced a decrease in total precipitation by 30–40%. Changes in the cloud water path are found to be much more sensitive to variations in aerosol concentrations than in CAPE, while changes in the ice water path are affected in a similar manner by changes in aerosol and CAPE. Other microphysical parameters such as the mean raindrop diameter demonstrated very little response to changes in CAPE but large responses to changes in aerosol concentrations. Finally, they concluded that a number of the aerosol indirect effects observed in their study were modulated by the amount of CAPE in the environment, with stronger aerosol effects in environments with weaker CAPE. Thus, both aerosol concentrations and environmental conditions need to be considered when assessing aerosol indirect forcing on deep convective storms.

[96] The regional-scale modeling studies also suggest that enhanced aerosol concentrations could either enhance or suppress precipitation processes and surface rainfall. These results are in good agreement with those of cloud-resolving modeling studies as shown in section 5.3.

5.5. IN Effect on Precipitation Processes

[97] Only a few CRMs have been used to study the effects of IN on precipitation processes because of the limited understanding of ice formation (see section 2). In addition, some aerosols can be transported by convective updrafts from the planetary boundary layer (PBL) to the middle and upper troposphere and can serve as IN [*Yin et al.*, 2005]. Because of this, it is very difficult to quantify the IN effect on precipitation processes. In addition, few of the previous CRMs were used to examine both IN and CCN effects on precipitation.

[98] *van den Heever et al.* [2006] showed that increasing either the GCCN or IN concentration produces the most rainfall at the surface, whereas enhanced CCN concentrations reduce surface rainfall. Higher IN concentrations produce ice at warmer temperatures and generate deeper anvils, but simultaneously increasing the concentrations of CCN and GCCN leads to more supercooled liquid water available for freezing and greater ice mixing ratios. Higher concentrations of GCCN and IN result in greater accumulated surface precipitation initially. By the end of the simulation period, however, the accumulated precipitation is the greatest for the case in which the aerosol concentrations are lowest. Their results suggested that such changes in the dynamical and microphysical characteristics of convective storms as a result of the variations in aerosol concentrations have potential climate consequences, through both the cloud radiative effect and the hydrological cycle.

[99] *Ekman et al.* [2007] studied the sensitivity of a continental storm to changes in IN concentration based on an observed case. They found that the increase in IN concentration, and thus heterogeneous nucleation, would generally result in enhanced updrafts due to latent heat release from the added diffusive growth of increased ice crystals. Such an effect was also identified to enhance homogeneous nucleation, i.e., to make CCN more effective in influencing ice nucleation. Since the dominant mechanism in providing ice particles for cirrus anvils in the modeled case is still homogeneous nucleation, the increase in IN concentration would lead to enlarged anvil coverage and increased precipitation. The finding of *Ekman et al.* [2007] suggests an interesting link between IN concentration and updraft strength and, consequently, homogeneous nucleation rate, anvil particle concentration, coverage, and radiation effects. It is also in qualitative agreement with observations made by *Heymsfield et al.* [2005].

[100] *Fan et al.* [2010b] studied the impact of different parameterization schemes on homogeneous nucleation and heterogeneous immersion nucleation for two isolated tropical deep convection cases. Similar to the finding of *Ekman et al.* [2007], they found that an increase in the immersion nucleation rate would lead to stronger convection, larger anvil coverage, and longer anvil lifetime. Precipitation and ice water path would both be enhanced under either wet or dry environmental conditions. Consequently, the homogeneous nucleation rate would also be enhanced, consistent with *Ekman et al.* [2007] and *Heymsfield et al.* [2005]. Note that *Ekman et al.* [2007] and *Fan et al.* [2010b] both mentioned the substantial uncertainty in modeled results due to various different schemes used to represent nucleation mechanisms, although such uncertainty does not seem to qualitatively affect their major conclusions. *Fan et al.* [2010a] also compared CCN and IN effects on convection and precipitation and found that the CCN effect is dominant. The IN effect does little to convection and precipitation, although ice microphysical properties could change significantly.

[101] *Zeng et al.* [2009a, 2009b] examined the effect of the ice crystal enhancement (IE) factor (defined as the ratio of the number of ice crystals to ice nuclei) on ice properties associated with tropical and midlatitude convective systems using a CRM. Their results showed that the IE factor in tropical clouds is about a thousand times larger than that in midlatitude clouds. This significant difference in the IE between the tropics and midlatitudes is consistent with

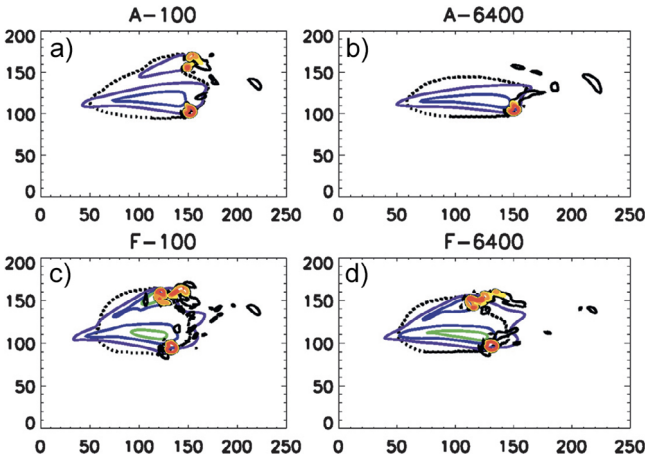

Figure 42. Model output showing storm development after 2 h in (a) the clean-aerosol (100 cm^{-3}) low convective available potential energy (CAPE) (491 J kg^{-1}) case; (b) the polluted-aerosol (6400 cm^{-3}) low-CAPE case; (c) the clean-aerosol high-CAPE (2828 J kg^{-1}) case; and (d) the polluted-aerosol high-CAPE case. The yellow, orange, and red contours are vertical velocity (5, 10, and 20 m s^{-1}) at 5.4 km above ground level. Purple, blue, and green contours represent total accumulated precipitation up to the current time (1, 10, and 20 mm, respectively). The dotted line is the outline of the cold pool at the surface. Adapted from *Storer et al.* [2010].

observations of stronger entrainment and detrainment in the tropics. However, surface precipitation is not affected by the change in IE as shown by *Fan et al.* [2010a].

6. LARGE-SCALE MODELING OF AEROSOL-PRECIPITATION EFFECTS

[102] On a global scale, aerosols could affect precipitation through microphysical and dynamical paths. The former path consists of a series of microphysical processes and microphysics-dynamics feedbacks, initiated by the activation of aerosols as CCN or IN. The resultant change in cloud radiation is commonly referred to as the indirect radiative forcing of aerosols [e.g., *Ramaswamy et al.*, 2001]. The dynamical path is implemented through changes in large-scale circulation by persistent aerosol direct forcing [e.g., *Wang*, 2004] or indirect forcing [*Ramaswamy and Chen*, 1997; *Rotstayn and Lohmann*, 2002]. The microphysical path would cause precipitation changes mainly confined to aerosol-laden regions, while the dynamical path could alter precipitation remote to these regions.

[103] To simulate the effects of aerosols on precipitation in a large-scale framework, models need to include the feedback of dynamical processes to aerosol forcing. The atmospheric transport model or chemical transport model, a commonly used tool to derive aerosol distribution and radiative forcing driven by prescribed meteorology, would not be useful for this purpose because of its lack of such feedbacks and for this reason is not discussed in this paper. In addition, recent advances in computational technology allow current CRMs to run efficiently over domains covering a continental scale. In fact, many details about regional modeling can be found in section 5. This section, therefore, concentrates on the efforts using global aerosol-climate models. The term aerosol-climate model is used in this section and refers to those general circulation models (GCMs), or global climate models as they are sometimes called, which include an aerosol module or simply include prescribed radiative effects of aerosols.

6.1. Major Methodology

[104] Precipitation is formed through a series of sophisticated processes with feedbacks involving aerosol physics and chemistry, cloud microphysics, and dynamics on different scales. It is located at the bottom of the "food chain" of aerosol-cloud processes, while serving as the largest sink of atmospheric aerosols. Many of these above processes occur on scales much smaller than the typical grid spacing of current global climate models. The first step toward modeling the effect of aerosols on precipitation using global climate models is thus to have a reasonable representation of aerosol processes in these models.

[105] The study of climate response to aerosol forcing requires long-term integrations using models on one hand equipped with needed details concerning aerosol processes and, on the other hand, having a good computational efficiency. In reality, mainly because of the computational cost, it has never been an easy task to include an interactive aerosol module in climate models to study the change in clouds and precipitation as a climate response to aerosol forcings. Therefore, an optimized balance between aerosol representation and model computational cost needs to be established. So far, the majority of research on modeling the climate impacts of aerosols has been conducted using models with prescribed aerosol profiles. This applies perhaps to all the GCMs that participated in the Fourth Assessment Report of the Intergovernmental Panel on Climate Change (IPCC AR4) [*Randall et al.*, 2007].

[106] The evolution of atmospheric aerosols can be represented by several important aerosol properties, such as size distribution, mixing state, and chemical composition. The size of an aerosol with a known chemical composition to a large extent determines both the optical and microphysical character of the particle. In many aerosol-climate models, particularly the earlier ones, only the aerosol mass mixing ratio was predicted. The size of aerosols in these models, when needed, was derived diagnostically using various empirical methods based on the predicted mass mixing ratio. In many such models, the radiative properties of aerosols were derived based on a given geometric size [*Haywood and Boucher*, 2000; *Penner et al.*, 2001; *Forster et al.*, 2007]. On the other hand, the mixing state of aerosols determines not only the value but also the sign of the radiative forcing of aerosols. Recent field experiments using single particle analysis have demonstrated the coexistence of external and internal mixtures in the atmosphere, and the latter is not always dominant [*Hara et al.*, 2003; *Schwarz et al.*, 2008; *Twohy et al.*, 2008] (also see section 3). From field

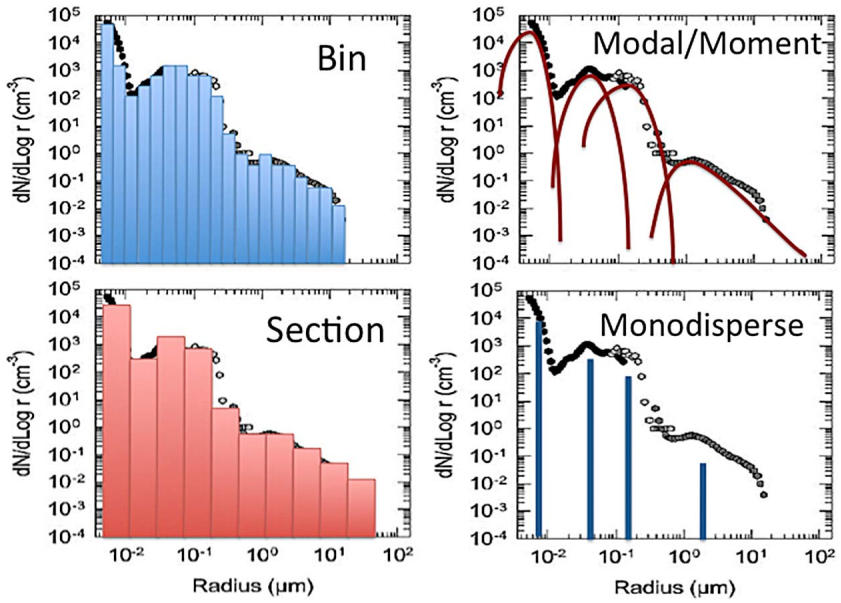

Figure 43. Diagram for various representations of aerosol size distributions in global models. Circles show an actual aerosol size distribution measured by *O'Dowd et al.* [2001], where four peaks in number concentration corresponding to different sizes appear. In bin and section models, the aerosol population properties would be approximated by predicted aerosol properties within various size bins (shown as colored vertical bars). For instance, the number concentrations of these size bins would derive the population size distribution as shown. In the moment method, the prediction would be based on a selected number of aerosol modes, each with a smooth distribution that can be defined by a distribution function (modal method) or using additional closures (moment method). In the monodisperse representation, aerosols corresponding to each mode are assumed to have the same size. Copyright Elsevier. Reprinted with permission.

experiments, internal mixtures containing an absorbing core (e.g., black carbon, or BC) coated by a scattering material [*Martins et al.*, 1998; *Pósfai et al.*, 1999; *Naoe and Okada*, 2001; *Okada et al.*, 2005; *Schwarz et al.*, 2008] are known to significantly enhance the bulk absorption per mass of aerosols compared to external mixtures of black carbon [*Ackerman and Toon*, 1981; *Horvath*, 1993; *Chýlek et al.*, 1995; *Bond and Bergstrom*, 2006; *Kim et al.*, 2008]. This specifically differs from the relatively well-mixed state of organic carbon (OC) and sulfate mixtures [e.g., *Okada et al.*, 2001; *Russell et al.*, 2002]. The majority of current aerosol-climate models include only external or internal mixtures. Among those models that include internal mixtures, a well-mixed assumption is usually adopted so that the radiative effects of aerosols are calculated using a volume-weighted refractive index over all predicted aerosol constituents [e.g., *Stier et al.*, 2005; *Kim et al.*, 2008].

[107] Increasing effort has been made in recent years to improve the representation of aerosols in GCMs (Figure 43). In a few studies where an aerosol model was used to predict number and mass concentrations of aerosol constituents in a series of relatively coarsely defined size bins, or sections [e.g., *Jacobson*, 2001; *Adams and Seinfeld*, 2002], the computational cost was still too high to include a series of multiple sections that could be internally as well as externally mixed in multiyear simulations. To reach a good balance between the computational burden and process details in climate impact studies, some of the current aerosol-climate models have adopted the multimoment approach [e.g., *Easter et al.*, 2004; *Vignati et al.*, 2004; *Liu et al.*, 2005; *Kim et al.*, 2008; *Bauer et al.*, 2008]. This method predicts multiple aerosol population properties including the number, mass, and size distribution (whether based on a prescribed type of function or not) of many aerosol modes (see Table 5 for a brief description of several selected models and Figure 44 for the model diagram of *Kim et al.* [2008]). Compared to the earlier mass-only model, or the "single-moment" scheme, the multimoment approach, when designed appropriately, improves the representation of aerosol size while remaining computationally efficient with the ability to perform multidecadal or even longer simulations.

6.2. Impact of Aerosols on Precipitation Through Microphysical Processes

[108] In global climate models, the representation of the impact of aerosols on cloud microphysics is generally implemented in a highly parameterized fashion due to the coarse spatial resolution of these models. Such a parameterization usually consists of two major steps: (1) the activation/nucleation of cloud droplets or ice crystals and (2) the "autoconversion" to convert small cloud droplets or ice crystals (typically from 10 to 100 μm in size) to precipitating hydrometeors, i.e., rain or snow (several hundreds of micrometers to a few millimeters). Note that the latter

TABLE 5. Examples of Size-Dependent Modules of Anthropogenic Aerosol in Global Interactive Aerosol-Climate Models

Model	Aerosol Model Type	Number of Aerosol Mode/Section	Mixing State	Typical Resolution	References
Stanford	sectional	17	all external or internal	4° × 5°, 22 layers	*Jacobson* [2001]
PNNL-MIRAGE	two-moment modal	4	all external or internal	2.8° × 2.8° (T42), 24 layers	*Easter et al.* [2004]
ECHAM-HAM	two-moment modal	7	all external or internal	1.8° × 1.8° (T63), 31 layers	*Vignati et al.* [2004], *Stier et al.* [2005]
MIT-NCAR	two-moment modal	7	external + core-shell + internal	2° × 2.5°, 26 layers	*Kim et al.* [2008]
PNNL/UMich/NCAR	two-moment modal	13	all external or internal	2° × 2.5°, 26 layers	*Wang et al.* [2009]
GISS-MATRIX	quadrature in moment, two-moment implementation	16	external + internal	4° × 5°, 23 layers	*Bauer et al.* [2008], *McGraw* [1997]

transition is a parameterization of a series of microphysical processes involving a random collection of small cloud droplets under the influence of updrafts or downdrafts and turbulent mixing at a subgrid-scale level.

[109] In fact, the majority of global aerosol-climate modeling efforts dealing with the microphysical impact of aerosols has focused on deriving the indirect radiative forcing of aerosols rather than studying the precipitation effect. The former task, in a model without explicitly predicting aerosol number concentration, would be done by using an empirical method to connect aerosol mass with CDNC, autoconversion rate, and precipitation efficiency to simulate various aerosol effects [*Rotstayn*, 2000; *Kiehl et al.*, 2000; *Menon et al.*, 2002; *Ming et al.*, 2005; *Penner et al.*, 2006; *Jones et al.*, 2007]. The aerosol-CDNC relationships used by different aerosol-climate models appear to agree with each other qualitatively and also with satellite estimations. However, the modeled results concerning the aerosol albedo effect, the cloud optical response to changes in aerosol level and thus CDNC, can vary significantly and also differ from satellite-based estimations. In addition, in performing more sophisticated tasks, such as simulating aerosol effects on cloud cover, height, lifetime, and outgoing longwave radiation that involve dynamic feedbacks, these models tend to disagree with each other even more evidently [*Quaas et al.*, 2009]. To date, the argument about whether the indirect forcing of aerosols should be treated as a forcing or a response still exists, and the estimation of such an effect remains one of the largest uncertainties in climate modeling. For more details about studies of indirect forcing of aerosols, the reader is referred to previous reviews including *Haywood and Boucher* [2000], *Ramaswamy et al.* [2001], and *Lohmann and Feichter* [2005].

[110] Several physics-based parameterizations for simulating the activation of liquid or ice cloud particles have been developed for global models [e.g., *Abdul-Razzak and Ghan*, 2000; *Nenes and Seinfeld*, 2003; *Kärcher and Lohmann*, 2003; *Liu and Penner*, 2005; *Barahona and Nenes*, 2007]. These schemes continue to benefit even the most up-to-date aerosol-climate models with improved aerosol and cloud microphysical representations. Efforts have also been made to include more physics-based descriptions of cloud microphysical processes beyond just the aerosol activation in the earlier generation of models. For example, *Rasch and Kristjánsson* [1998] and *Kristjánsson* [2002] introduced parameterizations of several microphysical processes into the Community Climate Model version 3 (CCM3) of the National Center of Atmospheric Research (NCAR), including autoconversion from cloud water to rain and from ice to snow and the collection of cloud water by rain and by snow. This implementation enables the model to simulate certain effects of aerosols on cloud droplet size and concentration and, most interestingly, on precipitation onset and quantity.

[111] As a major step forward, a two-moment microphysics scheme for cloud droplets and ice crystals has been developed recently for global climate models [e.g., *Lohmann et al.*, 1999, 2007; *Ming et al.*, 2007; *Morrison and Gettelman*, 2008; *Wang and Penner*, 2010] (see Table 6). The evaluation of these relatively comprehensive models is just beginning [*Gettelman et al.*, 2008; *Lohmann*, 2008; *Wang and Penner*, 2010]. This type of scheme requires that the model predict both mass and number concentration of a

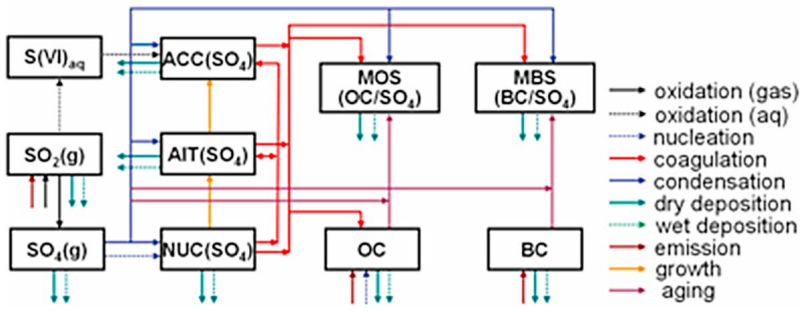

Figure 44. Diagram showing the size and mixing-state-resolving aerosol module. Adapted from *Kim et al.* [2008].

TABLE 6. Examples of Two-Moment Cloud Microphysical Schemes in Global Climate Models

Model	Hydrometeors Applied With Two-Moment Scheme	Cloud Type	Typical Resolution	Special Notes	References
ECHAM	cloud droplet, ice crystal	stratiform	2.8° × 2.8°, 19 layers	updraft perturbation using TKE and CAPE in nucleation	*Lohmann et al.* [1999, 2007]
GFDL	cloud droplet	convective and stratiform	2° × 2.5°, 24 layers	above-cloud base nucleation is estimated	*Ming et al.* [2007]
NCAR	cloud droplet, ice crystal	stratiform	1.9° × 2.5°, 26 layers	subgrid-scale variability is derived and applied to microphysical calculations	*Morrison and Gettelman* [2008], *Gettelman et al.* [2008]

given hydrometeor, i.e., the type of cloud particles categorized using size, phase, aggregate state, and often density. On the basis of the selected type of probability distribution function (PDF) for the size distribution of a given hydrometeor, and when the predicted number of moments equals the number of undefined parameters of the PDF, all microphysical conversions, along with the bulk motion characteristics of the hydrometeor, can be derived using integrations over size distributions that define various predicted moments. The effort to introduce the two-moment scheme for convective clouds in GCMs has just started. *Ming et al.* [2007] introduced a prognostic CDNC scheme in the convective parameterization of the Geophysical Fluid Dynamics Laboratory (GFDL) GCM. *Lohmann* [2008] tested a two-moment scheme for convective clouds in the ECHAM general circulation model. *Song and Zhang* [2011] tested a two-moment scheme including four hydrometeors for convective clouds using a single column climate model. Obviously, such a task is still very challenging due to the subgrid nature of convection in current climate models.

[112] The attempt to use a two-moment cloud microphysics scheme in GCMs is still in its early stage, and current schemes are still less comprehensive than their counterparts developed long ago for cloud-resolving models [e.g., *Wang and Chang*, 1993]. Nevertheless, by adopting such an approach, modeling aerosol effects on precipitation would become much more physics-based than in the earlier generation of models where only mass mixing ratios of hydrometeors were predicted. Especially when coupled with a size-dependent aerosol module, a two-moment cloud

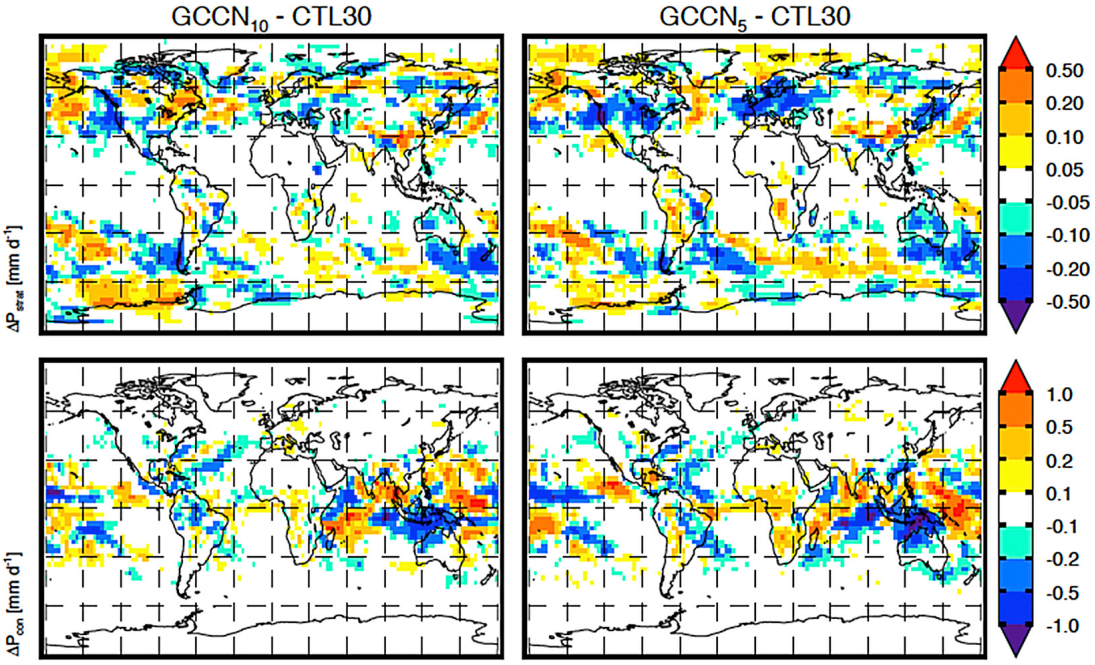

Figure 45. Differences in the global distribution of (top) stratiform and (bottom) convective precipitation between (left) GCCN10 and (right) GCCN5 simulations and CTL30 (note that different scales are used). In the GCCN10 case, the giant GCCN is defined as aerosols larger than 10 μm in radius, whereas in the GCCN5 case, it is defined as larger than 5 μm in radius. The results show that when more GCCN are available (GCCN5 case), both convective and stratiform precipitation would have larger regional scale changes, which could be interpreted as a reflection of a faster atmospheric water cycle. Note that these simulations were conducted using a prescribed climatological sea surface temperature. Adapted from *Posselt and Lohmann* [2008].

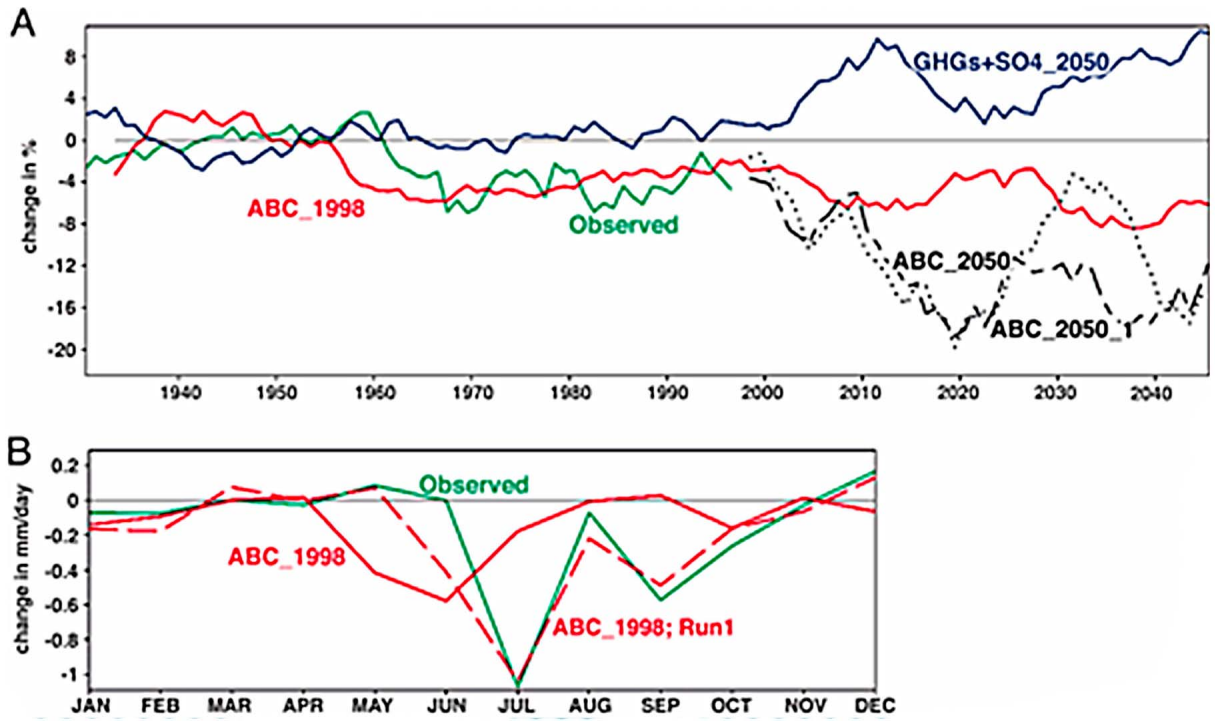

Figure 46. (a) Time series of observed and simulated summer (June–September) rainfall for India from observations and parallel climate model simulations. The results are the percent deviation of rainfall from the 1930–1960 average. Observed rainfall data were obtained from *Parthasarathy et al.* [1995]. The data are smoothed by an 11 year running mean average. (b) Trend in monthly mean rainfall from 1930 to 2000 over India. The uncertainty of the model trend, as estimated from five realizations, is ∼0.4 mm/d from May to July and <0.2 mm/d in the other months. For the observed trend, the 95% confidence level is ±0.9 mm/d (wet season) down to ±0.2 mm/d (January–March). The results demonstrate that only after including the effect of the Asian brown cloud (ABC; an atmospheric layer containing anthropogenic absorbing aerosols) in the model could the predicted precipitation reproduce the measured decreasing trend over the Indian subcontinent. Adapted from *Ramanathan et al.* [2005].

microphysics scheme provides a connection between the predicted number concentration of CCN by the aerosol module and predicted CDNC by the cloud microphysics module. Along with the two-moment scheme, subgrid-scale variability has also been introduced to further improve the modeled microphysical features of *Morrison and Gettelman* [2008], where the variability of cloud water is represented by a PDF derived from observations and extended to all related microphysical conversions.

[113] Studies have demonstrated that with the two-moment scheme, models tend to produce global total precipitation closer to observations than the previous generation of schemes [e.g., *Lohmann et al.*, 2007; *Gettelman et al.*, 2008]. On the other hand, in representing the formation of raindrops, a random process involving the collection of smaller cloud droplets, models with the two-moment scheme still need to include a parameterization of autoconversion and subsequent accretion growth of precipitation particles. This parameterization thus remains a major tuning job for simulating the effect of aerosols on precipitation. A recent sensitivity study demonstrated that by allowing raindrops to form directly from the activation of GCCN (a hypothesized path), the modeled hydrological cycle would become faster, compared to the case without such a path; this was manifested by faster rainfall and lower atmospheric water vapor content, although the total precipitation amount did not change much [*Posselt and Lohmann*, 2008] (also see Figure 45). Early attempts to bring the two-moment cloud microphysical scheme into the convection parameterization of GCMs have also identified the impact of aerosols on modeled precipitation features. *Lohmann* [2008] found that using the two-moment scheme and incorporating prescribed aerosol emissions could improve the modeled geographical distribution of precipitation changes from the past to the present climate when compared to observations. *Song and Zhang* [2011] found that the two-moment scheme alters the precipitation partition between convective and stratiform portions of modeled clouds, actually leading toward a ratio that is closer to observations than results derived using a simpler microphysical scheme. Both studies have identified a suppression of convective precipitation due to enhanced aerosol concentrations.

[114] Despite the advancement in introducing physics-based aerosol and cloud schemes into GCMs, verification of modeled precipitation changes due to aerosol microphysical effects remains a challenge. This issue inherits the problem in determining the reference state for the preindustrial climatology of CDNC, a result that is much needed for

TABLE 7. Brief Descriptions of Selected Modeling Studies That Address Aerosol Effects on Indian Summer Monsoon

Study	Climate Model	Aerosol Treatment	Aerosol Effect on Rainfall	Notes
Ramanathan et al. [2005]	NCAR PCM, coupled AOGCM	prescribed forcing based on observations or emission estimations	reduced in India as a total	ocean-land temperature gradient change by aerosols
Lau et al. [2006]	NASA fvGCM, prescribed 10 year SST observations	prescribed 3-D aerosol profile from CTM	increase in northern India and Bay of Bengal	"elevated heating pump"
Meehl et al. [2008]	NCAR CCSM3, coupled AOGCM	prescribed black carbon distribution based on CTM	enhanced during premonsoon while decreased during monsoon season over India	ocean-land temperature gradient by black carbon aerosols
Randles and Ramaswamy [2008]	GFDL GCM, prescribed climatological SST	prescribed based on offline calculations	enhanced in northwestern India during monsoon season due to absorbing aerosols	
Wang et al. [2009b]	NCAR CAM3 coupled with slab ocean	prognostic, size, and mixing dependent	northward switch in premonsoon season, northwest switch in monsoon season, both due to absorbing aerosols	absorbing aerosol alters large-scale stability by perturbing subcloud layer moist static energy over India
Collier and Zhang [2009]	NCAR CAM3, prescribed SST	prescribed based on CTM	enhanced during premonsoon season in central India, reduced in monsoon season	negative feedback to monsoon rainfall of the enhancement in clouds and precipitation during premonsoon

estimating the anthropogenic enhancement to cloud radiative forcing in the present day [e.g., *Rotstayn and Penner*, 2001; *Wang and Penner*, 2009]. For instance, models often introduce a lower bound to avoid low values of CDNC. This results in a spatially uniform distribution of CDNC, which leads to a substantial underestimation of the aerosol effect on cloud albedo [*Hoose et al.*, 2009]. In addition, more advanced schemes for aerosol and cloud microphysics also introduce new parameters. This would potentially add to the difficulty in examining whether the aerosol-cloud-precipitation microphysical effect would be able to explain some known variability in precipitation.

6.3. Impact of Aerosols on Precipitation Through Coupling With Large-Scale Dynamics

[115] The direct radiative forcing (DRF) of anthropogenic aerosols involves scattering and absorbing of solar radiation, or absorption and emission in the longwave radiation spectrum. The latter is only effective for large particles such as dust and will not be discussed much here. The optical effects of aerosols exert a negative forcing (cooling) at the Earth's surface by both scattering and absorbing solar radiation, and a positive forcing (warming) to the atmosphere by absorption. Because of their short lifetime of about 1 week, aerosols created from anthropogenic activities tend to concentrate over source regions or surrounding areas and hence apply a persistent forcing in these places.

[116] This type of persistent forcing can perturb atmospheric thermodynamic and dynamical processes and therefore influence precipitation-producing cloud systems in regions away from aerosol-laden areas. For example, studies using different GCMs all indicate that the direct radiative forcing of absorbing BC aerosols can lead to a northward shift of precipitation in the ITCZ, specifically over the Pacific Ocean [*Wang*, 2004; *Roberts and Jones*, 2004; *Chung and Seinfeld*, 2005]. *Ramaswamy and Chen* [1997] and *Rotstayn and Lohmann* [2002] both found that by including aerosol indirect forcing in their models, the dynamical consequence of such a forcing could have a remote impact on ITCZ precipitation, i.e., a shift in a direction opposite that caused by BC. An active research field aimed at understanding the effects of aerosols on precipitation through coupling with large-scale dynamics has developed. Current results indicate that the precipitation change caused by aerosols through this optical-thermodynamic-dynamical linkage is likely to be significant and could also be nonlinearly related to the aerosol forcing strength [e.g., *Wang*, 2007, 2009].

[117] Studies of the impact of aerosols on monsoon systems are rapidly growing. Correlations between estimated precipitation and circulation changes with the increasing trend of aerosols have unquestionably fueled the research in this direction [*Ramanathan et al.*, 2005] (see also Figure 46). Most of the studies are conducted using three-dimensional atmospheric GCMs or atmosphere–ocean coupled global circulation models (CGCM), which include either an interactive aerosol module or prescribed aerosol profiles. Paired simulations, which include and exclude aerosol effects, or include reference and altered aerosol profiles, allow comparisons to be made of the climate response to different aerosol forcing assumptions. Aerosol effects would be isolated, barring the assumption that model artifacts in simulating the monsoon system would not be significantly amplified by using different aerosol profiles. Model representations of aerosols and aerosol-climate interactions vary from study to study.

[118] The impact of aerosols, particularly absorbing aerosols, on the Indian summer monsoon has been extensively studied using models [*Ramanathan et al.*, 2001b; *Chung et al.*, 2002; *Ramanathan et al.*, 2005; *Lau et al.*, 2006, 2008; *Meehl et al.*, 2008; *Randles and Ramaswamy*, 2008; *Wang et al.*, 2009b; *Collier and Zhang*, 2009; *Krishnamurti et al.*, 2009; *Manoj et al.*, 2010]. Analyses looking at total precipitation over India mostly indicate an aerosol-caused decrease in rainfall during the summer monsoon season and

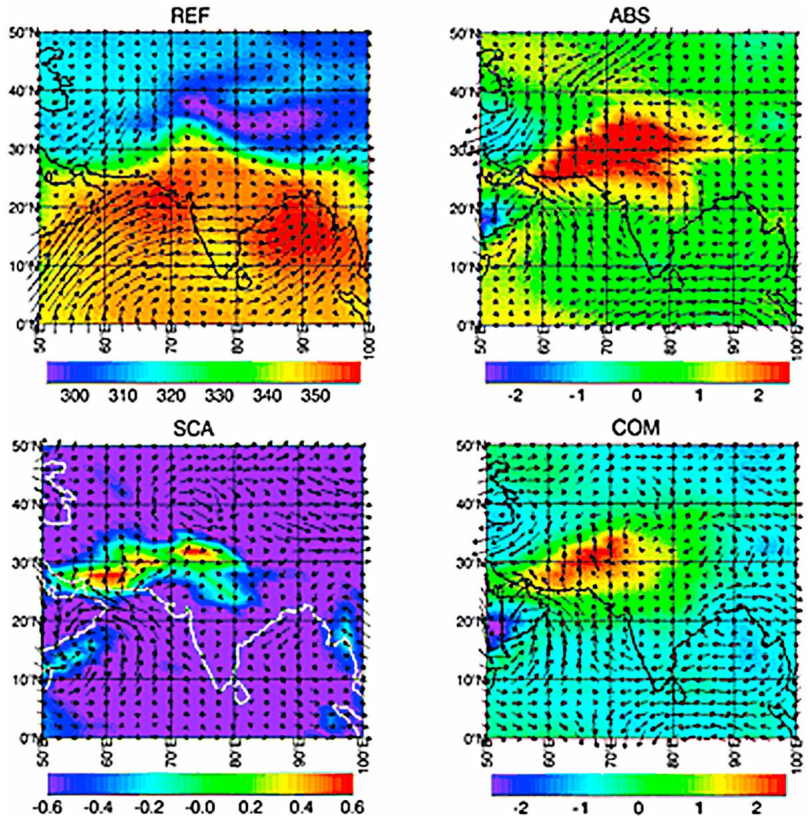

Figure 47. May–June mean wind and moist static energy (MSE) in the reference run (REF) that excludes the aerosol radiative effect. Also shown are the anomalies in May–June mean wind and MSE compared to the REF results derived from three model runs with radiative effects of (1) both scattering and absorbing aerosols (COM), (2) only absorbing aerosols (ABS), and (3) only scattering aerosols (SCA). All the aerosol chemical and physical processes in these three runs are the same. Data shown are averaged values for the lowermost three atmospheric layers based on year 41–60 means. The unit for the wind vector is 1 m s^{-1}. Moist static energy is in 10^3 J kg^{-1}. Note that in the three anomaly plots, a different color scale is used in SCA. A terrain correction has been applied to the REF result. The influence of absorbing aerosols is reflected in a perturbation to the moist static energy in the subcloud layer as shown in both ABS and COM cases. In comparison, the perturbation in the SCA case (due to the weak solar absorption of organic carbons) appears to be much smaller. Adapted from *Wang et al.* [2009b].

an increase during premonsoon and onset seasons. Several studies that analyzed precipitation patterns further suggested more complicated features, such as an increase in monsoon rainfall in certain regions, e.g., northwestern India. While qualitative and quantitative details may differ among them, these modeling studies all conclude that BC radiative forcing is large enough to perturb the Indian monsoon system and alter the precipitation pattern and amount in a statistically significant manner (see Table 7).

[119] Various mechanisms by which the direct radiative forcing of absorbing aerosols (solar heating of the atmosphere and dimming at the surface) modifies the monsoon circulation and rainfall have been suggested in modeling studies. *Wang et al.* [2009b] indicated that absorbing aerosols, whether coexisting with scattering aerosols or not, can alter the meridional gradient of moist static energy (MSE) in the subcloud layer over the Indian subcontinent, initiating heating of the PBL air and thus changing large-scale atmospheric stability (Figure 47). This would cause a northward extension of the monsoonal circulation and convective precipitation, which coincidently is in general agreement with observed monsoon precipitation changes in recent decades, particularly during the onset season (Figure 48). Such a pattern change is also in agreement with results produced in another study using a coupled atmosphere–ocean model although a prescribed aerosol profile was used [*Meehl et al.*, 2008] (see Figure 49). *Lau and Kim* [2006] proposed that the heating of absorbing aerosols on the slope of the Tibetan Plateau could initiate a positive feedback by drawing water convergence from oceans first and then form condensation and thus further heat the air over these elevated places; this is referred to as the "elevated heat pump" effect (EHP; see Figure 50). *Ramanathan et al.* [2005] suggested that aerosols could cause a decrease in surface evaporation (due to the dimming effect) and in the meridional sea surface temperature gradient. These two factors would affect monsoonal circulation and rainfall strength. The relative importance of these various mechanisms requires further research [*Lau et al.*, 2008].

[120] The potential impact of aerosols on the East Asian monsoon in winter was studied by *Niu et al.* [2010]. There is

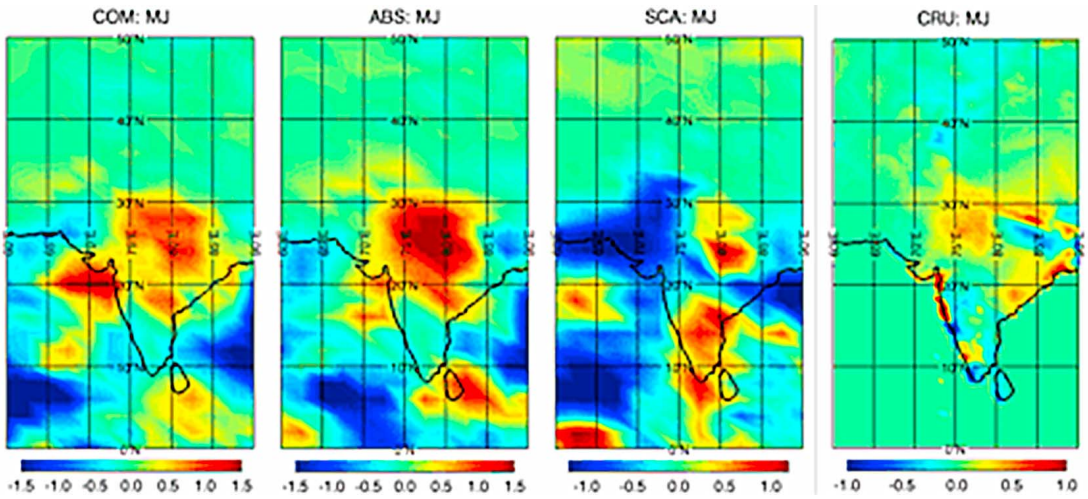

Figure 48. May–June (MJ) average changes in convective precipitation (dm season^{-1}) for India and surrounding regions derived from COM, ABS, and SCA runs (see Figure 47 for explanations). Also shown is the observed precipitation change (land only; dm/season) derived from data from the Climate Research Unit (CRU) of the University of East Anglia. Model results shown are based on year 41–60 mean differences with a reference run (REF) that excludes all aerosol effects. CRU results are derived from differences between 20 year means of 1981–2000 and 1946–1965 and based on the version 2.1 data set with 0.5 degree. Aerosol levels were derived based on present-day emission estimations. The effect of absorbing aerosols as shown in COM and ABS shows a northward precipitation shift that coincides with the observed precipitation pattern change reflected in CRU data. Adapted from *Wang et al.* [2009b].

a strong indication that the winter monsoon circulation that brings cold air from northwest to southeast China (the Siberian high-pressure system) has weakened significantly, resulting in noticeable increases in humidity and foggy days and decreases in wind speed and number of cold air outbreaks in China. Such trends are consistent with those simulated by the NCAR/CAM3 by including and removing the radiative effect of aerosols. Changes in the pattern of mean winter atmospheric pressure and airflow from the National Centers for Environmental Prediction (NCEP) reanalysis bear a close resemblance to those from the two types of simulations. This provides indirect evidence that aerosols may play a role in the development of the winter monsoon because aerosols diminish the surface radiation budget and reduce the thermal contrast between high and low latitudes and between ocean and land surfaces.

[121] The impact of aerosols on another monsoon system, the West African Monsoon (WAM), has also been studied. *Huang et al.* [2009] compared observational results with a global model simulation that included only direct radiative forcing of BC [*Wang*, 2004]. Both observations and model simulations showed that anomalously high African aerosol loading during boreal cold seasons was associated with significant reductions in cloud amount, cloud top height, and surface precipitation. This result suggests that the observed precipitation reduction in the WAM region is caused by the radiative effect of absorbing BC. The mechanism for this reduction, however, remains a mystery. In connection to the hypothesis of the aerosol-Indian summer monsoon effect proposed by *Wang et al.* [2009b], *Eltahir and Gong* [1996] found a correlation between WAM strength and the subtropical meridional gradient of subcloud MSE. So a similar mechanism could also explain the aerosol-WAM effect. Recently, *Lau et al.* [2009] used a GCM to show that the EHP effect due to Saharan dust and biomass burning BC has a significant impact on the climate and water cycle of the North Atlantic and the WAM. They found that during the boreal summer, as a result of large-scale atmospheric feedback triggered by absorbing aerosols, rainfall and cloudiness are enhanced over the West African/eastern Atlantic ITCZ and suppressed over the western Atlantic and Caribbean regions. This is related to the elevated dust layer that warms the air over West Africa and the eastern Atlantic and thus causes the air to rise. The response reflects a strengthening of the WAM, manifested in a northward shift of West African precipitation over land, increased low-level westerly flow over West Africa at the southern edge of the dust layer, and a near-surface westerly jet underneath the dust layer over the Sahara (Figure 51).

[122] The anthropogenic aerosol level in the Southern Hemisphere is lower than in the Northern Hemisphere. Therefore, the impact of local aerosols on the Australian monsoon system is expected to be relatively insignificant. However, since monsoon systems are closely associated with large-scale circulation, aerosol effects in the Northern Hemisphere could influence Southern Hemispheric circulation and thus precipitation by altering general circulation patterns. *Rotstayn et al.* [2007] hypothesized that Asian aerosols could lead to an increase in both rainfall and cloudiness over northwestern Australia, which would coincide with the observed rainfall trend in the region since the 1950s. They suggested that this would happen because the meridional

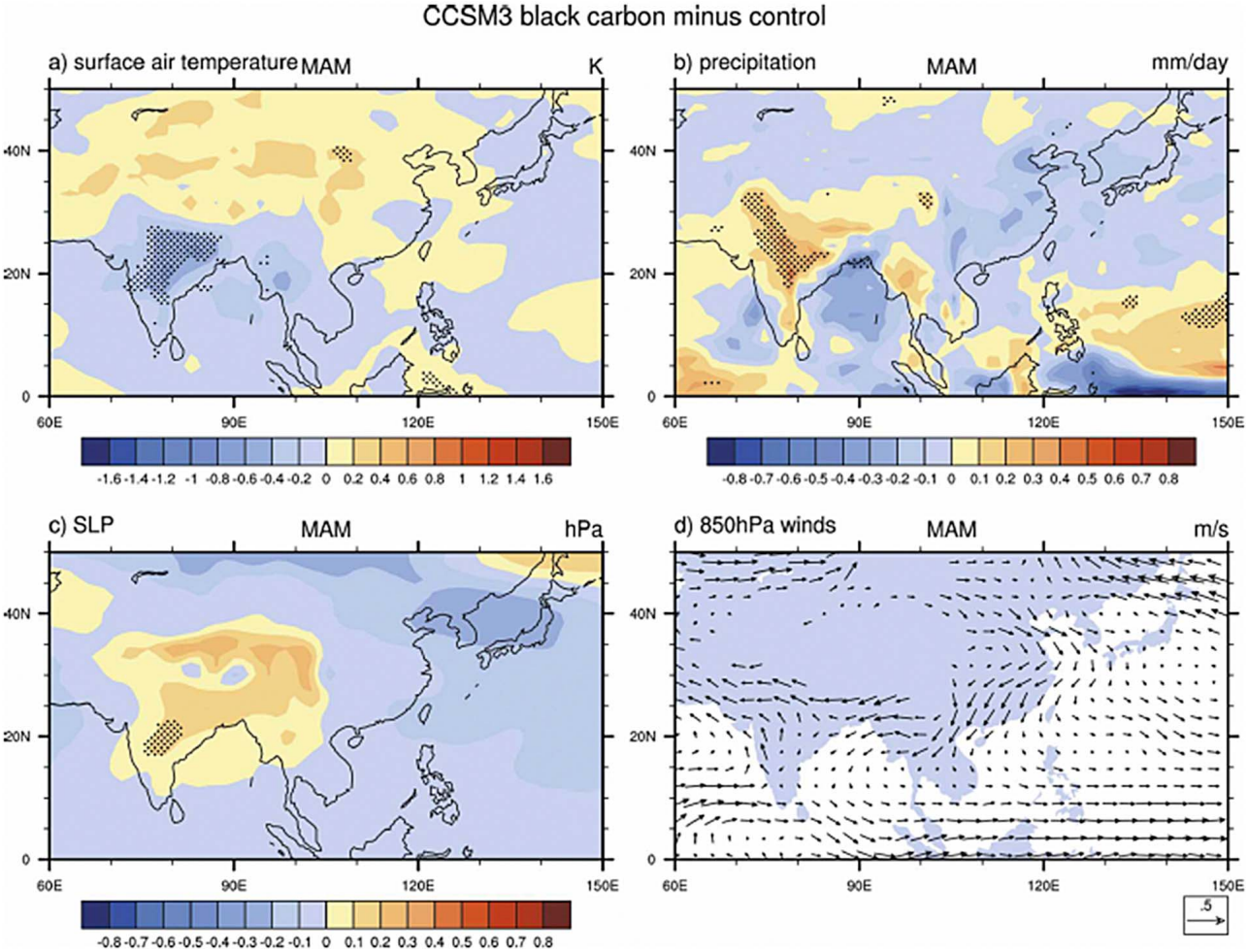

Figure 49. Effects of black carbon (BC) aerosols during the premonsoon season of March-April-May (MAM) on (a) surface air temperature (°C), (b) precipitation (mm d^{-1}), (c) SLP (hPa), and (d) 850 hPa winds (scaling vector of 0.5 m s^{-1} at bottom right). Stippling indicates areas where the ensemble mean signal divided by the interensemble standard deviation exceeds 1.0. Adapted from *Meehl et al.* [2008].

temperature gradient over the tropical Indian Ocean would be altered by Asian aerosols, which would further enhance monsoonal circulation toward Australia. A recent analysis of twentieth-century modeling results from 24 models participating in the Coupled Model Intercomparison Project Phase 3 (CMIP3), however, does not provide support to the above hypothesis [*Cai et al.*, 2010]. Despite the inclusion of either direct or both direct and indirect aerosol forcings in these models, their ensembles did not produce the hypothesized rainfall increase in northwestern Australia.

7. CURRENT AND FUTURE RESEARCH ON AEROSOL-PRECIPITATION INTERACTIONS

[123] We have described the impact of aerosols on precipitation systems from the perspective of microphysical processes, observational evidence, and a range of numerical model simulations. We have also described the discrepancies between results simulated by models, as well as those between simulations and observations. Understanding these discrepancies is a necessary step toward further resolving aerosol effects on cloud microphysics, dynamics, and precipitation within climate systems.

[124] From the discussion presented in sections 3–6, it is clear that isolating the aerosol effect on precipitation from other factors is still a challenge and that each of the current attempts to tackle this issue has its own advantages and disadvantages. Large-scale diagnosis of the aerosol effect on precipitation, through CCN, GCCN, and IN, is incomplete without considering microphysics (cloud, aerosol, and precipitation), cloud dynamics (life cycle), and the large-scale background environment (dynamical and thermodynamical forcing, radiative feedbacks, aerosol transport, and the water budget).

[125] Nevertheless, progress has been made in cloud microphysics involving CCN, GCCN, and IN, and their impact on clouds and precipitation ranging from the cloud scale to larger scales. Numerical models have assisted the physical interpretation of mechanisms associated with the aerosol-precipitation interaction. It is still quite difficult to quantify various aerosol effects on precipitation from either modeling or observational studies alone [*Khain et al.*, 2008;

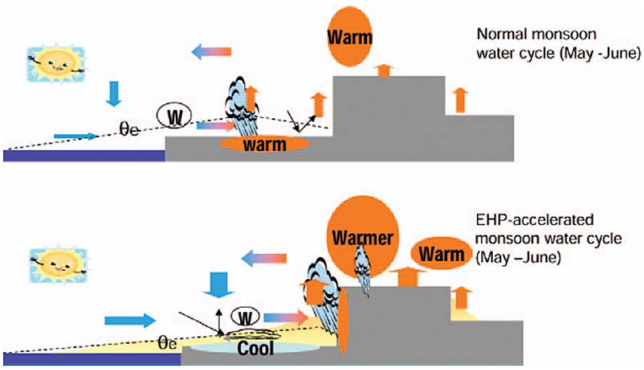

Figure 50. Schematic showing the monsoon water cycle with (top) no aerosol forcing and (bottom) the aerosol-induced "elevated heat pump" effect. W denotes the low-level monsoon westerly. The dashed line indicates the magnitude of the low-level equivalent potential temperature θe. Deep convection is indicated over regions of maximum θe. Adapted from *Lau et al.* [2008].

Stevens and Feingold, 2009; *Koren et al.*, 2010b]. Combining observations and modeling enables us to achieve a better understanding of the responses of cloud and precipitation to aerosols and their interactive feedbacks. The following summarizes the remaining scientific challenges and issues regarding aerosol-precipitation interactive processes.

7.1. Microphysics

[126] The fundamentals of the aerosol effect on cloud and precipitation formation are based on the concepts of CN activation into cloud drops and IN nucleation into cloud ice. The former can be described by Köhler curves, presuming that information such as the size distribution and chemical activity coefficient is known. Such information can be derived from measurements, so that aerosol properties can be prescribed accordingly in cloud models. However, prescribing aerosol properties is only suitable for case studies and not for simulations with durations longer than the lifetime of aerosols, which is about a few days. More elaborate simulations should be done by coupling the CRM with a detailed aerosol model that has the capability of resolving particle sizes, chemical compositions, and mixing state. The coupling must be done in such a way that the effects of cloud on aerosols, including aerosol scavenging and aerosol-recycling and even cloud chemistry, can be simulated simultaneously along with aerosol effects on cloud microphysical features.

[127] IN nucleation is much less understood than CN activation. The main difficulty comes from the poorly quantified properties of IN including their concentration, variety, and ice- nucleating capability. Measurement of these IN properties is still quite lacking, so even empirical descriptions of ice nucleation are tentative for most regions. A prognostic description of IN is possible and should also be incorporated into CRMs with a detailed aerosol model.

[128] Another area that needs further improvement is the cloud microphysical sensitivity to aerosol effects. Many bulk water schemes crudely simplify the collision efficiency between cloud drops and precipitation particles, so the effects of aerosols on cloud drop size and thus collision growth processes cannot be fully resolved.

7.2. Cloud-Scale Modeling

[129] In almost all previous cloud-resolving modeling studies, idealized or composite [e.g., *van den Heever et al.*, 2006] CCN concentrations were used in the simulations. Furthermore, the spatial distribution of CCN was assumed to be uniform, at least horizontally. A nonhomogeneous CCN distribution, consistent with nonhomogeneous initial meteorological conditions, is required to assess aerosol-

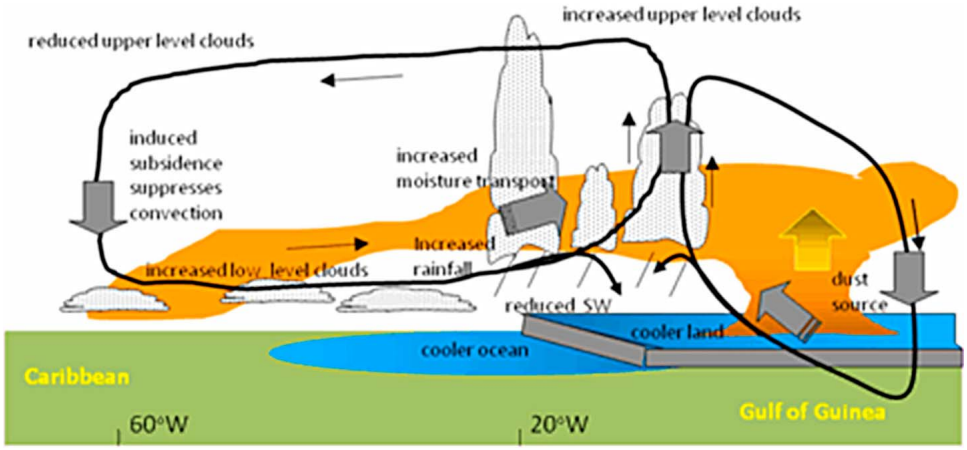

Figure 51. Schematic showing key features in the latitude domain of 5°N–15°N, associated with the "elevated heat pump" mechanism by radiative heating of Saharan dust: anomalous Walker-type and Hadley-type circulations; increased moisture transport from the eastern Atlantic and the Gulf of Guinea to West Africa; enhanced rainfall over the Sahel and the ITCZ off the cost of West Africa; subsidence and suppressed cloudiness in the central Atlantic and Caribbean and the Gulf of Guinea; and cooling of the West African Monso land and the upper ocean in the eastern Pacific underneath the dust plume. Adapted from *Lau et al.* [2009].

precipitation interactions using regional-scale models in the future. In addition to IN and GCCN, the chemistry of CCN needs to be considered in future modeling of aerosol-precipitation interactions. For example, *Fan et al.* [2007b], [*Ekman et al.*, 2004, 2006], and *Lee et al.* [2009b] found that aerosol chemical composition along with aerosol physics could affect precipitation processes.

[130] Furthermore, almost none of these CRM studies fully compared model results with observed cloud features such as dynamical and microphysical profiles, cloud extent, evolution of organization, radar reflectivity, and rainfall. This instantly raises the issue of gathering more data, perhaps through major field campaigns, that are suitable to both initialize model simulations (with meteorological and aerosol parameters) and validate model results (i.e., in situ cloud property observations, radar, lidar, and microwave remote sensing). Even though CRM-simulated results have provided valuable quantitative estimates of the indirect effects of aerosols, one needs to realize that these CRMs can only simulate clouds and cloud systems over a relatively small domain, for short periods, and under constraints given by specified large-scale meteorological conditions. Some CRM domains are too small to resolve whole clouds or precipitation systems. Close collaborations between the global and CRM communities are needed in order to explore how to extend CRM results to a regional and global perspective.

[131] Identifying regime-specific sensitivities using satellite data, in situ observations, and high-resolution, fine-scale modeling is a promising approach to improving the representation of clouds in larger-scale climate models [*Stevens and Feingold*, 2009].

7.3. Large-Scale Modeling

[132] As a critical factor determining climate response and feedback, the role of aerosols in influencing precipitation is undoubtedly a key issue in climate research and prediction. The future direction of global-scale research regarding this should focus on improving the model representation of aerosol-cloud related processes and, perhaps more important, observational constraints for aerosol-climate modeling. An immediate consequence of model advancement in spatial resolution and process representations is the realization that observation data at high resolution is required for model initialization and verification. Clearly, all currently available global-scale measurement networks do not necessarily meet this requirement. Further study of how to provide constraints for high-resolution global climate models is needed.

[133] With the rapid advancement in computational technology, climate models will step into an era of fast development. To better represent the effects of aerosols on clouds and precipitation, size-dependent cloud microphysics schemes along with size- and mixing-dependent aerosol schemes should be adopted in more models and used in long-term climate integrations. One issue that has remained in global climate modeling ever since its earliest days is the parameterization of convection. Because the requirement of several-kilometer resolution to resolve convection has been outside of the realm of possible resolutions for global climate models (and will likely still be the case in the near future), descriptions of convection processes along with aerosol-cloud-precipitation physics in these models have been empirically formulated using parameters resolved at model grid scales. Though still computationally expensive, today's global cloud-resolving models [i.e., *Tomita et al.*, 2005; *Miura et al.*, 2005; *Nasuno et al.*, 2008] are already being run in an exploratory manner and perhaps will reach the stage of performing long-term integrations with computationally more practical expenses earlier than one would expect. Recently, *Grabowski and Smolarkiewicz* [1999], *Khairoutdinov and Randall* [2001], and *Randall et al.* [2003] proposed a multiscale modeling framework (MMF) that replaces conventional cloud parameterizations with a CRM in each grid column of a GCM. The MMF can explicitly simulate deep convection, cloudiness and cloud overlap, cloud-radiation interactions, surface fluxes, and surface hydrology at the resolution of a CRM. It also has global coverage and two-way interactions between the CRMs and the parent GCM; initial simulations with aerosol-cloud interactions within a MMF have been performed [*Wang et al.*, 2011]. The MMF could be a natural extension of current cloud-resolving modeling activities. MMFs can also bridge the gap between traditional CRM simulations and nonhydrostatic global cloud-resolving models. Another less computationally demanding way of addressing the issue would be the development of an MMF approach that couples a global aerosol-climate model with a cloud-resolving model and detailed interactions between clouds, precipitation, and aerosols. Various cloud-related parameterizations in GCMs can be improved by using CRMs over selected regional domains within a MMF framework [e.g., *Lee et al.*, 2009].

[134] In addition to the cloud-resolving issue, many critical and nonlinear aerosol chemical and physical processes also occur on scales much smaller than the grid size of current global models, and so they need to be treated more carefully in these models. Sophisticated air quality models have been used recently to develop a reduced format model of urban aerosol processing under various environmental conditions, leading to much improved and computationally efficient representations of subgrid nonlinear aerosol processes in global models [*Cohen et al.*, 2011].

[135] Despite the progress in model development and computational technology, uncertainties in modeling aerosol-cloud-precipitation processes will always exist. Therefore, identifying and thus minimizing such uncertainties remains a constant task in the field. Attempts to use various inverse modeling skills in global model frameworks to optimize emissions of aerosols and aerosol precursors have been reported in the literature but are still at an early stage [e.g., *Collins et al.*, 2001; *Zhang et al.*, 2005; *Dubovik et al.*, 2008]. Further in-depth analyses on model process uncertainties require a very high computational demand that is still difficult to meet. Alternatively, the reduced format model of a given global aerosol-climate model could be derived through a limited number of simulations of the global model under a certain statistical framework [e.g., *Tatang et al.*, 1997]. The reduced format model is much more

computationally efficient, so it can be used in a full-scale parametric uncertainty analysis to mimic the behaviors of the global aerosol-climate model although with some limitations.

[136] Examining the effects of aerosols on precipitation remains a challenging task. Because of multiscale dynamical feedbacks involved in aerosol-cloud-precipitation connections, a global modeling framework might be needed for many cases to address such an issue. The effort using the so-called detection and attribution technique with GCMs to identify various aerosol effects is still at an early stage and mainly limited to aerosol-induced temperature changes [e.g., *Jones et al.*, 2011]. Applying the same skill to identify the aerosol-induced precipitation change is obviously much more difficult but should be considered in the near future. On the other hand, the effects of aerosols on precipitation can be examined at regional scales for certain weather regimes by combining relatively long-term high-quality measurements (e.g., the ones from the DOE ARM project) and process models [*Li et al.*, 2011a].

7.4. Observations

[137] Observations provide both initial conditions and validation data for models. The current generation of cloud-resolving models include reasonable, albeit not complete, microphysical parameterizations and can simulate the microphysical, dynamical, and chemical evolution during the life cycle of cloud systems. These models can also be used to explicitly calculate interactions between clouds, aerosols, and precipitation. However, all these advancements have raised challenging issues for corresponding measurements. Because of the range of scales involved in modern cloud modeling efforts, space-based remote sensing has served as an ever more necessary part of model validation.

[138] The availability of high-resolution surface precipitation data, compiled from satellite retrievals and surface rain gauge measurements in the recent two decades, has generally improved, though there is still a shortage of data. Still, how to detect aerosol signals along with clouds and precipitation, and specifically how to attribute the signal to the microphysical effects of aerosols, remains a topic that has barely been touched upon. Well-designed field campaigns and data analysis (e.g., for ARM sites) are required in the future to address this issue.

[139] Since more variables for the study of aerosol-cloud-precipitation interactions are available from both satellite (e.g., A-Train) sensors that provide global coverage and enhanced special ground-based observations (e.g., ARM) that provide a rich source of information, it is possible to investigate the climatological effects of aerosol-cloud-precipitation interactions beyond case-by-case studies, as demonstrated by *Li et al.* [2011a] and *Niu and Li* [2011]. If numerical models with adequate physics could reproduce such results obtained from very large ensembles of observations, it would provide solid evidence of the net ACPI effect that is currently still missing but of considerable climatological significance.

[140] Enlightened by the role of absorbing aerosols revealed in recent studies, measurements of the absorption strength and the spatial distribution of absorbing aerosols are still rare and should be specifically improved to validate model results [*Wang et al.*, 2009a; *Chin et al.*, 2009]. The most urgent need is to specify the vertical profile of aerosol absorption at least over highly polluted regions, which is a key indicator of the effects of absorbing aerosols in altering atmospheric stability and in governing the interaction and feedback between aerosols and atmospheric dynamics. Another much needed piece of information is global measurements of particle number concentration of both aerosols and cloud particles. Field experiments have provided and will continue to provide critical observational data in this regard. Current global networks including Aerosol Robotic Network (AERONET) and such satellites as Cloud-Aerosol Lidar and Infrared Pathfinder Satellite Observation (CALIPSO) and CloudSat provide valuable information about the optical properties of aerosols or its loading in terms of total extinction, but they do not convey any direct information about aerosol number concentration, size distribution, and chemical composition, which are key to understanding CCN effects. Out of necessity, AOD has been employed in large-scale modeling as a proxy for CCN because of its availability from satellite and surface networks. The two are indeed grossly correlated [*Andreae and Rosenfeld*, 2008], but their correlation is subject to a large uncertainty, often off by several factors of magnitude. Moreover, AOD is a poor indicator of aerosol number. AI is much better though not on a regional scale [*Penner et al.*, 2011]. This is not surprising, because AOD is determined primarily by aerosol extinction that is, in turn, influenced by aerosol scattering and thus proportional to the cross section; CCN effects are affected by many other factors. Given an appropriate composition and adequate supersaturation, aerosols of smaller size can provide more CCN than those of a larger size with the same bulk optical properties. Current attempts to use available satellite retrievals, such as those from MODIS, to estimate cloud droplet number concentration [e.g., *Bennartz*, 2007] are only of relative use for certain types of clouds. Next-generation satellites and global networks should be tailored toward extracting CCN as well as aerosol optical properties.

[141] Despite ever-escalating efforts and the virtually exponential increase in published studies concerning aerosol-cloud-precipitation interactions, we are still puzzled by many seemingly contradictory findings as reviewed above, although they really attest to the complexity of the problem. Disentangling meteorological and aerosol effects remains a daunting task. While individual endeavors have advanced our understanding substantially, it is highly recommended that a collective approach incorporating the strengths of all individual approaches while minimizing their limitations be undertaken to tackle the problem. Observation-based studies will likely continue to reveal new evidence of the ACPI, while cloud-resolving models will continue to help understand fundamental processes and to develop and test parameterizations for use with large-scale models. For the sake of testing and performing intercomparisons of large-scale models, "standard" tests may be developed on

the basis of well-defined experiments and/or observed relationships from analysis of large ensembles of data. In case of any discrepancies, it is essential to sort out contributing factors in terms of various direct and indirect effects.

[142] For additional in-depth details, the reader is referred to the following authors, who illustrate the complexity of aerosol interactions with convection: *Twomey et al.* [1984], *Albrecht* [1989], *Rosenfeld* [1999, 2000], *Khain et al.* [2004, 2005, 2008], *Cheng et al.* [2007], *Lynn et al.* [2005a], *van den Heever et al.* [2006], *Teller and Levin* [2006], *van den Heever and Cotton* [2007], *Wang* [2005], *Tao et al.* [2007], and *Levin and Cotton* [2009].

[143] **ACKNOWLEDGMENTS.** W.-K. Tao appreciates the inspiring and enthusiastic support by his mentor, Joanne Simpson, over the past 25 years and is grateful to R. Kakar at NASA headquarters for his continuous support of Goddard Cumulus Ensemble (GCE) model development and applications. This work is mainly supported by the NASA Headquarters Physical Climate Program and the NASA Precipitation Measurement Mission (PMM). He also thanks David Considine for support under the NASA Modeling Analysis Prediction (MAP). C. Wang thanks the NSF (AGS-0944121), the Singapore NRF through the Singapore-MIT Alliance for Research and Technology, and the corporate and foundation sponsors of the MIT Joint Program on the Science and Policy of Global Change for supporting his research. Z. Li's aerosol-related studies have been supported by NASA's Radiation Science program managed by H. Maring (NNX08AH71G), and DOE's Atmospheric System Research program managed by A. Williamson (DEFG0208ER64571), National Science Foundation managed by C. Lu (AGS-1118325), and the Ministry of Science and Technology of China (2006CB403706, 2011CB403405). C. Zhang thanks the support of the NOAA Office of Global Programs through awards under Cooperative Agreement NA17RJ1226 to the Cooperative Institute for Marine and Atmospheric Studies (CIMAS). J.-P. Chen acknowledges the support from projects NSC 98-2111-M-002-001 and NSC 99-2111-M-002-009-MY3. We'd like to thank M. Cribb for reading and editing the manuscript; Xiaowen Li for improving Figures 28, 33, and 35; and Takamichi Iguhi for providing Figure 25. We also thank Joyce Penner and two anonymous reviewers for their constructive comments that improved this paper significantly.

[144] The Editor responsible for this paper was Alan Robock. He thanks Joyce Penner and two anonymous reviewers.

REFERENCES

Abdul-Razzak, H., and S. J. Ghan (2000), A parameterization of aerosol activation: 2. Multiple aerosol types, *J. Geophys. Res.*, *105*(D5), 6837–6844, doi:10.1029/1999JD901161.

Abdul-Razzak, H., and S. J. Ghan (2004), Parameterization of the influence of organic surfactants on aerosol activation, *J. Geophys. Res.*, *109*, D03205, doi:10.1029/2003JD004043.

Abdul-Razzak, H., S. J. Ghan, and C. Rivera-Carpio (1998), A parameterization of aerosol activation: 1. Single aerosol type, *J. Geophys. Res.*, *103*(D6), 6123–6131, doi:10.1029/97JD03735.

Ackerman, A. S., O. B. Toon, D. E. Stevens, A. J. Heymsfield, V. Ramanathan, and E. J. Welton (2000), Reduction of tropical cloudiness by soot, *Science*, *288*, 1042–1047, doi:10.1126/science.288.5468.1042.

Ackerman, A. S., M. P. Kirkpatrick, D. E. Stevens, and O. B. Toon (2004), The impact of humidity above stratiform clouds on indirect aerosol climate forcing, *Nature*, *432*, 1014–1017, doi:10.1038/nature03174.

Ackerman, T. P., and O. B. Toon (1981), Absorption of visible radiation in atmosphere containing mixtures of absorbing and non-absorbing particles, *Appl. Opt.*, *20*, 3661–3667, doi:10.1364/AO.20.003661.

Adams, P. J., and J. H. Seinfeld (2002), Predicting global aerosol size distributions in general circulation models, *J. Geophys. Res.*, *107*(D19), 4370, doi:10.1029/2001JD001010.

Albrecht, B. A. (1989), Aerosols, cloud microphysics and fractional cloudiness, *Science*, *245*, 1227–1230, doi:10.1126/science.245.4923.1227.

Alpert, P., N. Halfon, and Z. Levin (2008), Does air pollution really suppress precipitation in Israel?, *J. Appl. Meteorol. Climatol.*, *47*, 933–943, doi:10.1175/2007JAMC1803.1.

Andreae, M. O., and D. Rosenfeld (2008), Aerosol-cloud-precipitation interactions: Part 1. The nature and sources of cloud-active aerosols, *Earth Sci. Rev.*, *89*, 13–41, doi:10.1016/j.earscirev.2008.03.001.

Andreae, M. O., D. Rosenfeld, P. Artaxo, A. A. Costa, G. P. Frank, K. M. Longo, and M. A. F. Silva-Dias (2004), Smoking rain clouds over the Amazon, *Science*, *303*, 1337–1342, doi:10.1126/science.1092779.

Arakawa, A., and W. H. Schubert (1974), Interaction of a cumulus cloud ensemble with large-scale environment: Part 1, *J. Atmos. Sci.*, *31*, 674–701, doi:10.1175/1520-0469(1974)031<0674:IOACCE>2.0.CO;2.

Archuleta, C. M., P. J. DeMott, and S. M. Kreidenweis (2005), Ice nucleation by surrogates for atmospheric mineral dust and mineral dust/sulfate particles at cirrus temperatures, *Atmos. Chem. Phys.*, *5*, 2617–2634, doi:10.5194/acp-5-2617-2005.

Barahona, D., and A. Nenes (2007), Parameterization of cloud droplet formation in large-scale models: Including effects of entrainment, *J. Geophys. Res.*, *112*, D16206, doi:10.1029/2007JD008473.

Bauer, S. E., D. L. Wright, D. Koch, E. R. Lewis, R. McGraw, L.-S. Chang, S. E. Schwartz, and R. Ruedy (2008), MATRIX (Multiconfiguration Aerosol TRacker of mIXing state): An aerosol microphysical module for global atmospheric models, *Atmos. Chem. Phys.*, *8*, 6003–6035, doi:10.5194/acp-8-6003-2008.

Bell, T. L., D. Rosenfeld, K.-M. Kim, J.-M. Yoo, M.-I. Lee, and M. Hahnenberger (2008), Midweek increase in U.S. summer rain and storm heights suggests air pollution invigorates rainstorms, *J. Geophys. Res.*, *113*, D02209, doi:10.1029/2007JD008623.

Bennartz, R. (2007), Global assessment of marine boundary layer cloud droplet number concentration from satellite, *J. Geophys. Res.*, *112*, D02201, doi:10.1029/2006JD007547.

Berg, W., T. L'Ecuyer, and C. Kummerow (2006), Rainfall climate regimes: The relationship of regional TRMM rainfall biases to the environment, *J. Appl. Meteorol. Climatol.*, *45*, 434–454, doi:10.1175/JAM2331.1.

Berg, W., T. L'Ecuyer, and S. van den Heever (2008), Evidence for the impact of aerosols on the onset and microphysical properties of rainfall from a combination of satellite observations and cloud resolving model simulations, *J. Geophys. Res.*, *113*, D14S23, doi:10.1029/2007JD009649.

Bigg, E. K. (1953), The formation of atmospheric ice crystals by the freezing of droplets, *Q. J. R. Meteorol. Soc.*, *79*, 510–519, doi:10.1002/qj.49707934207.

Bollasina, M., and S. Nigam (2009), Indian Ocean SST, evaporation, and precipitation during the South Asian summer monsoon in IPCC-AR4 coupled simulations, *Clim. Dyn.*, *33*, 1017–1032, doi:10.1007/s00382-008-0477-4.

Bollasina, M., S. Nigam, and M.-K. Lau (2008), Absorbing aerosols and summer monsoon evolution over South Asia: An observational portrayal, *J. Clim.*, *21*, 3221–3239, doi:10.1175/2007JCLI2094.1.

Bond, T. C., and R. W. Bergstrom (2006), Light absorption by carbonaceous particles: An investigative review, *Aerosol Sci. Technol.*, *40*, 27–67, doi:10.1080/02786820500421521.

Boucher, O., and U. Lohmann (1995), The sulfate-CCN-cloud albedo effect: A sensitivity study with two general circulation models, *Tellus, Ser. B*, *47*, 281–300.

Brechtel, F. J., S. M. Kreidenweis, and H. B. Swan (1998), Air mass characteristics, total particle concentration, and size distributions at Macquarie Island, Tasmania, during the First Aerosol Characterization Experiment (ACE 1), *J. Geophys. Res.*, *103*, 16,351–16,367, doi:10.1029/97JD03014.

Brenguier, J.-L., H. Pawlowska, L. Schüller, R. Preusker, J. Fischer, and Y. Fouquart (2000), Radiative properties of boundary layer clouds: Droplet effective radius versus number concentration, *J. Atmos. Sci.*, *57*, 803–821, doi:10.1175/1520-0469(2000)057<0803:RPOBLC>2.0.CO;2.

Browning, K. A., et al. (1993), The GEWEX Cloud System Study (GCSS), *Bull. Am. Meteorol. Soc.*, *74*, 387–399.

Bruintjes, R. T. (1999), A review of cloud seeding experiments to enhance precipitation and some new prospects, *Bull. Am. Meteorol. Soc.*, *80*, 805–820, doi:10.1175/1520-0477(1999)080<0805:AROCSE>2.0.CO;2.

Burrows, S. M., T. Butler, P. Jöckel, H. Tost, A. Kerkweg, U. Pöschl, and M. G. Lawrence (2009), Bacteria in the global atmosphere: Part 2. Modeling of emissions and transport between different ecosystems, *Atmos. Chem. Phys.*, *9*, 9281–9297, doi:10.5194/acp-9-9281-2009.

Cai, W., T. Cowan, A. Sullivan, J. Ribbe, and G. Shi (2010), Are anthropogenic aerosols responsible for the northwest Australia summer rainfall increase? A CMIP3 perspective and implications, *J. Clim.*, *10*, 2556–2564, doi:10.1175/2010JCLI3832.1.

Cantrell, W., and A. Heymsfield (2005), Production of ice in tropospheric clouds—A review, *Bull. Am. Meteorol. Soc.*, *86*, 795–807, doi:10.1175/BAMS-86-6-795.

Carrió, G. G., S. C. van den Heever, and W. R. Cotton (2007), Impacts of nucleating aerosol on anvil-cirrus clouds: A modeling study, *Atmos. Res.*, *84*, 111–131, doi:10.1016/j.atmosres.2006.06.002.

Chang, F.-L., and Z. Li (2002), Estimating the vertical variation of cloud droplet effective radius using multispectral near-infrared satellite measurements, *J. Geophys. Res.*, *107*(D15), 4257, doi:10.1029/2001JD000766.

Chang, F.-L., and Z. Li (2003), Retrieving the vertical profiles of water-cloud droplet effective radius: Algorithm modification and preliminary application, *J. Geophys. Res.*, *108*(D24), 4763, doi:10.1029/2003JD003906.

Chang, F.-L., and Z. Li (2005), A new method for detection of cirrus-overlapping-water clouds and determination of their optical properties, *J. Atmos. Sci.*, *62*, 3993–4009.

Changnon, S. A., R. G. Semonin, A. H. Auer, R. R. Braham, and J. Hales (1981), *METROMEX: A Review and Summary*, *Meteorol. Monogr. Ser.*, vol. 18, 181 pp., Am. Meteorol. Soc., Boston, Mass.

Chen, J.-P. (1994a), Predictions of saturation ratio for cloud microphysical models, *J. Atmos. Sci.*, *51*, 1332–1338, doi:10.1175/1520-0469(1994)051<1332:POSRFC>2.0.CO;2.

Chen, J.-P. (1994b), Theory of deliquescence and modified Köhler curves, *J. Atmos. Sci.*, *51*, 3505–3516, doi:10.1175/1520-0469(1994)051<3505:TODAMK>2.0.CO;2.

Chen, J.-P., and D. Lamb (1994), Simulation of cloud microphysical and chemical processes using a multi-component framework: Part I. Description of the microphysical model, *J. Atmos. Sci.*, *51*, 2613–2630, doi:10.1175/1520-0469(1994)051<2613:SOCMAC>2.0.CO;2.

Chen, J.-P., and S.-T. Liu (2004), Physically based two-moment bulk-water parameterization for warm cloud microphysics, *Q. J. R. Meteorol. Soc.*, *130*, 51–78.

Chen, J.-P., G. M. McFarquhar, A. J. Heymsfield, and V. Ramanathan (1997), A modeling and observational study of the detailed microphysical structure of tropical cirrus anvils, *J. Geophys. Res.*, *102*, 6637–6653, doi:10.1029/96JD03513.

Chen, J.-P., A. Hazra, and Z. Levin (2008), Parameterizing ice nucleation rates using contact angle and activation energy derived from laboratory data, *Atmos. Chem. Phys.*, *8*, 7431–7449, doi:10.5194/acp-8-7431-2008.

Chen, R., F. L. Chen, Z. Li, R. Ferraro, and F. Weng (2007), The impact of vertical variation of cloud droplet size on estimation of cloud liquid water path and detection of warm raining cloud, *J. Atmos. Sci.*, *64*, 3843–3853, doi:10.1175/2007JAS2126.1.

Chen, R., Z. Li, R. J. Kuligowski, R. Ferraro, and F. Weng (2011), A study of warm rain detection using A-Train satellite data, *Geophys. Res. Lett.*, *38*, L04804, doi:10.1029/2010GL046217.

Cheng, C.-T., W.-C. Wang, and J.-P. Chen (2007), A modeling study of aerosol impacts on cloud microphysics and radiative properties, *Q. J. R. Meteorol. Soc.*, *133*, 283–297, doi:10.1002/qj.25.

Cheng, C.-T., W.-C. Wang, and J.-P. Chen (2010), Simulation of the effects of increasing cloud condensation nuclei on mixed-phase clouds and precipitation of a front system, *Atmos. Res.*, *96*, 461–476, doi:10.1016/j.atmosres.2010.02.005.

Chin, M., A. Chu, R. Levy, L. Remer, Y. Kaufman, B. Holben, T. Eck, P. Ginoux, and Q. X. Gao (2004), Aerosol distribution in the Northern Hemisphere during ACE-Asia: Results from global model, satellite observations, and Sun photometer measurements, *J. Geophys. Res.*, *109*, D23S90, doi:10.1029/2004JD004829.

Chin, M., T. Diehl, O. Dubovik, T. F. Eck, B. N. Holben, A. Sinyuk, and D. G. Streets (2009), Light absorption by pollution, dust, and biomass burning aerosols: A global model study and evaluation with AERONET measurements, *Ann. Geophys.*, *27*, 3439–3464, doi:10.5194/angeo-27-3439-2009.

Chung, C. E., V. Ramanathan, and J. T. Kiehl (2002), Effects of the South Asian absorbing haze on the northeast monsoon and surface-air heat exchange, *J. Clim.*, *15*, 2462–2476, doi:10.1175/1520-0442(2002)015<2462:EOTSAA>2.0.CO;2.

Chung, S. H., and J. H. Seinfeld (2005), Climate response of direct radiative forcing of anthropogenic black carbon, *J. Geophys. Res.*, *110*, D11102, doi:10.1029/2004JD005441.

Chýlek, P., G. Videen, D. Ngo, R. G. Pinnick, and J. D. Klett (1995), Effect of black carbon on the optical properties and climate forcing of sulfate aerosols, *J. Geophys. Res.*, *100*, 16,325–16,332, doi:10.1029/95JD01465.

Chýlek, P., M. K. Dubey, U. Lohmann, V. Ramanathan, Y. J. Kaufman, G. Lesins, J. Hudson, G. Altmann, and S. Olsen (2006), Aerosol indirect effect over the Indian Ocean, *Geophys. Res. Lett.*, *33*, L06806, doi:10.1029/2005GL025397.

Clark, T. L. (1973), Numerical modeling of the dynamics and microphysics of warm cumulus convection, *J. Atmos. Sci.*, *30*, 857–878, doi:10.1175/1520-0469(1973)030<0857:NMOTDA>2.0.CO;2.

Clothiaux, E. E., T. P. Ackerman, G. C. Mace, K. P. Moran, R. T. Marchand, M. A. Miller, and B. E. Martner (2000), Objective determination of cloud heights and radar reflectivities using a combination of active remote sensors at the ARM CART sites, *J. Appl. Meteorol.*, *39*, 645–665, doi:10.1175/1520-0450(2000)039<0645:ODOCHA>2.0.CO;2.

Coakley, J. A., and C. D. Walsh (2002), Limits to the aerosol indirect radiative effect from observations of ship tracks, *J. Atmos. Sci.*, *59*, 668–680, doi:10.1175/1520-0469(2002)059<0668:LTTAIR>2.0.CO;2.

Coakley, J. A., Jr., et al. (2000), The appearance and disappearance of ship tracks on large spatial scales, *J. Atmos. Sci.*, *57*, 2765–2778, doi:10.1175/1520-0469(2000)057<2765:TAADOS>2.0.CO;2.

Cohen, J. B., R. G. Prinn, and C. Wang (2011), The impact of detailed urban-scale processing on the composition, distribution, and radiative forcing of anthropogenic aerosols, *Geophys. Res. Lett.*, *38*, L10808, doi:10.1029/2011GL047417.

Collier, J. C., and G. J. Zhang (2009), Aerosol direct forcing of the summer Indian monsoon as simulated by the NCAR CAM3, *Clim. Dyn.*, *32*, 313–332, doi:10.1007/s00382-008-0464-9.

Collins, W. D., P. J. Rasch, B. E. Eaton, B. V. Khattatov, J.-F. Lamarque, and C. S. Zender (2001), Simulating aerosols using a chemical transport model with assimilation of satellite aerosol

retrievals: Methodology for INDOEX, *J. Geophys. Res.*, *106*, 7313–7336, doi:10.1029/2000JD900507.

Conant, W. C., A. Nenes, and J. H. Seinfeld (2002), Black carbon radiative heating effects on cloud microphysics and implications for the aerosol indirect effect: 1. Extended Köhler theory, *J. Geophys. Res.*, *107*(D21), 4604, doi:10.1029/2002JD002094.

Cooper, W. A. (1986), Ice initiation in natural clouds, in *Precipitation Enhancement: A Scientific Challenge*, *AMS Meteorol. Monogr. Ser.*, vol. 21, edited by R. G. Braham Jr., pp. 29–32, Am. Meteorol. Soc., Boston, Mass.

Cotton, W. R., H. Zhang, G. M. McFarquhar, and S. M. Saleeby (2007), Should we consider polluting hurricanes to reduce their intensity?, *J. Weather Modif.*, *39*, 70–73.

Cziczo, D. J., D. M. Murphy, P. K. Hudson, and D. S. Thomson (2004), Single particle measurements of the composition of cirrus ice residue during CRYSTAL-FACE, *J. Geophys. Res.*, *109*, D04201, doi:10.1029/2003JD004032.

de Boer, G., T. Hashino, and G. J. Tripoli (2010), Ice nucleation through immersion freezing in mixed-phase stratiform clouds: Theory and numerical simulations, *Atmos. Res.*, *96*, 315–324, doi:10.1016/j.atmosres.2009.09.012.

de Leeuw, G., E. L. Andreas, M. D. Anguelova, C. W. Fairall, E. R. Lewis, C. O'Dowd, M. Schulz, and S. E. Schwarts (2011), Production flux of sea spray aerosol, *Rev. Geophys.*, *49*, RG2001, doi:10.1029/2010RG000349.

DeMott, P. J. (1990), An exploratory study of ice nucleation by soot aerosols, *J. Appl. Meteorol.*, *29*, 1072–1079, doi:10.1175/1520-0450(1990)029<1072:AESOIN>2.0.CO;2.

DeMott, P. J., D. C. Rogers, S. M. Kreidenweis, Y. Chen, C. H. Twohy, D. Baumgardner, A. J. Heymsfield, and K. R. Chan (1998), The role of heterogeneous freezing nucleation in upper tropospheric clouds: Inferences from SUCCESS, *Geophys. Res. Lett.*, *25*(9), 1387–1390, doi:10.1029/97GL03779.

DeMott, P. J., K. Sassen, M. Poellot, D. Baumgardner, D. C. Rogers, S. D. Brooks, A. J. Prenni, and S. M. Kreidenweis (2003), African dust aerosols as atmospheric ice nuclei, *Geophys. Res. Lett.*, *30*(14), 1732, doi:10.1029/2003GL017410.

DeMott, P. J., A. J. Prenni, X. Liu, S. M. Kreidenweis, M. D. Petters, C. H. Twohy, M. S. Richardson, T. Eidhammer, and D. C. Rogers (2010), Predicting global atmospheric ice nuclei distributions and their impacts on climate, *Proc. Natl. Acad. Sci. U. S. A.*, *107*, 11,217–11,222, doi:10.1073/pnas.0910818107.

Deryaguin, B. V., Y. S. Kurghin, S. P. Bakanov, and K. M. Merzhanov (1985), Influence of surfactant vapor on the spectrum of cloud drops forming in the process of condensation growth, *Langmuir*, *1*, 278–281, doi:10.1021/la00063a003.

Diehl, K., and S. Wurzler (2004), Heterogeneous drop freezing in the immersion mode: Model calculations considering soluble and insoluble particles in the drops, *J. Atmos. Sci.*, *61*, 2063–2072, doi:10.1175/1520-0469(2004)061<2063:HDFITI>2.0.CO;2.

Diehl, K., C. Quick, S. Matthias-Maser, S. K. Mitra, and R. Jaenicke (2001), The ice nucleating ability of pollen: Part I. Laboratory studies in deposition and condensation freezing modes, *Atmos. Res.*, *58*, 75–87, doi:10.1016/S0169-8095(01)00091-6.

Dorsey, N. E. (1948), The freezing of supercooled water, *Trans. Am. Philos. Soc.*, *38*, 248–328.

Dubovik, O., T. Lapyonok, Y. J. Kaufman, M. Chin, P. Ginoux, R. A. Kahn, and A. Sinyuk (2008), Retreving global aerosol sources from satellites using inverse modeling, *Atmos. Chem. Phys.*, *8*, 209–250, doi:10.5194/acp-8-209-2008.

Easter, R. C., S. J. Ghan, Y. Zhang, R. D. Saylor, E. G. Chapman, N. S. Laulainen, H. Abdul-Razzak, L. R. Leung, X. Bian, and R. A. Zaveri (2004), MIRAGE: Model description and evaluation of aerosols and trace gases, *J. Geophys. Res.*, *109*, D20210, doi:10.1029/2004JD004571.

Ekman, A., C. Wang, J. Ström, and J. Wilson (2004), Explicit simulation of aerosol physics in a cloud resolving model: A sensitivity study based on an observed convective cloud, *Atmos. Chem. Phys.*, *4*, 773–791, doi:10.5194/acp-4-773-2004.

Ekman, A., C. Wang, J. Ström, and R. Krejci (2006), Explicit simulation of aerosol physics in a cloud-resolving model: Aerosol transport and processing in the free troposphere, *J. Atmos. Sci.*, *63*, 682–696, doi:10.1175/JAS3645.1.

Ekman, A., A. Engström, and C. Wang (2007), The effect of aerosol composition and concentration on the development and anvil properties of a continental deep convective cloud, *Q. J. R. Meteorol. Soc.*, *133B*(627), 1439–1452, doi:10.1002/qj.108.

Eltahir, E., and C. Gong (1996), Dynamics of wet and dry years in West Africa, *J. Clim.*, *9*, 1030–1042, doi:10.1175/1520-0442(1996)009<1030:DOWADY>2.0.CO;2.

Facchini, M. C., M. Mircea, S. Fuzzi, and R. J. Charlson (1999), Cloud albedo enhancement by surface-active organic solutes in growing droplets, *Nature*, *401*, 257–259, doi:10.1038/45758.

Fan, J., R. Zhang, G. Li, and W.-K. Tao (2007a), Effects of aerosols and relative humidity on cumulus clouds, *J. Geophys. Res.*, *112*, D14204, doi:10.1029/2006JD008136.

Fan, J., R. Zhang, G. Li, W.-K. Tao, and X. Li (2007b), Simulation of cumulus clouds using a spectral microphysics cloud-resolving model, *J. Geophys. Res.*, *112*, D04201, doi:10.1029/2006JD007688.

Fan, J., et al. (2009), Dominant role by vertical wind shear in regulating aerosol effects on deep convective clouds, *J. Geophys. Res.*, *114*, D22206, doi:10.1029/2009JD012352.

Fan, J., J. M. Comstock, and M. Ovchinnikov (2010a), The cloud condensation nuclei and ice nuclei effects on tropical anvil characteristics and water vapor of the tropical tropopause layer, *Environ. Res. Lett.*, *5*, 044005, doi:10.1088/1748-9326/5/4/044005.

Fan, J., J. M. Comstock, M. Ovchinnikov, S. A. McFarlane, G. McFarquhar, and G. Allen (2010b), Tropical anvil characteristics and water vapor of the tropical tropopause layer: Impact of heterogeneous and homogeneous freezing parameterizations, *J. Geophys. Res.*, *115*, D12201, doi:10.1029/2009JD012696.

Fan, J., L. R. Leung, Z. Li, H. Morrison, H. Chen, Y. Zhou, Y. Qian, and Y. Wang (2012), Aerosol impacts on clouds and precipitation in eastern China: Results from bin and bulk microphysics, *J. Geophys. Res.*, *117*, D00K36, doi:10.1029/2011JD016537.

Feingold, G., and P. Y. Chuang (2002), Analysis of the influence of film-forming compounds on droplet growth: Implications for cloud microphysical processes and climate, *J. Atmos. Sci.*, *59*, 2006–2018, doi:10.1175/1520-0469(2002)059<2006:AOTIOF>2.0.CO;2.

Feingold, G., B. Stevens, W. R. Cotton, and R. L. Walko (1994), An explicit cloud microphysics/LES model designed to simulate the Twomey effect, *Atmos. Res.*, *33*, 207–233, doi:10.1016/0169-8095(94)90021-3.

Feingold, G., W. R. Cotton, S. M. Kreidenweis, and J. T. Davis (1999), The impact of giant cloud condensation nuclei on drizzle formation in stratocumulus: Implication for cloud radiative properties, *J. Atmos. Sci.*, *56*, 4100–4117, doi:10.1175/1520-0469(1999)056<4100:TIOGCC>2.0.CO;2.

Feingold, G., W. L. Eberhard, D. E. Veron, and M. Previdi (2003), First measurements of the Twomey indirect effect using ground-based remote sensors, *Geophys. Res. Lett.*, *30*(6), 1287, doi:10.1029/2002GL016633.

Feingold, G., R. Furrer, P. Pilewsskie, L. A. Remer, Q. Min, and H. Jonsson (2006), Aerosol indirect effect studies at Southern Great Plains during the May 2003 Intensive Operations Period, *J. Geophys. Res.*, *111*, D05S14, doi:10.1029/2004JD005648.

Ferek, R. J., et al. (2000), Drizzle suppression in ship tracks, *J. Atmos. Sci.*, *57*, 2705–2728, doi:10.1175/1520-0469(2000)057<2707:DSIST>2.0.CO;2.

Field, P. R., O. Möhler, P. Connolly, M. Krämer, R. Cotton, A. J. Heymsfield, H. Saathoff, and M. Schnaiter (2006), Some ice nucleation characteristics of Asian and Saharan desert dust, *Atmos. Chem. Phys.*, *6*, 2991–3006, doi:10.5194/acp-6-2991-2006.

Fitzgerald, J. W., and P. A. Spyers-Duran (1973), Changes in cloud nucleus concentration and cloud droplet size distribution associated

with pollution from St. Louis, *J. Appl. Meteorol.*, *12*, 511–516, doi:10.1175/1520-0450(1973)012<0511:CICNCA>2.0.CO;2.

Fletcher, N. H. (1962), *The Physics of Rainclouds*, 386 pp., Cambridge Univ. Press, New York.

Fletcher, N. H. (1969), Active sites and ice crystal nucleation, *J. Atmos. Sci.*, *26*(6), 1266–1271, doi:10.1175/1520-0469(1969)026<1266:ASAICN>2.0.CO;2.

Fornea, A. P., S. D. Brooks, J. B. Dooley, and A. Saha (2009), Heterogeneous freezing of ice on atmospheric aerosols containing ash, soot, and soil, *J. Geophys. Res.*, *114*, D13201, doi:10.1029/2009JD011958.

Forster, P., et al. (2007), Changes in atmospheric constituents and in radiative forcing, in *Climate Change 2007: The Physical Science Basis—Contribution of Working Group I to the Fourth Assessment Report of the Intergovernmental Panel on Climate Change*, edited by S. Solomon et al., pp. 129–234, Cambridge Univ. Press, Cambridge, U. K.

Fountoukis, C., and A. Nenes (2005), Continued development of a cloud droplet formation parameterization for global climate models, *J. Geophys. Res.*, *110*, D11212, doi:10.1029/2004JD005591.

Fridlind, A. M., et al. (2004), Evidence for the predominance of mid-tropospheric aerosols as subtropical anvil cloud nuclei, *Science*, *304*, 718–722, doi:10.1126/science.1094947.

Gettelman, A., H. Morrison, and S. J. Ghan (2008), A new two-moment bulk stratiform cloud microphysics scheme in the Community Atmosphere Model, version 3(CAM3): Part II. Single-column and global results, *J. Clim.*, *21*, 3660–3679, doi:10.1175/2008JCLI2116.1.

Ghan, S. J., C. C. Chuang, and J. E. Penner (1993), A parameterization of cloud droplet nucleation: Part I. Single aerosol types, *Atmos. Res.*, *30*, 198–221, doi:10.1016/0169-8095(93)90024-I.

Ghan, S. J., G. Guzman, and H. Abdul-Razzak (1998), Competition between sea salt and sulfate particles as cloud condensation nuclei, *J. Atmos. Sci.*, *55*, 3340–3347, doi:10.1175/1520-0469(1998)055<3340:CBSSAS>2.0.CO;2.

Givati, A., and D. Rosenfeld (2004), Quantifying precipitation suppression due to air pollution, *J. Appl. Meteorol.*, *43*, 1038–1056.

Grabowski, W. W., and P. Smolarkiewicz (1999), CRCP: A Cloud Resolving Convection Parameterization for modeling the tropical convecting atmosphere, *Physica D*, *133*, 171–178, doi:10.1016/S0167-2789(99)00104-9.

Hallett, J., and S. C. Mossop (1974), Production of secondary ice crystals during the riming process, *Nature*, *249*, 26–28, doi:10.1038/249026a0.

Han, Q., W. B. Rossow, and A. A. Lacis (1994), Near-global survey of effective droplet radii in liquid water clouds using ISCCP data, *J. Clim.*, *7*, 465–497, doi:10.1175/1520-0442(1994)007<0465:NGSOED>2.0.CO;2.

Han, Q. Y., W. B. Rossow, J. Chou, and R. Welch (1998), Global survey of the relationships of cloud albedo and liquid water path with droplet size using ISCCP, *J. Clim.*, *11*(7), 1516–1528, doi:10.1175/1520-0442(1998)011<1516:GSOTRO>2.0.CO;2.

Han, Q. Y., W. B. Rossow, J. Zeng, and R. Welch (2002), Three different behaviors of liquid water path of water clouds in aerosol-cloud interactions, *J. Atmos. Sci.*, *59*, 726–735, doi:10.1175/1520-0469(2002)059<0726:TDBOLW>2.0.CO;2.

Hansen, J., M. Sato, and R. Ruedy (1997), Radiative forcing and climate response, *J. Geophys. Res.*, *102*, 6831–6864, doi:10.1029/96JD03436.

Hara, K., S. Yamagata, T. Yamanouchi, K. Sato, A. Herber, Y. Iwasaka, M. Nagatani, and H. Nakata (2003), Mixing states of individual aerosol particles in spring Arctic troposphere during ASTAR 2000 campaign, *J. Geophys. Res.*, *108*(D7), 4209, doi:10.1029/2002JD002513.

Haywood, J. M., and O. Boucher (2000), Estimates of the direct and indirect radiative forcing due to tropospheric aerosols: A review, *Rev. Geophys.*, *38*, 513–543, doi:10.1029/1999RG000078.

Heintzenberg, J., K. Okada, and J. Ström (1996), On the composition of non-volatile material in upper tropospheric aerosols and cirrus crystals, *Atmos. Res.*, *41*, 81–88, doi:10.1016/0169-8095(95)00042-9.

Heymsfield, A. J., and L. M. Miloshevich (1993), Homogeneous ice nucleation and supercooled liquid water in orographic wave clouds, *J. Atmos. Sci.*, *50*, 2335–2353, doi:10.1175/1520-0469(1993)050<2335:HINASL>2.0.CO;2.

Heymsfield, A. J., and M. Sabin (1989), Cirrus crystal nucleation by homogeneous freezing of solution droplets, *J. Atmos. Sci.*, *46*, 2252–2264, doi:10.1175/1520-0469(1989)046<2252:CCNBHF>2.0.CO;2.

Heymsfield, A. J., L. M. Miloshevich, C. Schmitt, A. Bansemer, C. Twohy, M. R. Poellot, A. Fridlind, and H. Gerber (2005), Homogeneous ice nucleation in subtropical and tropical convection and its influence on cirrus anvil microphysics, *J. Atmos. Sci.*, *62*, 41–64, doi:10.1175/JAS-3360.1.

Hocking, L. M. (1959), The collision efficiency of water drops, *Q. J. R. Meteorol. Soc.*, *85*, 44–50, doi:10.1002/qj.49708536305.

Hoose, C., J. E. Kristjánsson, T. Iversen, A. Kirkevåg, Ø. Seland, and A. Gettelman (2009), Constraining cloud droplet number concentration in GCMs suppresses the aerosol indirect effect, *Geophys. Res. Lett.*, *36*, L12807, doi:10.1029/2009GL038568.

Hoose, C., J. E. Kristjánsson, and S. M. Burrows (2010a), How important is biological ice nucleation in clouds on a global scale?, *Environ. Res. Lett.*, *5*, 024009, doi:10.1088/1748-9326/5/2/024009.

Hoose, C., J. E. Kristjánsson, J.-P. Chen, and A. Hazra (2010b), A classical-theory-based parameterization of heterogeneous ice nucleation by mineral dust, soot, and biological particles in a global climate model, *J. Atmos. Sci.*, *67*, 2483–2503, doi:10.1175/2010JAS3425.1.

Horvath, H. (1993), Atmospheric light absorption: A review, *Atmos. Environ., Part A*, *27*, 293–317.

Huang, H., A. Adams, C. Wang, and C. Zhang (2009), Aerosol and West African monsoon precipitation: Observations and simulations, *Ann. Geophys.*, *27*, 4171–4181, doi:10.5194/angeo-27-4171-2009.

Huang, J., B. Lin, P. Minnis, T. Wang, X. Wang, Y. Hu, Y. Yi, and J. K. Ayers (2006a), Satellite-based assessment of possible dust aerosols semi-direct effect on cloud water path over East Asia, *Geophys. Res. Lett.*, *33*, L19802, doi:10.1029/2006GL026561.

Huang, J., P. Minnis, B. Lin, T. Wang, Y. Yi, Y. Hu, A. Sun-Mack, and K. Ayers (2006b), Possible influences of Asian dust aerosols on cloud properties and radiative forcing observed from MODIS and CERES, *Geophys. Res. Lett.*, *33*, L06824, doi:10.1029/2005GL024724.

Huang, J., C. Zhang, and J. M. Prospero (2009a), African aerosol and large-scale precipitation variability over West Africa, *Environ. Res. Lett.*, *4*, 015006, doi:10.1088/1748-9326/4/1/015006.

Huang, J., C. Zhang, and J. Prospero (2009b), Large-scale effect of aerosol on precipitation in the West African monsoon region, *Q. J. R. Meteorol. Soc.*, *135*, 581–594, doi:10.1002/qj.391.

Huang, J., C. Zhang, and J. Prospero (2009c), Aerosol-induced large-scale variability in precipitation over the tropical Atlantic, *J. Clim.*, *22*, 4970–4988, doi:10.1175/2009JCLI2531.1.

Huang, J., P. Minnis, H. Yan, Y. Yi, B. Chen, L. Zhang, and J. Ayers (2010), Dust aerosol effect on semi-arid climate over northwest China detected from A-Train satellite measurements, *Atmos. Chem. Phys.*, *10*, 6863–6872.

Huffman, P. J. (1973), Supersaturation spectra of AgI and natural ice nuclei, *J. Appl. Meteorol.*, *12*, 1080–1082, doi:10.1175/1520-0450(1973)012<1080:SSOAAN>2.0.CO;2.

Hui, W. J., B. I. Cook, S. Ravi, J. D. Fuentes, and P. D'Odorico (2008), Dust-rainfall feedbacks in the West African Sahel, *Water Resour. Res.*, *44*, W05202, doi:10.1029/2008WR006885.

Intergovernmental Panel on Climate Change (IPCC) (2001), *Climate Change 2001: The Physical Science Basis*, edited by J. T. Houghton et al., Cambridge Univ. Press, Cambridge, U. K.

Intergovernmental Panel on Climate Change (IPCC) (2007), *Intergovernmental Panel on Climate Change: Climate Change*

2007—The Physical Science Basis, edited by S. Solomon et al., Cambridge Univ. Press, Cambridge, U. K.

Isono, K., M. Kombayasi, and A. Ono (1959), The nature and the origin of ice nuclei in the atmosphere, *J. Meteorol. Soc. Jpn.*, *37*, 211.

Jacobson, M. (2001), Global direct radiative forcing due to multicomponent anthropogenic and natural aerosols, *J. Geophys. Res.*, *106*, 1551–1568, doi:10.1029/2000JD900514.

Jaenicke, R. (1993), Tropospheric aerosols, in *Aerosol-Cloud-Climate Interactions*, edited by P. V. Hobbs, pp. 1–31, Academic, San Diego, Calif., doi:10.1016/S0074-6142(08)60210-7.

Jiang, H., H. Xue, A. Teller, G. Feingold, and Z. Levin (2006), Aerosol effects on the lifetime of shallow cumulus, *Geophys. Res. Lett.*, *33*, L14806, doi:10.1029/2006GL026024.

Jiang, J. H., H. Su, M. R. Schoeberl, S. T. Massie, P. Colarco, S. Platnick, and N. J. Livesey (2008), Clean and polluted clouds: Relationships among pollution, ice clouds, and precipitation 603 in South America, *Geophys. Res. Lett.*, *35*, L14804, doi:10.1029/2008GL034631.

Jiang, J. H., H. Su, C. Zhai, S. T. Massie, M. R. Schoeberl, P. R. Colarco, S. Platnick, Y. Gu, and K.-N. Liou (2011), Influence of convection and aerosol pollution on ice cloud particle effective radius, *Atmos. Chem. Phys.*, *11*, 457–463, doi:10.5194/acp-11-457-2011.

Jin, M., J. M. Shepherd, and M. D. King (2005), Urban aerosols and their variations with clouds and rainfall: A case study for New York and Houston, *J. Geophys. Res.*, *110*, D10S20, doi:10.1029/2004JD005081.

Johnson, D. B. (1982), The role of giant and ultra-giant aerosol particles in warm rain initiation, *J. Atmos. Sci.*, *39*, 448–460, doi:10.1175/1520-0469(1982)039<0448:TROGAU>2.0.CO;2.

Jones, A., D. L. Roberts, M. J. Woodage, and C. E. Johnson (2001), Indirect sulphate aerosol forcing in a climate model with an interactive sulphur cycle, *J. Geophys. Res.*, *106*, 20,293–20,310, doi:10.1029/2000JD000089.

Jones, A., J. M. Haywood, and O. Boucher (2007), Aerosol forcing, climate response and climate sensitivity in the Hadley Centre climate model, *J. Geophys. Res.*, *112*, D20211, doi:10.1029/2007JD008688.

Jones, G. S., N. Christidis, and P. A. Stott (2011), Detecting the influence of fossil fuel and bio-fuel black carbon aerosols on near surface temperature changes, *Atmos. Chem. Phys.*, *11*, 799–816, doi:10.5194/acp-11-799-2011.

Jones, T. A., and S. A. Christopher (2010), Statistical properties of aerosol-cloud-precipitation interactions in South America, *Atmos. Chem. Phys.*, *10*, 2287–2305, doi:10.5194/acp-10-2287-2010.

Junge, C. E. (1952), Die konstitution des atmosphärischen aerosols, *Ann. Meteorol.*, *5*, 1–55.

Junge, C. E. (1955), The size distribution and aging of natural aerosols as determined from electrical and optical data on the atmosphere, *J. Meteorol.*, *12*, 13–25, doi:10.1175/1520-0469(1955)012<0013:TSDAAO>2.0.CO;2.

Kanakidou, M., et al. (2005), Organic aerosol and global climate modelling: A review, *Atmos. Chem. Phys.*, *5*, 1053–1123, doi:10.5194/acp-5-1053-2005.

Kanji, Z. A., and J. P. D. Abbatt (2006), Laboratory studies of ice formation via deposition mode nucleation onto mineral dust and n-hexane soot samples, *J. Geophys. Res.*, *111*, D16204, doi:10.1029/2005JD006766.

Kärcher, B., and U. Lohmann (2003), A parameterization of cirrus cloud formation: Heterogeneous freezing, *J. Geophys. Res.*, *108*(D14), 4402, doi:10.1029/2002JD003220.

Kaufman, Y. J., and R. S. Fraser (1997), The effect of smoke particles on clouds and climate forcing, *Science*, *277*, 1636–1639, doi:10.1126/science.277.5332.1636.

Kaufman, Y. J., O. Boucher, D. Tanré, M. Chin, L. A. Remer, and T. Takemura (2005), Aerosol anthropogenic component estimated from satellite data, *Geophys. Res. Lett.*, *32*, L17804, doi:10.1029/2005GL023125.

Khain, A. P. (2009), Notes on state of the art investigations of aerosol effects on precipitation: A critical review, *Environ. Res. Lett.*, *4*, 015004, doi:10.1088/1748-9326/4/1/015004.

Khain, A., and A. Pokrovsky (2004), Simulation of effects of atmospheric aerosols on deep turbulent convective clouds using a spectral microphysics mixed-phase cumulus cloud model: Part II. Sensitivity study, *J. Atmos. Sci.*, *61*, 2963–2982, doi:10.1175/JAS-3350.1.

Khain, A. P., M. Ovtchinnikov, M. Pinsky, A. Pokrovsky, and H. Krugliak (2000), Notes on the state-of-the-art numerical modeling of cloud microphysics, *Atmos. Res.*, *55*, 159–224, doi:10.1016/S0169-8095(00)00064-8.

Khain, A., A. Pokrovsky, M. Pinsky, A. Seigert, and V. Phillips (2004), Simulation of effects of atmospheric aerosols on deep turbulent convective clouds using a spectral microphysics mixed-phase cumulus cloud model: Part I. Model description and possible applications, *J. Atmos. Sci.*, *61*, 2983–3001, doi:10.1175/JAS-3281.1.

Khain, A., D. Roseenfeld, and A. Pokrovsky (2005), Aerosol impact on the dynamics and microphysics of deep convective clouds, *Q. J. R. Meteorol. Soc.*, *131*, 2639–2663, doi:10.1256/qj.04.62.

Khain, A. D., N. BenMoshe, and A. Pokrovsky (2008), Factors determining the impact of aerosols on surface precipitation from clouds: An attempt at classification, *J. Atmos. Sci.*, *65*, 1721–1748, doi:10.1175/2007JAS2515.1.

Khain, A., B. Lynn, and J. Dudhia (2010), Aerosol effects on intensity of land-falling hurricanes as seen from simulations with the WRF model with spectral bin microphysics, *J. Atmos. Sci.*, *67*, 365–384, doi:10.1175/2009JAS3210.1.

Khairoutdinov, M. F., and D. A. Randall (2001), A cloud resolving model as a cloud parameterization in the NCAR Community Climate System Model: Preliminary results, *Geophys. Res. Lett.*, *28*(18), 3617–3620, doi:10.1029/2001GL013552.

Khvorostyanov, V. I., and J. A. Curry (2009), Parameterization of cloud drop activation based on analytical asymptotic solutions to the supersaturation equation, *J. Atmos. Sci.*, *66*, 1905–1925, doi:10.1175/2009JAS2811.1.

Kiehl, J. T., T. L. Schneider, P. J. Rasch, and M. C. Barth (2000), Radiative forcing due to sulfate aerosols from simulations with the National Center for Atmospheric Research Community Climate Model, Version 3, *J. Geophys. Res.*, *105*, 1441–1457, doi:10.1029/1999JD900495.

Kim, B.-G., S. E. Schwartz, M. A. Miller, and Q. Min (2003), Effective radius of cloud droplets by ground-based remote sensing: Relationship to aerosol, *J. Geophys. Res.*, *108*(D23), 4740, doi:10.1029/2003JD003721.

Kim, D., C. Wang, A. M. L. Ekman, M. C. Barth, and P. Rasch (2008), Distribution and direct radiative forcing of carbonaceous and sulfate aerosols in an interactive size-resolving aerosol-climate model, *J. Geophys. Res.*, *113*, D16309, doi:10.1029/2007JD009756.

Klein, S. A., et al. (2009), Intercomparison of model simulations of mixed-phase clouds observed during the ARM mixed-phase Arctic cloud experiment: Part I. Single layer cloud, *Q. J. R. Meteorol. Soc.*, *135*, 979–1002, doi:10.1002/qj.416.

Klemp, J. B., and R. B. Wilhelmson (1978), Simulation of 3-dimensional convective storm dynamics, *J. Atmos. Sci.*, *35*, 1070–1096, doi:10.1175/1520-0469(1978)035<1070:TSOTDC>2.0.CO;2.

Knollenberg, R. G., K. Kelly, and J. C. Wilson (1993), Measurements of high number densities of ice crystal populations in the tops of tropical cumulonimbus, *J. Geophys. Res.*, *98*, 8639–8664, doi:10.1029/92JD02525.

Kogan, Y. L. (1991), The simulation of a convective cloud in a 3-D model with explicit microphysics: Part I. Model description and sensitivity experiments, *J. Atmos. Sci.*, *48*, 1160–1189, doi:10.1175/1520-0469(1991)048<1160:TSOACC>2.0.CO;2.

Köhler, H. (1936), The nucleus in and the growth of hygroscopic droplets, *Trans. Faraday Soc.*, *32*, 1152–1161, doi:10.1039/tf9363201152.

Koren, I., Y. J. Kaufman, L. A. Remer, and J. V. Martins (2004), Measurements of the effect of smoke aerosol on inhibition of cloud formation, *Science*, *303*, 1342–1345.

Koren, I., Y. J. Kaufman, D. Rosenfeld, L. A. Remer, and Y. Rudich (2005), Aerosol invigoration and restructuring of Atlantic convective clouds, *Geophys. Res. Lett.*, *32*, L14828, doi:10.1029/2005GL023187.

Koren, I., J. V. Martins, L. A. Remer, and H. Afargan (2008), Smoke invigoration versus inhibition of clouds over the Amazon, *Science*, *321*, 946–949, doi:10.1126/science.1159185.

Koren, I., G. Feingold, and L. A. Remer (2010a), The invigoration of deep convective clouds over the Atlantic: Aerosol effect, meteorology or retrieval artifact?, *Atmos. Chem. Phys.*, *10*, 8855–8872, doi:10.5194/acp-10-8855-2010a.

Koren, I., L. A. Remer, O. Altaratz, J. V. Martins, and A. David (2010b), Aerosol-induced changes of convective cloud anvils produce strong climate warming, *Atmos. Chem. Phys.*, *10*, 5001–5010, doi:10.5194/acp-10-5001-2010b.

Korolev, A. V., and P. Field (2008), The effect of dynamics on mixed-phase clouds: Theoretical considerations, *J. Atmos. Sci.*, *65*, 66–86, doi:10.1175/2007JAS2355.1.

Krishnamurti, T. N., A. Chakraborty, A. Martin, W. K. Lau, K.-M. Kim, Y. Sud, and G. Walker (2009), Impact of Arabian Sea pollution on the Bay of Bengal winter monsoon rains, *J. Geophys. Res.*, *114*, D06213, doi:10.1029/2008JD010679.

Kristjánsson, J. E. (2002), Studies of the aerosol indirect effect from sulfate and black carbon aerosols, *J. Geophys. Res.*, *107*(D15), 4264, doi:10.1029/2001JD000887.

Kulmala, M., A. Laaksonen, P. Korhonen, T. Vesala, T. Ahonen, and J. C. Barrett (1993), The effect of atmospheric nitric acid vapor on cloud condensation nucleus activation, *J. Geophys. Res.*, *98*, 22,949–22,958, doi:10.1029/93JD02070.

Kulmala, M., A. Laaksonen, R. J. Charlson, and P. Korhonen (1997), Clouds without supersaturation, *Nature*, *388*, 336–337, doi:10.1038/41000.

La Mer, V. K. (Ed.) (1962), *Retardation of Evaporation by Monolayers: Transport Processes*, 277 pp., Academic, New York.

Langmuir, I., and D. B. Langmuir (1927), The effect of monomolecular films on the evaporation of ether solutions, *J. Phys. Chem.*, *31*(11), 1719–1731, doi:10.1021/j150281a011.

Lasher-Trapp, S. G., C. A. Knight, and J. M. Straka (2001), Early radar echoes from ultragiant aerosol in a cumulus congestus: Modeling and observations, *J. Atmos. Sci.*, *58*, 3545–3562, doi:10.1175/1520-0469(2001)058<3545:EREFUA>2.0.CO;2.

Lau, K.-M., and K.-M. Kim (2006), Observational relationships between aerosol and Asian monsoon rainfall, and circulation, *Geophys. Res. Lett.*, *33*, L21810, doi:10.1029/2006GL027546.

Lau, K. M., M. K. Kim, and K. M. Kim (2006), Asian monsoon anomalies induced by aerosol direct effects, *Clim. Dyn.*, *26*, 855–864, doi:10.1007/s00382-006-0114-z.

Lau, K.-M., et al. (2008), The Joint Aerosol-Monsoon Experiment: A new challenge for monsoon climate research, *Bull. Am. Meteorol. Soc.*, *89*, 369–383, doi:10.1175/BAMS-89-3-369.

Lau, K. M., K. M. Kim, Y. C. Sud, and G. K. Walker (2009), A GCM study of the response of the atmospheric water cycle of West Africa and the Atlantic to Saharan dust radiative forcing, *Ann. Geophys.*, *27*, 4023–4037, doi:10.5194/angeo-27-4023-2009.

Leaitch, W. R., C. M. Banic, G. A. Isaac, M. D. Couture, P. S. K. Liu, I. Gultepe, S.-M. Li, L. I. Kleinman, P. H. Daum, and J. I. MacPherson (1996), Physical and chemical observations in marine stratus during the 1993 North Atlantic Regional Experiment: Factors controlling cloud droplet number concentrations, *J. Geophys. Res.*, *101*(D22), 29,123–29,135, doi:10.1029/96JD01228.

Lebsock, M. D., G. L. Stephens, and C. Kummerow (2008), Multisensor satellite observations of aerosol effects on warm clouds, *J. Geophys. Res.*, *113*, D15205, doi:10.1029/2008JD009876.

L'Ecuyer, T. S., W. Berg, J. Haynes, M. Lebsock, and T. Takemura (2009), Global observations of aerosol impacts on precipitation occurrence in warm maritime clouds, *J. Geophys. Res.*, *114*, D09211, doi:10.1029/2008JD011273.

Lee, K., Z. Li, Y. J. Kim, and A. Kokhanovsky (2009), Atmospheric aerosol monitoring from satellite observations: A history of three decades, in *Atmospheric and Biological Environmental Monitoring*, edited by Y. J. Kim et al., pp. 13–38, Springer, New York, doi:10.1007/978-1-4020-9674-7_2.

Lee, S. S. (2011), Dependence of aerosol-precipitation interactions on humidity in a multiple-cloud system, *Atmos. Chem. Phys.*, *11*, 2179–2196, doi:10.5194/acp-11-2179-2011.

Lee, S. S., and G. Feingold (2010), Precipitating cloud-system response to aerosol perturbations, *Geophys. Res. Lett.*, *37*, L23806, doi:10.1029/2010GL045596.

Lee, S. S., L. J. Donner, V. T. J. Phillips, and Y. Ming (2008a), The dependence of aerosol effects on clouds and precipitation on cloud-system organization, shear and stability, *J. Geophys. Res.*, *113*, D16202, doi:10.1029/2007JD009224.

Lee, S. S., L. J. Donner, V. T. J. Phillips, and Y. Ming (2008b), Examination of aerosol effects on precipitation in deep convective clouds during the 1997 ARM summer experiment, *Q. J. R. Meteorol. Soc.*, *134*(634), 1201–1220, doi:10.1002/qj.287.

Lee, S. S., L. J. Donner, and V. T. J. Phillips (2009a), Impacts of aerosol chemical composition on microphysics and precipitation in deep convection, *Atmos. Res.*, *94*, 220–237, doi:10.1016/j.atmosres.2009b.05.015.

Lee, S. S., L. J. Donner, and V. T. J. Phillips (2009b), Sensitivity of aerosol and cloud effects on radiation to cloud types: Comparison between deep convective clouds and warm stratiform clouds over one-day period, *Atmos. Chem. Phys.*, *9*, 2555–2575, doi:10.5194/acp-9-2555-2009c.

Lerach, D. G., B. J. Gaudet, and W. R. Cotton (2008), Idealized simulations of aerosol influences on tornadogenesis, *Geophys. Res. Lett.*, *35*, L23806, doi:10.1029/2008GL035617.

Levin, Z., and W. R. Cotton (Eds.) (2009), *Aerosol Pollution Impact on Precipitation: A Scientific Review*, 386 pp., Springer, New York, doi:10.1007/978-1-4020-8690-8.

Li, G., Y. Wang, and R. Zhang (2008a), Implementation of a two-moment bulk microphysics scheme to the WRF model to investigate aerosol-cloud interaction, *J. Geophys. Res.*, *113*, D15211, doi:10.1029/2007JD009361.

Li, G., Y. Wang, K.-H. Lee, Y. Diao, and R. Zhang (2008b), Increased winter precipitation over the North Pacific from 1984–1994 to 1995–2005 inferred from the Global Precipitation Climatology Project, *Geophys. Res. Lett.*, *35*, L13821, doi:10.1029/2008GL034668.

Li, G., Y. Wang, K.-H. Lee, Y. Diao, and R. Zhang (2009a), The impacts of aerosols on development and precipitation of a mesoscale squall line, *J. Geophys. Res.*, *114*, D17205, doi:10.1029/2008JD011581.

Li, Z., et al. (2007), Preface to special section on East Asian Studies of Tropospheric Aerosols: An International Regional Experiment (EAST-AIRE), *J. Geophys. Res.*, *112*, D22S00, doi:10.1029/2007JD008853.

Li, Z., X. Zhao, R. Kahn, M. Mishchenko, L. Remer, K.-H. Lee, M. Wang, I. Laszlo, T. Nakajima, and H. Maring (2009b), Uncertainties in satellite remote sensing of aerosols and impact on monitoring its long-term trend: A review and perspective, *Ann. Geophys.*, *27*, 2755–2770, doi:10.5194/angeo-27-2755-2009.

Li, Z., F. Niu, J. Fan, Y. Liu, D. Rosenfeld, and Y. Ding (2011a), The long-term impacts of aerosols on the vertical development of clouds and precipitation, *Nat. Geosci.*, *4*, 888–894, doi:10.1038/ngeo1313.

Li, Z., et al. (2011b), East Asian studies of tropospheric aerosols and their impact on regional climate (EAST-AIRC): An overview, *J. Geophys. Res.*, *116*, D00K34, doi:10.1029/2010JD015257.

Lin, J. C., T. Matsui, R. A. Pielke Sr., and C. Kummerow (2006), Effects of biomass burning-derived aerosols on precipitation and clouds in the Amazon Basin: A satellite-based empirical study, *J. Geophys. Res.*, *111*, D19204, doi:10.1029/2005JD006884.

Liu, G., H. Shao, J. A. Coakley Jr., J. A. Curry, J. A. Haggerty, and M. A. Tschudi (2003), Retrieval of cloud droplet size from visible and microwave radiometric measurements during INDOEX: Implication to aerosols' indirect radioactive effect, *J. Geophys. Res.*, *108*(D1), 4006, doi:10.1029/2001JD001395.

Liu, J., Y. Zheng, Z. Li, and M. Cribb (2011), Analysis of cloud condensation nuclei properties at a polluted site in southeastern China during the AMF-China Campaign, *J. Geophys. Res.*, *116*, D00K35, doi:10.1029/2011JD016395.

Liu, X., and J. E. Penner (2005), Ice nucleation parameterization for global models, *Meteorol. Z.*, *14*, 499–514, doi:10.1127/0941-2948/2005/0059.

Liu, X., and J. Wang (2010), How important is organic aerosol hygroscopicity to aerosol indirect forcing?, *Environ. Res. Lett.*, *5*, 044010, doi:10.1088/1748-9326/5/4/044010.

Liu, X., J. E. Penner, and M. Herzog (2005), Global modeling of aerosol dynamics: Model description, evaluation, and interactions between sulfate and nonsulfate aerosols, *J. Geophys. Res.*, *110*, D18206, doi:10.1029/2004JD005674.

Liu, Y., and P. H. Daum (2002), Indirect warming effect from dispersion forcing, *Nature*, *419*, 580–581, doi:10.1038/419580a.

Lohmann, U. (2008), Global anthropogenic aerosol effects on convective clouds in ECHAM-HAM, *Atmos. Chem. Phys.*, *8*, 2115–2131, doi:10.5194/acp-8-2115-2008.

Lohmann, U., and J. Feichter (2005), Global indirect aerosol effects: A review, *Atmos. Chem. Phys.*, *5*, 715–737, doi:10.5194/acp-5-715-2005.

Lohmann, U., J. Feichter, C. C. Chuang, and J. E. Penner (1999), Prediction of the number of cloud droplets in the ECHAM GCM, *J. Geophys. Res.*, *104*(D8), 9169–9198, doi:10.1029/1999JD900046.

Lohmann, U., P. Stier, C. Hoose, S. Ferrachat, S. Kloster, E. Roeckner, and J. Zhang (2007), Cloud microphysics and aerosol indirect effects in the global climate model ECHAM5-HAM, *Atmos. Chem. Phys.*, *7*, 3425–3446, doi:10.5194/acp-7-3425-2007.

Low, T. B., and R. List (1982), Collision, coalescence and breakup of raindrops: 1. Experimentally established coalescence efficiencies and fragment size distributions in breakup, *J. Atmos. Sci.*, *39*, 1591–1606, doi:10.1175/1520-0469(1982)039<1591:CCABOR>2.0.CO;2.

Lüönd, F., O. Stetzer, A. Welti, and U. Lohmann (2010), Experimental study on the ice nucleation ability of size selected kaolinite particles in the immersion mode, *J. Geophys. Res.*, *115*, D14201, doi:10.1029/2009JD012959.

Lynn, B. H., A. Khain, J. Dudhia, D. Rosenfeld, A. Pokrovsky, and A. Seifert (2005a), Spectral (bin) microphysics coupled with a mesoscale model (MM5): Part I. Model description and first results, *Mon. Weather Rev.*, *133*, 44–58, doi:10.1175/MWR-2840.1.

Lynn, B. H., A. Khain, J. Dudhia, D. Rosenfeld, A. Pokrovsky, and A. Seifert (2005b), Spectral (bin) microphysics coupled with a mesoscale model (MM5): Part II. Simulation of a CaPE rain event with a squall line, *Mon. Weather Rev.*, *133*, 59–71, doi:10.1175/MWR-2841.1.

Mace, G. G., and S. Benson (2008), The vertical structure of cloud occurrence and radiative forcing at the SGP ARM site as revealed by 8 years of continuous data, *J. Clim.*, *21*(11), 2591, doi:10.1175/2007JCLI1987.1.

Manoj, M. G., P. C. S. Devera, and P. D. Safai (2010), Absorbing aerosols facilitate transition of Indian monsoon breaks to active spells, *Clim. Dyn.*, *37*, 2181–2198, doi:10.1007/s00382-010-0971-3.

Marcolli, C., S. Gedamke, T. Peter, and B. Zobrist (2007), Efficiency of immersion mode ice nucleation on surrogates of mineral dust, *Atmos. Chem. Phys.*, *7*, 5081–5091, doi:10.5194/acp-7-5081-2007.

Martin, G. M., D. W. Johnson, and A. Spice (1994), The measurement and parameterization of effective radius of droplets in warm stratocumulus clouds, *J. Atmos. Sci.*, *51*, 1823–1842, doi:10.1175/1520-0469(1994)051<1823:TMAPOE>2.0.CO;2.

Martins, J. V., P. V. Hobbs, R. E. Weiss, and P. Artaxo (1998), Sphericity and morphology of smoke particles from biomass burning in Brazil, *J. Geophys. Res.*, *103*(D24), 32,051–32,057, doi:10.1029/98JD01153.

Mason, B. J. (1971), *The Physics of Clouds*, Clarendon, Oxford, U. K.

Massie, S. T., A. Heymsfield, C. Schmitt, D. Müller, and P. Seifert (2007), Aerosol indirect effects as a function of cloud top pressure, *J. Geophys. Res.*, *112*, D06202, doi:10.1029/2006JD007383.

Mather, G. K., D. E. Terblanche, F. E. Steffens, and L. Fletcher (1997), Results of the South African cloud seeding experiments using hygroscopic flares, *J. Appl. Meteorol.*, *36*, 1433–1447, doi:10.1175/1520-0450(1997)036<1433:ROTSAC>2.0.CO;2.

Matsui, T., H. Masunaga, R. A. Pielke Sr., and W.-K. Tao (2004), Impact of aerosols and atmospheric thermodynamics on cloud properties within the climate system, *Geophys. Res. Lett.*, *31*, L06109, doi:10.1029/2003GL019287.

Matsui, T., H. Masunaga, S. M. Kreidenweis, R. A. Pielke Sr., W.-K. Tao, M. Chin, and Y. J. Kaufman (2006), Satellite-based assessment of marine low cloud variability associated with aerosol, atmospheric stability, and the diurnal cycle, *J. Geophys. Res.*, *111*, D17204, doi:10.1029/2005JD006097.

McCumber, M., W. K. Tao, J. Simpson, R. Penc, and S. T. Soong (1991), Comparison of ice-phase microphysical parameterization schemes using numerical simulations of tropical convection, *J. Appl. Meteorol.*, *30*, 985–1004, doi:10.1175/1520-0450-30.7.985.

McGraw, R. (1997), Description of aerosol dynamics by the quadrature method of moments, *Aerosol Sci. Technol.*, *27*, 255–265, doi:10.1080/02786829708965471.

Meehl, G. A., J. M. Arblaster, and W. D. Collins (2008), Effects of black carbon aerosols on the Indian monsoon, *J. Clim.*, *21*, 2869–2882, doi:10.1175/2007JCLI1777.1.

Menon, S., A. D. Del Genio, D. Koch, and G. Tselioudis (2002), GCM simulations of the aerosol indirect effect: Sensitivity to cloud parameterization and aerosol burden, *J. Atmos. Sci.*, *59*, 692–713, doi:10.1175/1520-0469(2002)059<0692:GSOTAI>2.0.CO;2.

Meyers, M. P., P. J. DeMott, and W. R. Cotton (1992), New primary ice-nucleation parameterization in an explicit cloud model, *J. Appl. Meteorol.*, *31*, 708–721, doi:10.1175/1520-0450(1992)031<0708:NPINPI>2.0.CO;2.

Meyers, M. P., R. L. Walko, J. Y. Harrington, and W. R. Cotton (1997), New RAMS cloud microphysics parameterization: Part II. The two-moment scheme, *Atmos. Res.*, *45*, 3–39, doi:10.1016/S0169-8095(97)00018-5.

Ming, Y., V. Ramaswamy, P. A. Ginoux, L. H. Horowitz, and L. M. Russell (2005), Geophysical Fluid Dynamics Laboratory general circulation model investigation of the indirect radiative effects of anthropogenic sulfate aerosol, *J. Geophys. Res.*, *110*, D22206, doi:10.1029/2005JD006161.

Ming, Y., V. Ramaswamy, L. J. Donner, and V. T. J. Phillips (2006), A new parameterization of cloud droplet activation applicable to general circulation models, *J. Atmos. Sci.*, *63*, 1348–1356, doi:10.1175/JAS3686.1.

Ming, Y., et al. (2007), Modeling the interactions between aerosols and liquid water clouds with a self-consistent cloud scheme in a general circulation model, *J. Atmos. Sci.*, *64*, 1189–1209, doi:10.1175/JAS3874.1.

Miura, H., H. Tomita, T. Nasuno, S. Iga, M. Satoh, and T. Matsuno (2005), A climate sensitively test using a global cloud resolving model under an aqua planet condition, *Geophys. Res. Lett.*, *32*, L19717, doi:10.1029/2005GL023672.

Möhler, O., et al. (2006), Efficiency of the deposition mode ice nucleation on mineral dust particles, *Atmos. Chem. Phys.*, *6*, 3007–3021, doi:10.5194/acp-6-3007-2006.

Morrison, H., and A. Gettelman (2008), A new two-moment bulk stratiform cloud microphysics scheme in the Community Atmosphere Model, version 3(CAM3): Part I. Description and numerical tests, *J. Clim.*, *21*, 3642–3659, doi:10.1175/2008JCLI2105.1.

Morrison, H., and W. W. Grabowski (2008), Modeling supersaturation and subgrid-scale mixing with two-moment bulk warm microphysics, *J. Atmos. Sci.*, *65*, 792–812, doi:10.1175/2007JAS2374.1.

Morrison, H., and W. W. Grabowski (2010), An improved representation of rimed snow and conversion to graupel in a multi-component bin microphysics scheme, *J. Atmos. Sci.*, *67*, 1337–1360, doi:10.1175/2010JAS3250.1.

Morrison, H., and J. O. Pinto (2005), Mesoscale modeling of springtime arctic mixed phase clouds using a new two-moment bulk microphysics scheme, *J. Atmos. Sci.*, *62*, 3683–3704, doi:10.1175/JAS3564.1.

Mossop, S. C., and J. Hallett (1974), Ice crystal concentration in cumulus clouds: Influence of the drop spectrum, *Science*, *186*, 632–634, doi:10.1126/science.186.4164.632.

Nakajima, T., A. Higurashi, K. Kawamoto, and J. Penner (2001), A possible correlation between satellite-derived cloud and aerosol microphysical parameters, *Geophys. Res. Lett.*, *28*, 1171–1174, doi:10.1029/2000GL012186.

Naoe, H., and K. Okada (2001), Mixing properties of submicrometer aerosol particles in the urban atmosphere—with regard to soot particles, *Atmos. Environ.*, *35*, 5765–5772, doi:10.1016/S1352-2310(01)00367-3.

Nasuno, T., H. Tomita, S. Iga, H. Miura, and M. Satoh (2008), Multiscale organization of convection simulated with explicit cloud processes on an aquaplanet, *J. Atmos. Sci.*, *64*(6), 1902–1921, doi:10.1175/JAS3948.1 DOI:dx.doi.org.

National Research Council (NRC) (2005), *Radiative Forcing of Climate Change: Expanding the Concept and Addressing Uncertainties*, Natl. Acad. Press, Washington, D. C.

Nenes, A., and J. H. Seinfeld (2003), Parameterization of cloud droplet formation in global climate models, *J. Geophys. Res.*, *108*(D14), 4415, doi:10.1029/2002JD002911.

Nenes, A., W. C. Conant, and J. H. Seinfeld (2002), Black carbon radiative heating effects on cloud microphysics and implications for the aerosol indirect effect: 2. Cloud microphysics, *J. Geophys. Res.*, *107*(D21), 4605, doi:10.1029/2002JD002101.

Nesbitt, S. W., R. Cifelli, and S. A. Rutledge (2006), Storm morphology and rainfall characteristics of TRMM precipitation features, *Mon. Weather Rev.*, *134*, 2702–2721, doi:10.1175/MWR3200.1.

Niedermeier, D., et al. (2010), Heterogeneous freezing of droplets with immersed mineral dust particles—Measurements and parameterization, *Atmos. Chem. Phys.*, *10*, 3601–3614, doi:10.5194/acp-10-3601-2010.

Nigam, S., and M. Bollasina (2010), "Elevated heat pump" hypothesis for the aerosol-monsoon hydroclimate link: "Grounded" in observations?, *J. Geophys. Res.*, *115*, D16201, doi:10.1029/2009JD013800.

Niu, F., and Z. Li (2011), Cloud invigoration and suppression by aerosols over the tropical region based on satellite observations, *Atmos. Chem. Phys. Discuss.*, *11*, 5003–5017, doi:10.5194/acpd-11-5003-2011.

Niu, F., Z. Li, C. Li, K.-H. Lee, and M. Wang (2010), Increase of wintertime fog in China: Potential impacts of weakening of the Eastern Asian monsoon circulation and increasing aerosol loading, *J. Geophys. Res.*, *115*, D00K20, doi:10.1029/2009JD013484.

Novakov, T., and J. E. Penner (1993), Large contributions of organic aerosols to cloud condensation nuclei concentrations, *Nature*, *365*, 823–826, doi:10.1038/365823a0.

O'Dowd, C. D., M. H. Smith, I. E. Consterdine, and J. A. Lowe (1997), Marine aerosol, sea-salt, and the marine sulphur cycle: A short review, *Atmos. Environ.*, *31*, 73–80, doi:10.1016/S1352-2310(96)00106-9.

O'Dowd, C. D., E. Becker, and M. Kulmala (2001), Mid-latitude North-Atlantic aerosol characteristics in clean and polluted air, *Atmos. Res.*, *58*, 167–185, doi:10.1016/S0169-8095(01)00098-9.

Ogura, Y., and N. A. Phillips (1962), Scale analysis of deep and shallow convection in the atmosphere, *J. Atmos. Sci.*, *19*, 173–179, doi:10.1175/1520-0469(1962)019<0173:SAODAS>2.0.CO;2.

Ohashi, Y., and H. Kida (2002), Local circulation developed in the vicinity of both coastal and inland urban areas: Numerical study with a mesoscale atmospheric model, *J. Appl. Meteorol.*, *41*, 30–45, doi:10.1175/1520-0450(2002)041<0030:LCDITV>2.0.CO;2.

Okada, K., M. Ikegami, Y. Zaizen, Y. Makino, J. B. Jensen, and J. L. Gras (2001), The mixture state of individual aerosol particles in the 1997 Indonesian haze episode, *J. Aerosol Sci.*, *32*(11), 1269–1279, doi:10.1016/S0021-8502(01)00062-3.

Okada, K., M. Ikegami, Y. Zaizen, Y. Tsutsumi, Y. Makino, J. B. Jensen, and J. L. Gras (2005), Soot particles in the free troposphere over Australia, *Atmos. Environ.*, *39*, 5079–5089, doi:10.1016/j.atmosenv.2005.05.015.

Orville, R. E., R. Zhang, J. N. Gammon, D. Collins, B. Ely, and S. Steiger (2001), Enhancement of cloud-to-ground lightening over Houston, Texas, *Geophys. Res. Lett.*, *28*(13), 2597–2600, doi:10.1029/2001GL012990.

Panicker, A. S., G. Pandithurai, and S. Dipu (2010), Aerosol indirect effect during successive contrasting monsoon years over Indian subcontinent using MODIS data, *Atmos. Environ.*, *44*, 1937–1943, doi:10.1016/j.atmosenv.2010.02.015.

Parthasarathy, B. A., A. A. Munot, and D. R. Kothavale (1995), Monthly and seasonal rainfall series for all-India homogeneous regions and meteorological subdivisions: 1871–1994, *Res. Rep. RR-065*, Indian Inst. of Trop. Meteorol., Pune, India.

Penner, J. E., et al. (2001), Aerosols, their direct and indirect effects, in *Climate Change 2001: The Scientific Basis*, edited by J. T. Houghton et al., pp. 289–348, Cambridge Univ. Press, Cambridge, U. K.

Penner, J. E., X. Dong, and Y. Chen (2004), Observational evidence of a change in radiative forcing due to the indirect aerosol effect, *Nature*, *427*, 231–234, doi:10.1038/nature02234.

Penner, J. E., J. Quaas, T. Storelvmo, T. Takemura, O. Boucher, H. Guo, A. Kirkevåg, J. E. Kristjánsson, and Ø. Seland (2006), Model intercomparison of indirect aerosol effects, *Atmos. Chem. Phys.*, *6*, 3391–3405, doi:10.5194/acp-6-3391-2006.

Penner, J. E., L. Xu, and M. Wang (2011), Satellite methods underestimate indirect climate forcing by aerosols, *Proc. Natl. Acad. Sci. U. S. A.*, *108*, 13,404–13,408, doi:10.1073/pnas.1018526108.

Petters, M. D., and S. M. Kreidenweis (2007), A single parameter representation of hygroscopic growth and cloud condensation nucleus activity, *Atmos. Chem. Phys.*, *7*, 1961–1971, doi:10.5194/acp-7-1961-2007.

Phillips, V. T. J., T. W. Choularton, A. M. Blyth, and J. Latham (2002), The influence of aerosol concentrations on the glaciation and precipitation of a cumulus cloud, *Q. J. R. Meteorol. Soc.*, *128*(581), 951–971, doi:10.1256/0035900021643601.

Phillips, V. T. J., et al. (2005), Anvil glaciation in a deep cumulus updraught over Florida simulated with the Explicit Microphysics Model: I. Impact of various nucleation processes, *Q. J. R. Meteorol. Soc.*, *131*, 2019–2046, doi:10.1256/qj.04.85.

Pinsky, M., A. P. Khain, and M. Shapiro (2000), Stochastic effect on cloud droplet hydrodynamic interaction in a turbulent flow, *Atmos. Res.*, *53*, 131–169, doi:10.1016/S0169-8095(99)00048-4.

Pinsky, M., A. P. Khain, and M. Shapiro (2001), Collision efficiency of drops in a wide range of Reynolds numbers: Effects

of pressure on spectrum evolution, *J. Atmos. Sci.*, *58*, 742–764, doi:10.1175/1520-0469(2001)058<0742:CEODIA>2.0.CO;2.

Pinsky, M., A. P. Khain, L. Magaritz, and A. Sterkin (2008), Simulation of droplet size distributions and drizzle formation using a new trajectory ensemble model of cloud topped boundary layer: Part 1. Model description and first results in non-mixing limit, *J. Atmos. Sci.*, *65*, 2064–2086, doi:10.1175/2007JAS2486.1.

Platnick, S. (2000), Vertical photon transport in cloud remote sensing problems, *J. Geophys. Res.*, *105*(D18), 22,919–22,935, doi:10.1029/2000JD900333.

Pósfai, M., J. R. Anderson, P. R. Buseck, and H. Sievering (1999), Soot and sulfate aerosol particles in the remote marine troposphere, *J. Geophys. Res.*, *104*, 21,685–21,693, doi:10.1029/1999JD900208.

Posselt, R., and U. Lohmann (2008), Influence of giant CCN on warm rain processes in the ECHAM5 GCM, *Atmos. Chem. Phys.*, *8*, 3769–3788, doi:10.5194/acp-8-3769-2008.

Pruppacher, H. R., and J. D. Klett (1997), *Microphysics of Clouds and Precipitation*, Kluwer Acad., Dordrecht, Netherlands.

Qian, Y., D. Gong, J. Fan, L. R. Leung, R. Bennartz, D. Chen, and W. Wang (2009), Heavy pollution suppresses light rain in China: Observations and modeling, *J. Geophys. Res.*, *114*, D00K02, doi:10.1029/2008JD011575.

Quaas, J., et al. (2009), Aerosol indirect effects—General circulation model intercomparison and evaluation with satellite data, *Atmos. Chem. Phys.*, *9*, 8697–8717, doi:10.5194/acp-9-8697-2009.

Radke, L. F., J. A. Coakley Jr., and M. D. King (1989), Direct and remote sensing observations of the effects of ships on clouds, *Science*, *246*, 1146–1149, doi:10.1126/science.246.4934.1146.

Ramanathan, V., P. J. Crutzen, J. T. Kiehl, and D. Rosenfeld (2001a), Aerosols, climate, and the hydrological cycle, *Science*, *294*, 2119–2124, doi:10.1126/science.1064034.

Ramanathan, V., et al. (2001b), Indian Ocean Experiment: An integrated analysis of the climate forcing and effects of the great Indo-Asian haze, *J. Geophys. Res.*, *106*, 28,371–28,398, doi:10.1029/2001JD900133.

Ramanathan, V., C. Chung, D. Kim, T. Bettge, L. Buja, J. T. Kiehl, W. M. Washington, Q. Fu, D. R. Sikka, and M. Wild (2005), Atmospheric brown clouds: Impact on South Asian climate and hydrologic cycle, *Proc. Natl. Acad. Sci. U. S. A.*, *102*, 5326–5333, doi:10.1073/pnas.0500656102.

Ramaswamy, V., and C.-T. Chen (1997), Linear additivity of climate response for combined albedo and greenhouse perturbations, *Geophys. Res. Lett.*, *24*, 567–570, doi:10.1029/97GL00248.

Ramaswamy, V., O. Boucher, J. Haigh, D. Hauglustaine, J. Haywood, G. Myhre, T. Nakajima, Y. G. Shi, and S. Solomon (2001), Radiative forcing of climate change, in *Climate Change 2001: The Scientific Basis—Contribution of Working Group I to the Third Assessment Report of the Intergovernmental Panel on Climate Change*, edited by J. T. Houghton et al., pp. 349–416, Cambridge Univ. Press, New York.

Randall, D., M. Khairoutdinov, A. Arakawa, and W. Grabowski (2003), Breaking the cloud parameterization deadlock, *Bull. Am. Meteorol. Soc.*, *84*, 1547–1564, doi:10.1175/BAMS-84-11-1547.

Randall, D. A., et al. (2007), Climate models and their evaluation, in *Climate Change 2007: The Physical Science Basis—Contribution of Working Group I to the Fourth Assessment Report of the Intergovernmental Panel on Climate Change*, edited by S. Solomon et al., pp. 589–662, Cambridge Univ. Press, Cambridge, U. K.

Randles, C. A., and V. Ramaswamy (2008), Absorbing aerosols over Asia: A Geophysical Fluid Dynamics Laboratory general circulation model sensitivity study of model response to aerosol optical depth and aerosol absorption, *J. Geophys. Res.*, *113*, D21203, doi:10.1029/2008JD010140.

Rasch, P. J., and J. E. Kristjánsson (1998), A comparison of the CCM3 model climate using diagnosed and predicted condensate parameterizations, *J. Clim.*, *11*, 1587–1614, doi:10.1175/1520-0442(1998)011<1587:ACOTCM>2.0.CO;2.

Ravi, S., et al. (2011), Aeolian processes and the biosphere, *Rev. Geophys.*, *49*, RG3001, doi:10.1029/2010RG000328.

Reisin, T. G., Y. Yin, Z. Levin, and S. Tzivion (1998), Development of giant drops and high reflectivity cores in Hawaiian clouds: Numerical simulation using a kinematic model with detailed microphysics, *Atmos. Res.*, *45*, 275–297, doi:10.1016/S0169-8095(97)00081-1.

Roberts, D. L., and A. Jones (2004), Climate sensitivity to black carbon aerosol from fossil fuel combustion, *J. Geophys. Res.*, *109*, D16202, doi:10.1029/2004JD004676.

Roelofs, G. J., L. G. Ganzeveld, and J. Lelieveld (1998), Simulation of global sulfate distribution and the influence on effective cloud drop radii with a coupled photochemistry-sulfur cycle model, *Tellus, Ser. B*, *50*, 224–242.

Roelofs, G. J., P. Stier, J. Feichter, E. Vignati, and J. Wilson (2006), Aerosol activation and cloud processing in the global aerosol-climate model ECHAM5-HAM, *Atmos. Chem. Phys.*, *6*, 2389–2399, doi:10.5194/acp-6-2389-2006.

Rogers, R. R., and M. K. Yau (1989), *A Short Course in Cloud Physics*, Pergamon, New York.

Rosenfeld, D. (1999), TRMM observed first direct evidence of smoke from forest fires inhibiting rainfall, *Geophys. Res. Lett.*, *26*, 3105–3108, doi:10.1029/1999GL006066.

Rosenfeld, D. (2000), Suppression of rain and snow by urban and industrial air pollution, *Science*, *287*, 1793–1796, doi:10.1126/science.287.5459.1793.

Rosenfeld, D., and G. Feingold (2003), Explanation of the discrepancies among satellite observations of the aerosol indirect effects, *Geophys. Res. Lett.*, *30*(14), 1776, doi:10.1029/2003GL017684.

Rosenfeld, D., and I. Lensky (1998), Satellite-based insights into precipitation formation processes in continental and maritime convective clouds, *Bull. Am. Meteorol. Soc.*, *79*, 2457–2476, doi:10.1175/1520-0477(1998)079<2457:SBIIPF>2.0.CO;2.

Rosenfeld, D., and C. W. Ulbrich (2003), Cloud microphysical properties, processes, and rainfall estimation opportunities, in *Radar and Atmospheric Science: A Collection of Essays in Honor of David Atlas*, *Meteorol. Monogr. Ser.*, vol. 52, edited by R. M. Wakimoto and R. Srivastava, chap. 10, pp. 237–258, Am. Meteorol. Soc., Boston, Mass.

Rosenfeld, D., and W. L. Woodley (2000), Convective clouds with sustained highly supercooled liquid water down to −37°C, *Nature*, *405*, 440–442, doi:10.1038/35013030.

Rosenfeld, D., Y. Rudich, and R. Lahav (2001), Desert dust suppressing precipitation: A possible desertification feedback loop, *Proc. Natl. Acad. Sci. U. S. A.*, *98*, 5975–5980, doi:10.1073/pnas.101122798.

Rosenfeld, D., et al. (2008), Flood or drought: How do aerosols affect precipitation?, *Science*, *321*, 1309–1313, doi:10.1126/science.1160606.

Rotstayn, L. D. (2000), On the tuning of autoconversion parameterizations in climate models, *J. Geophys. Res.*, *105*, 15,495–15,507, doi:10.1029/2000JD900129.

Rotstayn, L. D., and U. Lohmann (2002), Tropical rainfall trends and the indirect aerosol effect, *J. Clim.*, *15*, 2103–2116, doi:10.1175/1520-0442(2002)015<2103:TRTATI>2.0.CO;2.

Rotstayn, L. D., and J. E. Penner (2001), Indirect aerosol forcing, quasiforcing, and climate response, *J. Clim.*, *14*, 2960–2975, doi:10.1175/1520-0442(2001)014<2960:IAFQFA>2.0.CO;2.

Rotstayn, L. D., et al. (2007), Have Australian rainfall and cloudiness increased due to the remote effects of Asian anthropogenic aerosols?, *J. Geophys. Res.*, *112*, D09202, doi:10.1029/2006JD007712.

Russell, L. M., S. F. Maria, and S. C. B. Myneni (2002), Mapping organic coatings on atmospheric particles, *Geophys. Res. Lett.*, *29*(16), 1779, doi:10.1029/2002GL014874.

Rutledge, S. A., R. A. Houze Jr., M. I. Biggerstaff, and T. Matejka (1988), The Oklahoma-Kansas mesoscale convective system of 10–11 June 1985: Precipitation structure and single-Doppler radar analysis, *Mon. Wea. Rev.*, *116*, 1409–1430.

Saleeby, S. M., and W. R. Cotton (2004), A large-droplet mode and prognostic number concentration of cloud droplets in the Colorado State University Regional Atmospheric Modeling System (RAMS): Part I. Module descriptions and supercell test simulations, *J. Appl. Meteorol.*, *43*, 182–195, doi:10.1175/1520-0450(2004)043<0182:ALMAPN>2.0.CO;2.

Saleeby, S. M., W. Berg, S. C. van den Heever, and T. L'Ecuyer (2010), Impact of cloud-nucleating aerosols in cloud-resolving model simulations of warm-rain precipitation in the East China Sea, *J. Atmos. Sci.*, *67*, 3916–3930, doi:10.1175/2010JAS3528.1.

Sassen, K. (2002), Indirect climate forcing over the western US from Asian dust storms, *Geophys. Res. Lett.*, *29*(10), 1465, doi:10.1029/2001GL014051.

Sassen, K., D. Starr, G. G. Mace, M. R. Poellot, S. H. Melfi, W. L. Eberhard, J. D. Spinhirne, E. W. Eloranta, D. E. Hagan, and J. Hallett (1995), The 5–6 December 1991 FIRE IFO II jet stream cirrus case study: Possible influences of volcanic aerosols, *J. Atmos. Sci.*, *52*, 97–123, doi:10.1175/1520-0469(1995)052<0097:TDFIIJ>2.0.CO;2.

Sassen, K., P. J. DeMott, J. Prospero, and M. R. Poellot (2003), Saharan dust storms and indirect aerosol effects on clouds: CRYSTAL-FACE results, *Geophys. Res. Lett.*, *30*(12), 1633, doi:10.1029/2003GL017371.

Schwartz, S. E., Harshvardan, and C. M. Benkovitz (2002), Influence of anthropogenic aerosol on cloud optical depth and albedo shown by satellite measurements and chemical transport modeling, *Proc. Natl. Acad. Sci. U. S. A.*, *99*, 1784–1789, doi:10.1073/pnas.261712099.

Schwarz, J. P., et al. (2008), Coatings and their enhancement of black carbon light absorption in the tropical atmosphere, *J. Geophys. Res.*, *113*, D03203, doi:10.1029/2007JD009042.

Sedunov, Y. S. (1967), Kinetics of initial stage of condensation in clouds, *Izv. Acad. Sci. USSR Atmos Oceanic Phys.*, *3*, 34–46.

Seifert, A., and K. D. Beheng (2006), A two-moment cloud microphysics parameterization for mixed-phase clouds: Part 2. Maritime vs. continental deep convective storms, *Meteorol. Atmos. Phys.*, *92*, 67–82, doi:10.1007/s00703-005-0113-3.

Seifert, A., A. Khain, U. Blahak, and K. D. Beheng (2005), Possible effects of collisional breakup on mixed-phase deep convection simulated by a spectral (bin) cloud model, *J. Atmos. Sci.*, *62*, 1917–1931, doi:10.1175/JAS3432.1.

Sekiguchi, M., T. Nakajima, K. Suzuki, K. Kawamoto, A. Higurashi, D. Rosenfeld, I. Sano, and S. Mukai (2003), A study of the direct and indirect effects of aerosols using global satellite data sets of aerosol and cloud parameters, *J. Geophys. Res.*, *108*(D22), 4699, doi:10.1029/2002JD003359.

Shepherd, J. M. (2005), A review of current investigations of urban-induced rainfall and recommendations for the future, *Earth Interact.*, *9*(12), 1–27, doi:10.1175/EI156.1.

Shepherd, J. M., and S. J. Burian (2003), Detection of urban-induced rainfall anomalies in a major coastal city, *Earth Interact.*, *7*, 1–17.

Sheridan, L. M., J. Y. Harrington, D. Lamb, and K. Sulia (2009), Influence of ice aspect ratio on the evolution of ice size spectra during vapor depositional growth, *J. Atmos. Sci.*, *66*, 3732–3743, doi:10.1175/2009JAS3113.1.

Sherwood, S. (2002), Aerosols and ice particle size in tropical cumulonimbus, *J. Clim.*, *15*, 1051–1063, doi:10.1175/1520-0442(2002)015<1051:AAIPSI>2.0.CO;2.

Shulman, M. L., M. C. Jacobson, R. J. Charlson, R. E. Synovec, and T. E. Young (1996), Dissolution behavior and surface tension effects of organic compounds in nucleating cloud droplets, *Geophys. Res. Lett.*, *23*(3), 277–280, doi:10.1029/95GL03810.

Song, X., and G. J. Zhang (2011), Microphysics parameterization for convective clouds in a global climate model: Description and single-column model tests, *J. Geophys. Res.*, *116*, D02201, doi:10.1029/2010JD014833.

Sorooshian, A., G. Feingold, M. D. Lebsock, H. Jiang, and G. Stephens (2009), On the precipitation susceptibility of clouds to aerosol perturbations, *Geophys. Res. Lett.*, *36*, L13803, doi:10.1029/2009GL038993.

Sorooshian, A., et al. (2010), Deconstructing the precipitation susceptibility construct: Improving methodology for aerosol-cloud precipitation studies, *J. Geophys. Res.*, *115*, D17201, doi:10.1029/2009JD013426.

Squires, P. (1952), The growth of cloud drops by condensation: I. general characteristics, *Aust. J. Sci. Res., Ser. A*, *5*, 66–86.

Squires, P. (1958), The microstructure and colloidal stability of warm clouds, *Tellus*, *10*, 256–271.

Squires, P., and S. Twomey (1961), The relation between cloud drop spectra and the spectrum of cloud nuclei, in *Physics of Precipitation*, *Geophys. Monogr. Ser.*, vol. 5, edited by H. Weickmann, pp. 211–219, AGU, Washington, D. C.

Squires, P., and S. Twomey (1966), A comparison of cloud nucleus measurements over central North America and Caribbean Sea, *J. Atmos. Sci.*, *23*, 401–404, doi:10.1175/1520-0469(1966)023<0401:ACOCNM>2.0.CO;2.

Steiger, S. M., and R. E. Orville (2003), Cloud-to-ground lightning enhancement over southern Louisiana, *Geophys. Res. Lett.*, *30*(19), 1975, doi:10.1029/2003GL017923.

Steiger, S. M., R. E. Orville, and G. Huffines (2002), Cloud-to-ground lightning characteristics over Houston, Texas: 1989–2000, *J. Geophys. Res.*, *107*(D11), 4117, doi:10.1029/2001JD001142.

Stephens, G. L., et al. (2002), The CloudSat mission and the A-TRAIN: A new dimension to space-based observations of clouds and precipitation, *Bull. Am. Meteorol. Soc.*, *83*, 1771–1790, doi:10.1175/BAMS-83-12-1771.

Stevens, B., and G. Feingold (2009), Untangling aerosol effects on clouds and precipitation in a buffered system, *Nature*, *461*, 607–613, doi:10.1038/nature08281.

Stier, P., et al. (2005), The aerosol-climate model ECHAM-HAM, *Atmos. Chem. Phys.*, *5*, 1125–1156, doi:10.5194/acp-5-1125-2005.

Storelvmo, T., J. E. Kristjánsson, G. Myhre, M. Johnsrud, and F. Stordal (2006), Combined observational and modeling based study of the aerosol indirect effect, *Atmos. Chem. Phys.*, *6*, 3583–3601, doi:10.5194/acp-6-3583-2006.

Storer, R. L., S. C. van den Heever, and G. L. Stephens (2010), Modeling aerosol impacts on convection under differing storm environments, *J. Atmos. Sci.*, *67*, 3904–3915, doi:10.1175/2010JAS3363.1.

Ström, J., and S. Ohlsson (1998), In situ measurements of enhanced crystal number densities in cirrus clouds caused by aircraft exhaust, *J. Geophys. Res.*, *103*(D10), 11,355–11,361, doi:10.1029/98JD00807.

Tao, W.-K. (2003), Goddard Cumulus Ensemble (GCE) model: Application for understanding precipitation processes, in *Cloud Systems, Hurricanes, and the Tropical Rainfall Measuring Mission (TRMM)—A Tribute to Dr. Joanne Simpson*, *Meteorol. Monogr. Ser.*, vol. 29, pp. 107–138, Am. Meteorol. Soc. Boston, Mass.

Tao, W. K. (2007), Cloud resolving modeling, *J. Meteorol. Soc. Jpn.*, *85B*, 305–330, doi:10.2151/jmsj.85B.305.

Tao, W.-K., and M. Moncrieff (2009), Multiscale cloud system modeling, *Rev. Geophys.*, *47*, RG4002, doi:10.1029/2008RG000276.

Tao, W.-K., X. Li, A. Khain, T. Matsui, S. Lang, and J. Simpson (2007), Role of atmospheric aerosol concentration on deep convective precipitation: Cloud-resolving model simulations, *J. Geophys. Res.*, *112*, D24S18, doi:10.1029/2007JD008728.

Tatang, M. A., W. Pan, R. G. Prinn, and G. J. McRae (1997), An efficient method for parametric uncertainty analysis of numerical geophysical models, *J. Geophys. Res.*, *102*, 21,925–21,932, doi:10.1029/97JD01654.

Teller, A., and Z. Levin (2006), The effects of aerosols on precipitation and dimensions of subtropical clouds: A sensitivity study using a numerical cloud model, *Atmos. Chem. Phys.*, *6*, 67–80, doi:10.5194/acp-6-67-2006.

Thompson, A. M., W.-K. Tao, K. E. Pickering, J. R. Scala, and J. Simpson (1997), Tropical deep convection and ozone formation, *Bull. Am. Meteorol. Soc.*, *78*, 1043–1054, doi:10.1175/1520-0477(1997)078<1043:TDCAOF>2.0.CO;2.

Tomita, H., H. Miura, H. Iga, T. Nasuno, and M. Satoh (2005), A global cloud-resolving simulation: Preliminary results from an aqua planet experiment, *Geophys. Res. Lett.*, *32*, L08805, doi:10.1029/2005GL022459.

Tsai, I.-C., J.-P. Chen, P.-Y. Lin, W.-C. Wang, and I. S. A. Isaksen (2010), Sulfur cycle and sulfate radiative forcing simulated from a coupled global climate-chemistry model, *Atmos. Chem. Phys.*, *10*, 3693–3709, doi:10.5194/acp-10-3693-2010.

Twohy, C., et al. (2005), Evaluation of the aerosol indirect effect in marine stratocumulus clouds: Droplet number, size, liquid water path, and radiative impact, *J. Geophys. Res.*, *110*, D08203, doi:10.1029/2004JD005116.

Twohy, C., et al. (2008), Interaction of Saharan dust with liquid and ice clouds, paper presented at the 15th International Conference on Clouds and Precipitation, Universidad Nacional Autónoma de México, Cancun, Mexico, 7–11 July.

Twomey, S. (1959a), The nuclei of natural cloud formation: Part I. The chemical diffusion method and its application to atmospheric nuclei, *Geofis. Pura Appl.*, *43*, 227–242, doi:10.1007/BF01993559.

Twomey, S. (1959b), The nuclei of natural cloud formation: Part II. The supersaturation in natural clouds and the variation of cloud droplet concentration, *Geofis. Pura Appl.*, *43*, 243–249, doi:10.1007/BF01993560.

Twomey, S. (1977), The influence of pollution on the shortwave albedo of clouds, *J. Atmos. Sci.*, *34*, 1149–1152, doi:10.1175/1520-0469(1977)034<1149:TIOPOT>2.0.CO;2.

Twomey, S., M. Piepgrass, and T. L. Wolfe (1984), An assessment of the impact of pollution on global cloud albedo, *Tellus, Ser. B*, *36*, 356–366, doi:10.1111/j.1600-0889.1984.tb00254.x.

Vali, G. (1994), Freezing rate due to heterogeneous nucleation, *J. Atmos. Sci.*, *51*(13), 1843–1856, doi:10.1175/1520-0469(1994)051<1843:FRDTHN>2.0.CO;2.

Vali, G. (2008), Repeatability and randomness in heterogeneous freezing nucleation, *Atmos. Chem. Phys.*, *8*, 5017–5031, doi:10.5194/acp-8-5017-2008.

Vali, G., and E. J. Stansbury (1966), Time dependent characteristics of the heterogeneous nucleation of ice, *Can. J. Phys.*, *44*, 477–502, doi:10.1139/p66-044.

van den Heever, S. C., and W. R. Cotton (2007), Urban aerosol impacts on downwind convective storms, *J. Appl. Meteorol. Climatol.*, *46*, 828–850, doi:10.1175/JAM2492.1.

van den Heever, S. C., G. Carrio, W. R. Cotton, P. J. DeMott, and A. J. Prenni (2006), Impacts of nucleating aerosol on Florida convection: Part I. Mesoscale simulations, *J. Atmos. Sci.*, *63*, 1752–1775, doi:10.1175/JAS3713.1.

van den Heever, S. C., G. L. Stephens, and N. B. Wood (2011), Aerosol indirect effects on tropical convection characteristics under conditions of radiative-convective equilibrium, *J. Atmos. Sci.*, *68*, 699–718, doi:10.1175/2010JAS3603.1.

Vignati, E., J. Wilson, and P. Stier (2004), M7: An efficient size-resolved aerosol microphysics module for large-scale aerosol transport models, *J. Geophys. Res.*, *109*, D22202, doi:10.1029/2003JD004485.

Wang, C. (2004), A modeling study on the climate impacts of black carbon aerosols, *J. Geophys. Res.*, *109*, D03106, doi:10.1029/2003JD004084.

Wang, C. (2005), A model study of the response of tropical deep convection to the increase of CCN concentration: 1. Dynamics and microphysics, *J. Geophys. Res.*, *110*, D21211, doi:10.1029/2004JD005720.

Wang, C. (2007), Impact of direct radiative forcing of black carbon aerosols on tropical convective precipitation, *Geophys. Res. Lett.*, *34*, L05709, doi:10.1029/2006GL028416.

Wang, C. (2009), The sensitivity of tropical convective precipitation to the direct radiative forcings of black carbon aerosols emitted from major regions, *Ann. Geophys.*, *27*, 3705–3711, doi:10.5194/angeo-27-3705-2009.

Wang, C., and J. S. Chang (1993), A three-dimensional numerical model of cloud dynamics, microphysics, and chemistry: 1. Concepts and formulation, *J. Geophys. Res.*, *98*, 14,827–14,844, doi:10.1029/92JD01393.

Wang, C., G.-R. Jeong, and N. Mahowald (2009a), Particulate absorption of solar radiation: Anthropogenic aerosols vs. dust, *Atmos. Chem. Phys.*, *9*, 3935–3945, doi:10.5194/acp-9-3935-2009.

Wang, C., D. Kim, A. M. L. Ekman, M. C. Barth, and P. J. Rasch (2009b), Impact of anthropogenic aerosols on Indian summer monsoon, *Geophys. Res. Lett.*, *36*, L21704, doi:10.1029/2009GL040114.

Wang, M., and J. Penner (2009), Aerosol indirect forcing in a global model with particle nucleation, *Atmos. Chem. Phys.*, *9*, 239–260, doi:10.5194/acp-9-239-2009.

Wang, M., and J. E. Penner (2010), Cirrus clouds in a global climate model with a statistical cirrus cloud scheme, *Atmos. Chem. Phys.*, *10*, 5449–5474, doi:10.5194/acp-10-5449-2010.

Wang, M., J. E. Penner, and X. Liu (2009c), Coupled IMPACT aerosol and NCAR CAM3 model: Evaluation of predicted aerosol number and size distribution, *J. Geophys. Res.*, *114*, D06302, doi:10.1029/2008JD010459.

Wang, M., S. J. Ghan, M. Ovchinnikov, X. Liu, R. C. Easter Jr., E. I. Kassianov, Y. Qian, and H. Morrison (2011), Aerosol indirect effects in a multi-scale aerosol-climate model PNNL-MMF, *Atmos. Chem. Phys.*, *11*(11), 5431–5455, doi:10.5194/acp-11-5431-2011.

Warner, J. (1968), A reduction in rainfall associated with smoke from sugar-cane fires: An inadvertent weather modification?, *J. Appl. Meteorol.*, *7*, 247–251, doi:10.1175/1520-0450(1968)007<0247:ARIRAW>2.0.CO;2.

Warner, J., and S. Twomey (1967), The production of cloud nuclei by cane fires and the effects on cloud droplet concentration, *J. Atmos. Sci.*, *24*, 704–706, doi:10.1175/1520-0469(1967)024<0704:TPOCNB>2.0.CO;2.

Wetzel, M. A., and L. L. Stowe (1999), Satellite-observed patterns in stratus microphysics, aerosol optical thickness, and shortwave radiative forcing, *J. Geophys. Res.*, *104*(D24), 31,287–31,299, doi:10.1029/1999JD900922.

Whitby, K. T. (1978), The physical characteristics of sulfur aerosols, *Atmos. Environ.*, *12*, 135–159, doi:10.1016/0004-6981(78)90196-8.

Wilcox, E. M., K. M. Lau, and K.-M. Kim (2010), A northward shift of the North Atlantic Ocean Intertropical Convergence Zone in response to summertime Saharan dust outbreaks, *Geophys. Res. Lett.*, *37*, L04804, doi:10.1029/2009GL041774.

Williams, E., et al. (2002), Contrasting convective regimes over the Amazon: Implications for cloud electrification, *J. Geophys. Res.*, *107*(D20), 8082, doi:10.1029/2001JD000380.

Xue, H., and G. Feingold (2006), Large-eddy simulations of trade wind cumuli: Investigation of aerosol indirect effects, *J. Atmos. Sci.*, *63*, 1605–1622, doi:10.1175/JAS3706.1.

Yankofsky, S. A., Z. Levin, T. Bertold, and N. Sandlerman (1981), Some basic characteristics of bacterial freezing nuclei, *J. Appl. Meteorol.*, *20*, 1013–1019, doi:10.1175/1520-0450(1981)020<1013:SBCOBF>2.0.CO;2.

Yin, Y., K. S. Carslaw, and G. Feingold (2005), Vertical transport and processing of aerosols in a mixed-phase convective cloud and the feedback on cloud development, *Q. J. R. Meteorol. Soc.*, *131*, 221–245, doi:10.1256/qj.03.186.

Yuan, T., Z. Li, R. Zhang, and J. Fan (2008), Increase of cloud droplet size with aerosol optical depth: An observation and modeling study, *J. Geophys. Res.*, *113*, D04201, doi:10.1029/2007JD008632.

Yuan, T., J. V. Martins, Z. Li, and L. A. Remer (2010), Estimating glaciation temperatures of deep convective clouds with remote sensing data, *Geophys. Res. Lett.*, *37*, L08808, doi:10.1029/2010GL042753.

Yuan, T., L. A. Remer, K. E. Pickering, and H. Yu (2011), Observational evidence of aerosol enhancement of lightning activity and convective invigoration, *Geophys. Res. Lett.*, *38*, L04701, doi:10.1029/2010GL046052.

Zeng, X., W.-K. Tao, M. Zhang, A. Y. Hou, S. Xie, S. Lang, X. Li, D. Starr, X. Li, and J. Simpson (2009a), The indirect effect of ice nuclei on atmospheric radiation, *J. Atmos. Sci.*, *66*, 41–61, doi:10.1175/2008JAS2778.1.

Zeng, X., W.-K. Tao, M.-H. Zhang, A. Y. Hou, S. Xie, S. Lang, X. Li, D. Starr, and X. Li (2009b), A contribution by ice nuclei to global warming, *Q. J. R. Meteorol. Soc.*, *135*, 1614–1629, doi:10.1002/qj.449.

Zhang, H., G. M. McFarquhar, S. M. Saleeby, and W. R. Cotton (2007), Impacts of Saharan dust as CCN on the evolution of an idealized tropical cyclone, *Geophys. Res. Lett.*, *34*, L14812, doi:10.1029/2007GL029876.

Zhang, H., G. M. McFarquhar, W. R. Cotton, and Y. Deng (2009), Direct and indirect impacts of Saharan dust acting as condensation nuclei on tropical cyclone eyewall development, *Geophys. Res. Lett.*, *36*, L06802, doi:10.1029/2009GL037276.

Zhang, J., H. Chen, Z. Li, X. Fan, L. Peng, Y. Yu, and M. Cribb (2010), Analysis of cloud layer structure in Shouxian, China, using RS92 radiosonde aided by 95 GHz cloud radar, *J. Geophys. Res.*, *115*, D00K30, doi:10.1029/2010JD014030.

Zhang, R., G. Li, J. Fan, D. L. Wu, and M. J. Molina (2007), Intensification of Pacific storm track linked to Asian pollution, *Proc. Natl. Acad. Sci. U. S. A.*, *104*(13), 5295–5299, doi:10.1073/pnas.0700618104.

Zhang, S., J. E. Penner, and O. Torres (2005), Inverse modeling of biomass burning emissions using Total Ozone Mapping Spectrometer aerosol index for 1997, *J. Geophys. Res.*, *110*, D21306, doi:10.1029/2004JD005738.

J.-P. Chen, Department of Atmospheric Sciences, National Taiwan University, Taipei, Taiwan 10617.

Z. Li, Earth System Science Interdisciplinary Center and Department of Atmospheric and Oceanic Sciences, University of Maryland, College Park, MD 20740, USA.

W.-K. Tao, Laboratory for Mesoscale Atmospheric Processes, NASA Goddard Space Flight Center, Code 612, Greenbelt, MD 20771, USA. (wei-kuo.tao-1@nasa.gov)

C. Wang, Department of Earth, Atmospheric, and Planetary Sciences, Massachusetts Institute of Technology, Cambridge, MA 02139, USA.

C. Zhang, Rosenstiel School of Marine and Atmospheric Science, University of Miami, Miami, FL 33149, USA.